CZECH UNIVERSITY OF LIFE SCIENCES IN PRAGUE

FACULTY OF FORESTRY AND WOOD SCIENCE

EFFECT OF NANOCELLULOSE REINFORCED ADHESIVE ON THE STRENGTH AND STIFFNESS OF WOODEN JOINTS

Prague 2022 **Ing. Gourav Kamboj**

CZECH UNIVERSITY OF LIFE SCIENCES IN PRAGUE

FACULTY OF FORESTRY AND WOOD SCIENCE

EFFECT OF NANOCELLULOSE REINFORCED ADHESIVE ON THE STRENGTH AND STIFFNESS OF WOODEN JOINTS

DISSERTATION

Study program:	Wood Processing and Forest Machinery
Department (department / institute):	Department of Wood Processing and Biomaterials
Dissertation supervisor:	doc. Ing. Milan Gaff, PhD.

Prague 2022

Ing. Gourav Kamboj

Assignment

The assignment of the final thesis (hereinafter referred to as the ‘assignment’) is a document by which the university determines the student's study obligations in the elaboration of the final thesis. The assignment usually includes a final thesis, the title of the final thesis, the name, surname and titles of the student, the name, surname, and titles of the supervisor, and if there is an external supervisor, the name, surname and titles of the consultant, training department, the name, surname and titles of the supervisor, the final annotation thesis, the language in which the thesis is prepared, and the date of approval of the assignment.

I declare that I have written a dissertation on the topic of the effect of nanocellulose reinforced adhesive on the strength and stiffness of wood joints independently, with the use of literature and based on consultations and supervisor recommendations. I agree to the publishing of the dissertation pursuant to Act no. 111/1998 Coll., on schools, as amended, regardless of the outcome of its defense.

In Prague on……. Ing. Gourav Kamboj

ACKNOWLEDGEMENT

I would like to thank my supervisor Assoc. Professor Milan Gaff for his guidance, support and for giving me the opportunity to work in his research group; without his help it would not have possible to complete this research. I would like to express my gratitude to Professor Jerzy Smardzewski from the Poznan University of Life Sciences, Poznan, whose expertise in wood joints was invaluable in formulating the research questions and methodology.

I would like to thank Professor Eva Haviarova from Purdue University, West Lafayette, USA and Dr. Anil Kumar Sethy, Scientist at the Institute of Wood Sciences and Technology, Bangalore, India, for their technical support and insightfull feedback that helped me push my work to a higher level.

I would like to thank the woodworking lab members for extending all the necessary support for my research study. I would also like to thank all my colleagues: Fatemeh Razeai, Roberto Corleto, Gianlucca Ditommaso, Sumanta Das, and Salvio Marino for their help and motivation. Last but not the least, I would like to express my gratitude to my parents and family members in India for their constant motivation, love, support.

The dissertation was only possible by the financial support of the Internal Grant Agency of the Faculty of Forestry and Wood FLD CULS and IGA_B_06_2019 ‘Advanced research supporting the forestry and wood-processing sectors adaptation to global change and the 4th industrial revolution’, no. CZ.02.1.01 / 0.0 / 0.0 / 16_019 / 0000803.

Abstract

Adhesives play an essential role in the wood industry. The performance of existing wood joints is highly dependent on the performance of the wood species, geometry type, and type of adhesive. Polyvinyl acetate (PVAc) and polyurathene (PUR) are predominantly used in furniture as well as structural applications. In this study, two types of adhesive (PVAc and 1C-PUR) were used in wood joints (dowel, finger, dovetail, and lap joints). The joint performance improvement was investigated by adding nanocellulose. Nanocellulose (cellulose nanofiber and cellulose nanocrystals) is of natural origin and possesses remarkable mechanical properties. However, dispersion on nanocellulose in adhesive, especially in PUR, has been a challenging. To overcome this difficulty, chemical modification (acetylation) of nanocelluose was also attempted. The performance of the nanocelluose reinforced adhesives (PVAc and PUR) was assessed with a lap shear test. A study with a scanning electron microscope (SEM) was carried out to assess the bondline. The effect of cyclic moisture (8-19%) exposure on the performance of the nanocellulose reinforced adhesive bond was also assessed. The optimum value of elastic stiffness and shear strength was obtained with the addition of 1% nanocellulose. The resulting mechanical properties of lap shear joints were investigated and the difference between the pure adhesive and nanocellulose reinforced adhesive were discussed.

Keywords: Wood joints, Nanocellulose, Polyvinyl acetate (PVAc), Polyurethane (1C-PUR), Mechanical characteristics

Hypothesis and Objectives

Goal

The main goal of this study is to assess what types of wood species, adhesive and joint geometry affects the elastic stiffness of glued wood joints. The elastic stiffness of wood joints and resistence against moisture changes could be further improved by adding cellulose nanofiber (CNF) and cellulose nanocrystals (CNC) to the wood adhesive (PVAc and PUR).

Hypothesis

- The elastic stiffness of glued wood joints could be affected by reinforced adhesive.
- Adding cellulose nanofiber (CNF) and cellulose nanocrystals (CNC) to the wood adhesive (PVAc and PUR) could improve the elastic stiffness of joints.

Objectives

- Determining the effect of joint geometry and adhesive type on the performance of joint (Finger, Dowel, and Dovetail).
- Determining the effect of nanocellulose reinforced adhesive (PVAc and 1C-PUR) on the bond performance (lap joint).
- Determining the effect of moisture cycling conditioning on the properties of nanocellulose reinforced adhesive bonded joints (lap joint).

Table of Contents

List of Figures

List of tables

List of published articles

1. **Kamboj, G**. Záborský, V. Girl, T. Influence of Geometry on the stiffness of corner finger joint. Bioresources 14(2):2019,2946-2960 DOI: 10.15376/biores.14. 2. 2946-2960
2. Záborský, V. **Kamboj, G.** Sikora, A. Boruvka, V. Effect of selected factors on spruce dowel joint stiffness. Bioresources, 2018, 14(1): 14. DOI: 10.15376/biores.14.1.1127-1140
3. **Kamboj, G.** Gaff, M. Smardzewski, J. Haviaova, E. Boruvka, V. Sethy, A. K. Numerical and experimental investigation on the elastic stiffness of glued dovetail joint. Construction and Building Materials 2020, 263:120613. DOI: 10.1016/j.conbuildmat.2020.120613
4. **Kamboj, G.,** Gašparík, M., Gaff, M., Kačík, F., Sethy, A.K., Corleto, R., Razaei, F., Ditommaso, G., Sikora, A., Kaplan, L., Kubš, J., Das, S., Macků, J. (2020). Surface quality and cutting power requirement after edge milling of thermally modified Meranti (Shorea spp.) wood" Journal of Building Engineering, 29 (2020) 119793, May 2020, 101213 DOI: https://doi.org/10.1016/j.jobe.2020.101213
5. Ditommaso, G., Gaff, M., Kačik, F., Sikora, A., Sethy, A., Corleto, R., Razaei, F., Kaplan, L., Kubš, J., Das, S., **Kamboj, G.,** Gašparík, M., Šedivka, P., Hýsek, Š., Macku, J., Sedlecký, M., (2020). "Interaction of technical and technological factors on qualitative and energy/ecological/economic indicators in the production and processing of thermally modified Merbau wood" Journal of Cleaner Production, 252 (2020) 119793, 10 April 2020, DOI:https://doi.org/10.1016/j.jclepro.2019.119793
6. Gaff, M., Razaei, F., Sikora, A., Hýsek, Š., Sedlecký, M., Ditommaso, G., Corleto, R., **Kamboj, G.,** Sethy, A., Vališ, M., Řipa, K., (2020). " Interactions of monitored factors upon tensile glue shear strength on laser cut wood", Composite Structures, 234 (2020): 80-88, Februar 2020. DOI:https://doi.org/10.1016/j.compstruct.2019.111679
7. Razaei, F., Gaff, M., Kumar Sethy, A., **Kamboj, G.,** Ditommaso, G., Corleto, R., Das, S., Gašparík, M., (2020). Surface quality measurement by contact and laser methods on thermally modified spruce wood after plain milling, The

International Journal of Advanced Manufacturing Technology, August 2020, DOI: https://link.springer.com/article/10.1007/s00170-020-05983-7

8. Corleto, R. Gaff, M. Niemz, P. Sethy, A. K. Todaro, L. Ditomasso, G. Rezaei, F. Sikora, A. Kaplan, L. Das, S. **Kamboj, G.,** et al. (2020). Effect of thermal modification on properties and milling behaviour of african Padauk (Petrocarpus soyauxii Taub) wood. Journal of Materials Research and Technology 9(4): 9315-9327. DOI: 10.1016/j.jmrt.2020.06.018

List of prepared manuscripts

9. **Kamboj, G.,** Gaff, M., Smardzewski, J., Sethy, A.K., Haviarova, E., Hui, D., Fatemeh, R., Kacik, F. Effect of Nanocellulose (CNF and CNC) reinforcement on strength and stiffness of PVAc bonded joints.
10. **Kamboj, G.,** Gaff, M., Smardzewski, J., Sethy, A.K., Haviarova, E., Hui, D., Kacik, F. Incorporating of cellulose nanofiber and cellulose nanocrystals to enhance the strength and stiffness property of polyurethane adhesive (1 C-PUR).

1 Introduction and overview

1.1 Wood joints

Woodworking offers a multitude of opportunities to create a joint. Whenever material intersects, a joint must be made. Several joinery techniques and technologies have been developed. Wood joints are the most important components in furniture creation, because they are a critical part and the primary cause of failure. The designer needs to design the product in such a way so that it performs the best in service. In order for a functional design, it is important to understand loads acting on the structure and the stress acting on the joints. Wooden furniture is held together by joints. Different types of joints are unique in their construction, and it is important to know their mechanical properties when subjected to various stresses, namely shear, compression, and tension. The characteristics of wood joints, such as stiffness, strength, flexibility, toughness, and appearance, are derived from the properties of the joining material and how they are used in the wood joints. Therefore, different joinery techniques are used to meet these requirements. Some traditional wood-working joints are the dowel, finger, dovetail, mortise and tenon and butt joints. Proulx (1996) stated that the strength and durability of furniture depends on the structural integrity of its joinery. Several factors are responsible for the strength of joints, such as their geometry, properties of the wood species, and type of adhesive. Boadu and Antwi-Boasiako (2017) found that the geometry of dovetail joints improved their grain-to-grain connection in furniture products, making these products more resistant to bending force and warping than mortise and tenon joints. They also studied chairs produced with mortise-tenon and dovetail joints, which had longer wider and thicker tails and tenon were stronger than those manufactured with shorter, narrower, and thinner tails and tenons. Jokerst (1981) shows that finger joint geometry largely dictates the potential strength of a joint. Geometric parameters of joints include finger length, finger pitch, tip thickness, and slope. All these parameters are related to each other, so changing one parameter will change all the others. This interdependency between joint parameters complicates research of the effect of a single parameter on joint strength (Jokerst 1981). Another common type of structural joint is the dowel joint (Segovia and Pizzi 2012; Tas et al., 2014). This joint type has a great advantage in terms of economy and the ratio of production difficulty to the resulting joint properties. Today there is a wide range of dowels

themselves, varying in diameter, length, and surface treatment (Nutsch et al. 2006), which can be defined by several different characteristics (Eckelman et al., 2002), of which the elastic stiffness of the joint is very important. In the construction of chairs, joints are highly resistive to bending under compressive and tensile forces (Smardzewski 2015 b). For better resistance under bending stress, dovetail joints could offer an alternative to mortise and tenon joints (Zhang and Eckelman 1993, Hoadley 2000). Asomani 2009 found that dovtetail joints were 70% stronger than mortise and tenon joints in chair legs and rails. Su and Wang 2007 also observed that the strength of dovetail joints is greater than mortise-tenon and dowel joints. The stiffness of the furniture depends on the rigidity of the furniture joints, and it is one of the most important criteria for high-quality furniture (Eckelman and Kwiatkowski 1978, Eckelman and Rabiej 1985, Kotaś et al. 1957, Kotaś 1957, Ganowicz et al., 1978,). Considerable research has been conducted on the influence of each geometric parameter on joint strength. Therefore, the development of a suitable and correct design of furniture construction requires carrying out appropriate strength which is very important for the industry. Based on this, it is possible to design a piece of furniture that is characterised by strong joinery and that meets all the aesthetic and functional requirements. Even though a universally accepted design formula that calculates the joint strength has not been developed, some useful studies have been conducted. Joints are mostly tested by experimental and numerical methods. Experimental testing has been extensively reported to assess the mechanical properties of wood joints. While the experimental method is a precise method of assessing the mechanical behavior of joints, numerical simulations provide an opportunity to assess the distribution of stresses in the joints. It also provides information about the post elastic behaviour, which is most important to reduce damage in the experiment and optimise the furniture design. (Chuan et al. 2008, Ceccotti 2010). For a long time, the Finite Element Method (FEM) has been popular among scholars for calculating the mechanical properties of wood joints, such as elastic stiffness and strength. The elastic stiffness of joints is influenced by several factors, such as the type of load, joint thickness, type of adhesive, and the type of bonded wood or composite material. Adhesive bonding of solid wood, wood particles for various shapes and sizes, and wood fibres, is necessary in the production of modern wood products, whether they are used in construction, furniture, or in other applications.

1.2 Wood species

The anatomical properties of wood used in furniture construction are also equally important. Kiaei and Samariha (2011) noted the anatomical, physical, and mechanical properties of timber are the main source of the strength performance of wood in joints. The wood species is an important factor in the strength and stiffness of wood joints. It is therefore important to test different wood species to see if there is any variance between these species in their ability to form a strong furniture joint. This information was presented by the USDA Wood Handbook (2010) about the detailed differences between various wood species. There are two broad classes of wood species: hardwood and softwood. The generalisation of the categories is based on the cellular structure of the wood itself. The cellular structure of a particular species of wood influences the overall strength of the joints. It is important for furniture producers to have a better understanding of these properties to be able to select the right kind of timber for joint construction. The influence of mechanical properties of wood on joint strength has been extensively studied. For example, Haviarova et al., (2013) found that the difference in shear strength and modulus of elasticity in timber is partially responsible for variations in the strength of joints produced.

Mechanical fasteners are not sufficient for the production of modern wood products with varying shapes and sizes of wood joints. Adhesive bonding of solid wood, wood particles of varying shapes and sizes and wood fibre is therefore necessary to produce modern wood products, whether they are used for construction, furniture, or in other applications.

1.3 Wood adhesive

Adhesive bonding technology has been studied for many years, and it played an essential role in the development and growth of timber structures involving adhesive joints instead of mechanical joints. The widespread use of adhesive bonding can be attributed to its inherent advantages, such as the fact that the use of an adhesive joint can distribute the applied load over the entire bonded area and create more uniform distribution of stress. Adhesive adds very little weight to the joint structure, it has superior fatigue resistance compared to other joining methods, it is suitable for joining of dissimilar material, and it can reduce manufacturing costs. In the

rehabilitation and repair of wood structures, the adhesive has proven to be efficiently and economically competitive when compared with alternative repair procedures. Adhesive bonding of wood components has played an essential role in the development and growth of the forest product industry.

1.3.1 Polyvinyl acetate adhesive (PVAc)

Polyvinyl acetate (PVAc) is a clear, water-white, thermoplastic synthetic resin, produced from its monomer by emulsion polymerization. PVAc adhesive is suitable for wood, paper and plastics, and it is also used as a general building adhesive. PVAc adhesive has long been used in wood bonding and furniture construction. These adhesives, easily set at room temperature, are cost-effective and easy to use. These waterborne adhesives set as the water is absorbed into the wood, leading to their wide use in manufacturing and construction operations involving wood. PVAc is a linear polymer with an aliphatic backbone; this makes it a very flexible adhesive as opposed to the rigid nature of copolymers, normally used as a wood adhesive. PVAc sets through evaporation and diffusion of water into the substrate, and also by polymerisation of polymer particles as the water evaporates. PVAc is applied easily through different methods, such as brushing, flowing, spraying, roll coating, knife coating or silk screening (Ebnesajjad 2008, Pizzi 2005). The main advantages of PVAc are its easy and wide application, resistance to aging, elasticity, low cost, and availability, and non-toxicity. Özçifçi and Yapici, 2008 determined that the adhesion strength of beech and pine wood bonded with PVAc adhesive along the tangential direction is stronger than along the radial direction. Burdurlu et al., (2006) achieved similar results with Calabrian pine wood bonded with PVAc and PUR (polyurethane) adhesives, recommending that the bonding process on tangential surfaces be performed with higher pressure. On the other side, there are some disadvantages, such as low resistance to weather and moisture, poor resistance to most solvents, slow curing and setting speed, and creeping under substantial load.

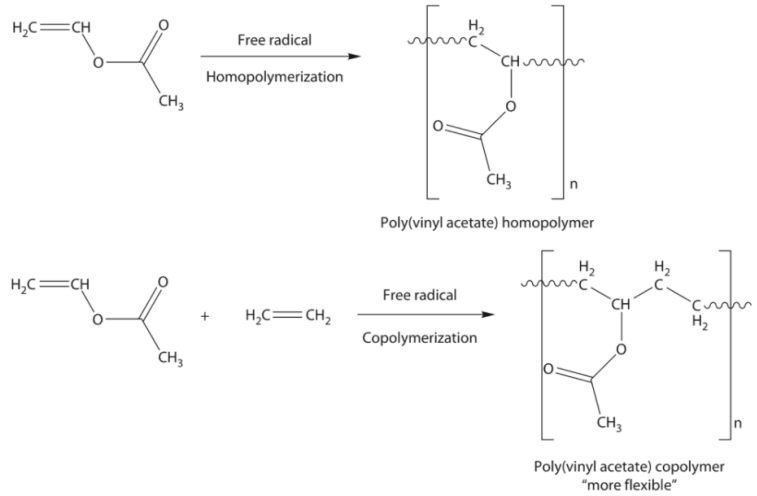

Figure 1 Polyvinyl acetate is made by the self-polymerisation of vinyl acetate, usually under free radical conditions. The chains can be altered by adding ethylene to form a copolymer (Rowell 2013).

1.3.2 Polyurethane adhesive (PUR)

For several decades, one-component polyurethane (1 C-PUR) has been used rapidly and successfully in the wood industry. One-component polyurethane (1C-PUR) has been used in the field of engineered wood gluing for the last two decades, as it offers several advantages, including fast curing at room temperature, an invisible glue line, no formaldehyde, and no mixing during the processing time (Kägi et al., 2006). Many researchers have found that 1C-PUR adhesives are capable of reaching high bond strength in glued wood structures, and they show comparatively ductile behaviour under load (Pizzi and Mittal 2003; Kägi et al., 2006; Brandmair et al., 2012). Müller et al., (2009) studied the fracture energy of adhesive bonding, finding that the higher ductility of 1C-PUR results in significantly enhanced failure load in certain load situations. Kläusler et al., 2013 investigated the effect of moisture conditions on stress and strain behaviour of 1C-PUR, PRF and MUF adhesives; they discovered the ductility of the tested 1C-PUR polymers in several climate stages in contrast to the brittleness of MUF and PRF adhesive. The fracture strain of MRF and MUF specimens was below 5%, whereas it reached at least 20% in 1C-PUR adhesives.

1.4 Technical properties of wood adhesive

It is very important to study the use of wood adhesive and its technical properties.

These properties were discussed below.

1.4.1 Bonding and science of adhesion

Adhesive increases the strength and stiffness of wood-based materials. The adhesion of the glue depends on the wood-adhesive bonding chain. The degrees of penetration of adhesive into the porous network of interconnected cells define the bonding perfomance of adhesive between two wood elements. To see the bonding performance, many studies have been conducted through microscopic examination and associated techniques to establish a relationship with the bond performance. Adhesive bonding problems and designing new adhesive systems and processes may be facilitated by understanding the fundamentals of adhesive penetration (Kamke and Lee 2007). The interphase region is an uneven layer. The geometry of the interphase is assumed to affect the bond performance.

Adhesive bonding joints must transfer stress from component to component through the interphase region. The structural interphase and its volume and shape dedicate the magnitude of stress concentration and ultimately have a significant impact on the performance of the bond.

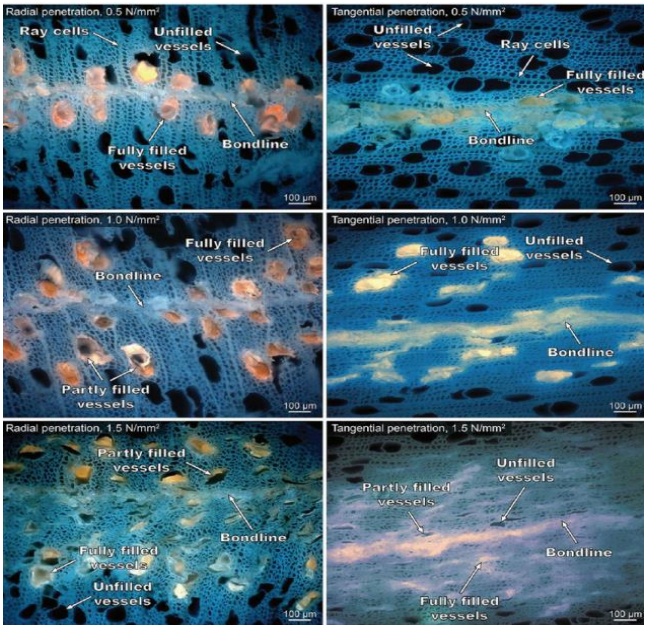

Figure 2 Example of an epi-fluorescence microphotograph with the penetration of UF resin into poplar at three different pressures applied during the press cycle: 0.5 N/mm2 , 1 N/mm2 , and 1.5 N/mm2 for radial and tangential penetration (Gavrilović-Grmuša et al 2016)

1.4.2 Wood adhesive penetration

Researchers have studied the penetration of wood adhesives. The penetration of adhesive into wood can be categorised into two groups:

1. Gross penetration
2. Cell wall penetration

In gross penetration, the liquid resin flows into the porous structure of wood, mostly filling cell lumens. Hydrodynamic flow and capillary action could be explained as gross penetration. Cell wall penetration occurs when resin diffuses into the cell wall or flows into the micro-fissures. In wood, the least resistance to the hydrodynamic flow is in the longitudinal direction, following through the lumens in the long and slender tracheid of softwood, or through the vessels of hardwoods. Since vessels are connected end-to-end with perforation plates and there is no pit membrane, the cell type dominates the penetration of adhesive in hardwoods. With an optical microscope, resin has been observed in pit chambers of both hardwood and softwood species, and in cell lumens in which the only entry pathway for the resin was through the pit. Adhesive penetration influences link 4 through 7. All of the potential adhesion mechanisms are influenced by the penetration. The concept of mechanical interlocking depends on the penetration of the adhesive phase beyond the external wood surface. In addition, the combined adhesion force due to covalent bonding and the formation of secondary chemical bonds is directly related to the area of surface in contact between the adhesive and cell wall.

A chain link analogy for an adhesive bond is shown in Fig. 3; we can see that the bond is only as good as the weakest link in the chain. Adhesive penetration plays a vital role in the analogy. Link 1 is the pure adhesive phase, unaffected by the substrates. Links 2 and 3 represent the adhesive boundary layer that may have cured under the influence of the substrates and is no longer homogeneous. Links 4 and 5 represent the interface between the boundary layer and the substrate and constitute the adhesion mechanism. The mechanism may be mechanical interlocking, covalent bonding, or secondary chemical bonds due to electrostatic forces. Links 6 and 7 represent wood cells that have been modified by the process of preparing the wood surface or the bonding process itself. Links 8 to 9 reperesent unmodified wood, which would have a lower limit of structure integrity, making it the weakest link.

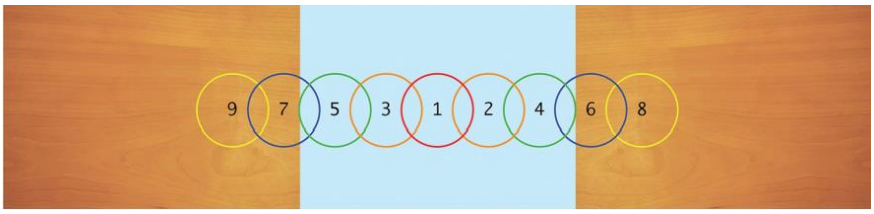

Figure 3: Chain link analogy for an adhesive bond in wood (Onur Ülker 2016)

1.4.3 Adhesion and cohesion

Adhesion is the tendency of dissimilar surfaces to bond to one another. The internal forces between the molecules that are responsible for adhesion are chemical bonding, dispersive bonding and diffusive bonding. These interamolecular forces can make cumulative bonding and bring certain emergent mechanical effects.

Cohesion means sticking or staying together. Cohesive force is the tendency of similar molecules to stick together. They attract mutually. Cohesive forces are caused by the shape and structure of the molecules, which makes the distribution of orbiting electrons irregular when molecules get close to one another. The chain link analogy for adhesion and cohesion is shown in Fig. 4. The adhesive and cohesive definition refers to the forces that keep the adhesive and the substrate (adhesion) and the adhesive itself (cohesion) together. As wood is increasingly used in furniture and engineered wood products worldwide, concerns about the integrity of the wood and adhesive used are rising. The bondline is a crucial issue for wood product application, especially in different moisture conditions. The properties of wood products are affected by many factors, including the quality of wood adhesives and the bonding process, wetting of the substrate surface, heat and pressure on the bond line, and drying time (Frihart 2013). The aim is to obtain higher functional strength. Fibre fillers are used in adhesives, improving surface wetting, bond rigidity, and more. Chawla 1998 shows that materials are stronger and stiffer in fibrous form. Many reinforcing fibres, such as glass and carbon fibres, polymer fibre and inorganic nanoparticles have been studied as additives for modifying wood adhesives, but their use introduces some environmental and sustainability issues to otherwise green materials (Singha and Thakur 2008).

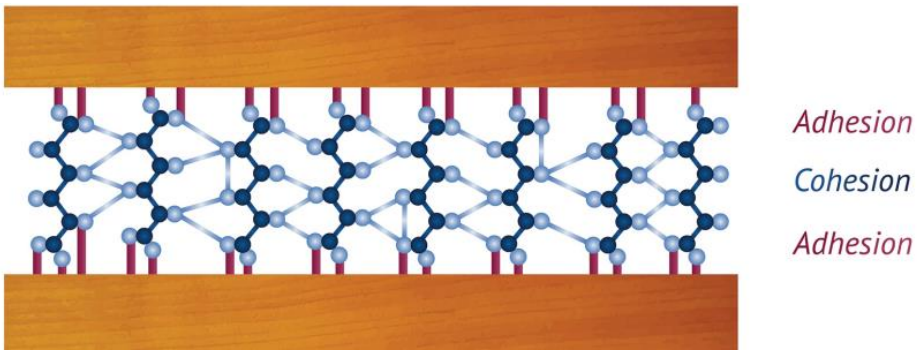

Figure 4 Chain link of adhesion and cohesion (Onur Ülker 2016)

1.5 Nanocellulose

Nanocellulose (CNF and CNC) as a renewable material has gained attention as potential reinforcement for adhesives, but its practical application remains scarce. Many researchers have investigated nanocellulose applications in polymer and composites, but a few related to adhesive for wood bonding. Recent studies have focused on the reinforcement of urea formaldehyde (UF), melamine formaldehyde (MF), phenol formaldehyde (PF) and polyvinyl acetate adhesive (PVAc) with the addition of nanocellulose. Property of nanocellulose to act as both binders and structural reinforcement in various adhesive system adds its potential, beside by reducing the harmful emission of formaldehyde, it also can improve the mechanical properties and enhance the performance of adhesive (Vineeth et al., 2019).

1.5.1 Nanocellulose reinforced PVAc and PUR adhesive:

The wood industry is under pressure to eliminate formaldehyde from its products. PVAc is a good adhesive to replace some wood adhesives containing formaldehyde. The main drawback of PVAc adhesive is its limitation to be used in humid conditions and at elevated temperatures. So far, some approaches been used to increase the performance of PVAc adhesive; firstly, copolymerization of vinyl acetate with more hydrophobic monomers (Zhou 1991), and the blending of PVAc with adhesive or hardeners (Lu 1996). These strategies can increase some properties of PVAc adhesive at the expense of reducing some other properties. However, some additives are so acidic that they can damage the wood surface, which can affect the overall performance of wood joints. The introduction of nanotechnology has opened new opportunities for the industry to develop a new generation of composites with high performance. In the past, research showed that nano-aluminum and nano- clay can be used to improve the performance of wood

adhesive, but there has been some concern related to the health risk posed by nano-clay and nano-oxide particles. Therefore, eco-friendly nano-materials (nanocellulose) introduce, which has high strength and stiffness property. Among the several opportunities which offered by the nanotechnology for the forst based product industry, the reinforcement of adhesive with nanocellulose has been already potential opportunity, which has been explored (Cai and Niska 2012). López-Suevos et al., (2010) used CNF (cellulose nanofiber) with the addition of acid and sodium hydroxide to reinforce PVAc-latex adhesive; the results showed excellent heat resistant properties of the produced panels. Chaabouni and Boufi (2017) investigated the influence of the addition of CNF to PVAc adhesive with 10 wt% content and observed a significant benefit in shear strength and water resistance performance. Considering the strong reinforcing potential of CNF when incorporating the polymer matrix, the matrix of CNF and PVAc adhesive might contribute to imporving the performance of wood joints bonded with PVAc in humid conditions at elevated temperature. The use of nanocellulose gel as reinforcement of PVAc adhesive should be easy to process and the simple mixing route. To the best of our knowledge, only one reported work by López-Suevos et al. (2010) has been subjected to the application of CNF for PVAc wood adhesive reinforcement. A study conducted by Jiang et al., 2018 where the commercial polyvinyl acetate and starch adhesives mixed with dicarboxylic acid cellulose nanofiber (CNF), by adding the optimum amount of CNF , the lap joint strength increased up to 74.5%.

Kaboorani et al., 2012 used NCC (nanocrystaline cellulose) in the wood adhesive to improve the performance of polyvinyl acetate adhesive. This study was conducted with the addition of NCC to polyvinyl acetate at different loads (1%, 2%, and 3%) and the use of blends as a wood binder. The block shear test shows that NCC can improve the bonding strength of polyvinyl acetate.. The thermal stability, hardness, modulus of elasticity, and creep of polyvinyl acetate film were also enhanced by the addition of NCC. Cellulose nanocrystal (CNC) is used as a reinforcing filler in different polymers, and its special physicochemical properties, good mechanical properties, renewability and biodegradability have drawn attention to it (Girouard et al., 2016, Lei et al., 2019). The high crystallinity in CNC gives it good thermostability, because the presence of interchain hydrogen bonds at high temperatures cannot easily break the crystalline region and are difficult for cellulose to melt (Ng et al., 2015, Tonoli et al., 2012). Polyurethane demonstrated the typical behaviour of an elastomer material with high flexibility and deformation. The addition of nanocellulose with ceratin content and conditions

substantially affected the mechanical properties of polyurethane adhesive (Pei et al., 2011). The highest value of tensile strength resulted is 5 time more deformation with a 10 wt% load of CNF, which increased from 6.5 MPa for neat polyurethane to 10.5 MPa (Ivdre et al., 2016). The reinforcement effect of nanocellulose in whisker form, the modulus of PUR increased by 253% with the addition of 4 wt% filler. The young modulus and shear strength increased of the composites, while strain at break decreased by increasing the content of nanocellulose in the form of fibres and crystals. The improvement in shear strength is indicative of strong interfacial bonding between the composites, while the reduction in tensile strain is attributed to the restricted polymer segments causing the formation of rigid nanocellulose (Aranguren et al., 2013, Wu et al., 2007). When comparing the increase in tensile properties between nanocellulose fibres and whiskers, we found a more noticeable in nanocomposites with CNF than with CNC (Azeredo et al., 2010, Floros et al., 2012). This is due to the formation of an interconnected nanocellulose network with increasing filler content. For cellulose nanofibre, the formation of the network is assisted by its flexibility, resulting from the high aspect ratio and the presence of amorphous domains along the nanofibres. The stronger interaction between CNF and polyurethane as hosting polymers restricts the motion of polymeric chains, resulting in greater young's modulus and shear strength (Auad et al., 2010). CNC has received significant attention for how it improves the thermal properties of PUR adhesive due to its high thermal stability. Dou et al., (2014) found CNC improved temperature at 5 % weight loss of polyurethane from 326.6 to 333.9 °C. Therefore, nanocellulose (CNF and CNC) is an abundant natural green material. Depending on the type of nanocellulose reinforced, modification of its structure and compatibility between polymer matrix, enhance the properties of an adhesive by addition of a small amount of nanocellulose.

However, synthetic adhesives are currently widely used in the wood industry. Fibre reinforcement has the potential to reliably improve the mechanical properties of adheisve needed in the joints. Nanocellulose therefore has many advantages for this application: it is renewable, biodegradeable, it has low density, it has good mechanical properties, and it is non-toxic.

2 Material and methodology

This chapter discusses material information, the preparation of nanocellulose reinforced adhesive, and the preparation of wood joints (dowel, finger, dovetail, and lap shear joint). Nanocellulose reinforced material characterisation for surface morphology, chemical properties, and thermal properties with an FTIR, DSC, and SEM analysis are also discussed.

2.1 Material

Defect-free beech (*Fagus sylvatica*) and spruce (*Picea abies* L) wood was used for the test specimens. The specimens for the mechanical testing were made from dried lumber with wood working machines at a vocational school in Spišská Nová Ves (Slovakia) and the Czech University of Life Sciences. Four types of wood joints were prepared (dowel, finger, dovetail, and lap). For dowel joints, two types of joint geometries were used with diameters of 8 mm and 12 mm and a length of 50 mm. For finger joints, the planks were first machined into specimens with a 58 mm × 20 mm cross section. The planks were subsequently shortened to 215 mm. The basic dimensions of the test specimens were 58 mm × 20 mm × 215 mm. Two types of geometries (2 teeth and 5 teeth) were used with straight fingers machined by a planner. Dovetail joint specimens were prepared with dimensions of 214 × 60 × 24 mm (L × W × H). Wood lamellas were prepared for the lap shear test using the standard procedure. The individual lamellas were cut in dimensions of 150 × 35 × 5 mm (L × W × H). The average density for beech wood was 0.725 g/cm^3, and 0.450 g/cm^3 for spruce wood. All specimens were conditioned at a temperature of 20 ± 2 °C and RH of 65 ± 3% to an equilibrium moisture content of 12%. The effect of moisture cycling on the strength of glued lap shear joints was studied by subjecting the samples to the moisture cycles at a constant temperature of 30 ± 2 °C. The conditioned samples with 12% moisture content were first exposed to 30 ± 2 °C and 43 ± 2 RH to arrive at 8% EMC, followed by exposure to 30 ± 2 °C and 86 ± 2 RH to reach 19% EMC. Then the samples were brought down to 8% EMC again by exposing them to 30 ± 2 °C and 43 ± 2 RH, and finally conditioned back to 12% moisture content by exposing them to 20 ± 2 °C and 65 ± 3% RH. Only one moisture cycle was performed in this study. The configurations of the test specimen are shown in Fig. 5.

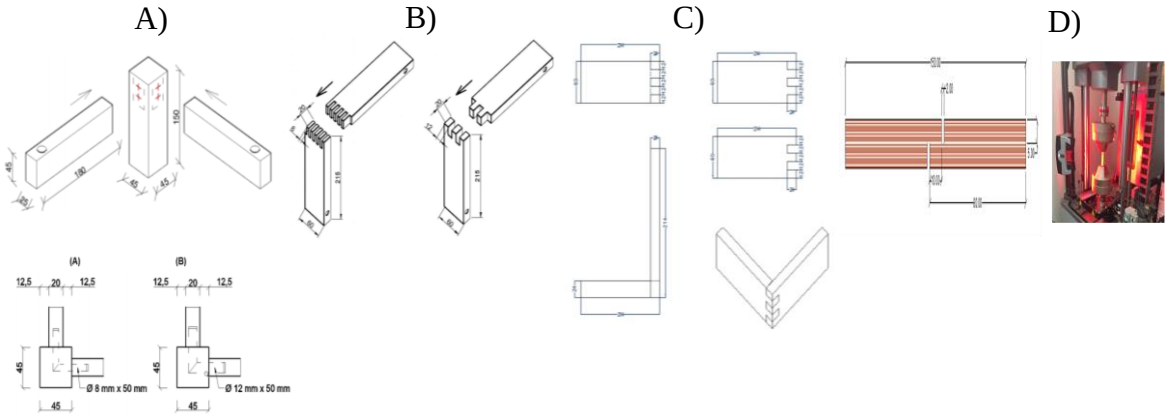

Figure 5 Sechamtic diagram of a (A) dowel joint with 8 mm dia and 12 mm dia; (B) Finger joint with 5 teeth and 2 teeth; (C) Dovetail Joint; (D) Shear lap joint

Polyvinyl acetate adhesive (PVAc) AG-COLL 8761 / L D3 and polyurethane adhesive (PUR) were used for the test samples. The technical specification of both adhesives is shown in Table 1. The adhesive was applied manually with a roller on both the wood surfaces, with a range of 150 - 180 g/m^2 for PVAc and 180 -250 g/m^2 for PUR adhesive.

Table 1: Technical parameters of PVAc AG-COLL 8761 / L D3 and PUR (1C - AkzoNobel 2010) adhesive

Technical parameters for AG-COLL 8761 / L D3 adhesives	
Viscosity (mPas)	5000-7000 (at 23 ° C)
Working time (min)	15-20
Density (g / cm3)	0.9-1.1 (at 23 ° C)
Open time (min)	15
Dry matter content (g)	49–51
pH	to 4.5
Shear strength according to EN 205 (MPa)	11.9
Technical parameters for PUR adhesive (1C – AkzoNobel 2010)	
Viscosity (mPas)	6000 – 19000
Working time (min)	15-20
Density (g / cm3)	1.16
Open time (min)	90

2.2 Specification of nanocellulose and chemical material

Cellulose nanocrystals (CNC) NCV100-NASD90 used as a reinforcing material were purchased from Celluforce, Windsor, Canada. Cellulose nanofibre (CNF) was supplied by the University of Maine, Orono, Maine, USA. The CNC was prepared by sulfuric

acid hydrolysis, and CNF was produced through high pressure grinding. The produced CNC and CNF were in dry powder form. The width and length of the CNC are 20 ± 5 nm and 150 ± 39 nm; the dimensions of the CNFs are 20 ± 14 nm and 1030 ± 334 nm, respectively. Acetic acid (CH_3COOH), acetone (C_3H_6O), and acetic anhydride (C_4H6O_3) were purchased from Lach - Ner (Neratovice, Czech Republic). Potassium acetate (Reagent Plus ≥99%) used as a catalyst was purchasd from Sigma-Aldrich.

2.3 Modification of nanocellulose

Nanocellulose was modified based on the acetylation method. Cellulose nanofibre (CNF) dry powder with a weight of 0.25 g was dissolved in 10 ml acetic acid (CH3COOH) at room temperature by using sonication (SONOPLUS HD 3100, Berlin, Germany) for 15 min. To remove the acetic acid (CH3COOH) from the CNF, a suspension centrifuge process was performed at a speed of 15000 rpm for 15 min. CNF suspension inside of the centrifuge tube can be seen in two separated layers; one is acetic acid, and the second layer is CNF. Excess acetic acid was decanted, and the resulting CNF was washed with acetone. The obtained CNF was further subjected to centrifuge (15000 rpm, 15 min) by three folds and decanting, and further diluted with distilled water. The obtained CNFs were mixed with 25 ml acetic anhydride with a 5% catalyst of postassium acetate (CH_3CO_2K). The suspension was heated at a temperature of 105 °C for 4 hrs with continuous stirring in the soxhlet apparatus. To decant the untreated acetic anhydride, the suspension was successfully centrifuged 3 times with acetone and finally with distilled water. The obtained CNFs were dried at room temperature.

2.4 Creation of nanocellulose reinforced adhesive

CNF (cellulose nanofiber) and CNC (cellulose nanocrystal) 0.5w%, 1w%, and 2w% were mixed in PVAc (polyvinyl acetate) and PUR (polyurethane) adhesive with a high-speed homogenizer (**T 18 digital ULTRA - TURRAX® IKA-Werke, Staufen, Germany**) followed by sonication (**SONOPLUS HD 3100, Berlin, Germany**). One part of nanocellulose suspension was added to two parts of PVAc and PUR adhesive mixed thoroughly with s high-speed homogenizer followed by sonication.

3 Methodology of mechanical testing

All dowel, finger, and dovetail joint specimens were conditioned and kept at 12% moisture content before and during the testing time. The calculation was performed according to ISO 13061-1 (2014), and the density of the specimen was evaluated pursuant to ISO 13061-2 (2014). A universal testing machine TIRA 50 (TIRA System GmbH, Schalkau, Germany) was used to measure the elastic stiffness of corner joints by applying a compressive and tensile load. Figure 6 shows the experimental testing of corner joints and their mounting in the testing machine.

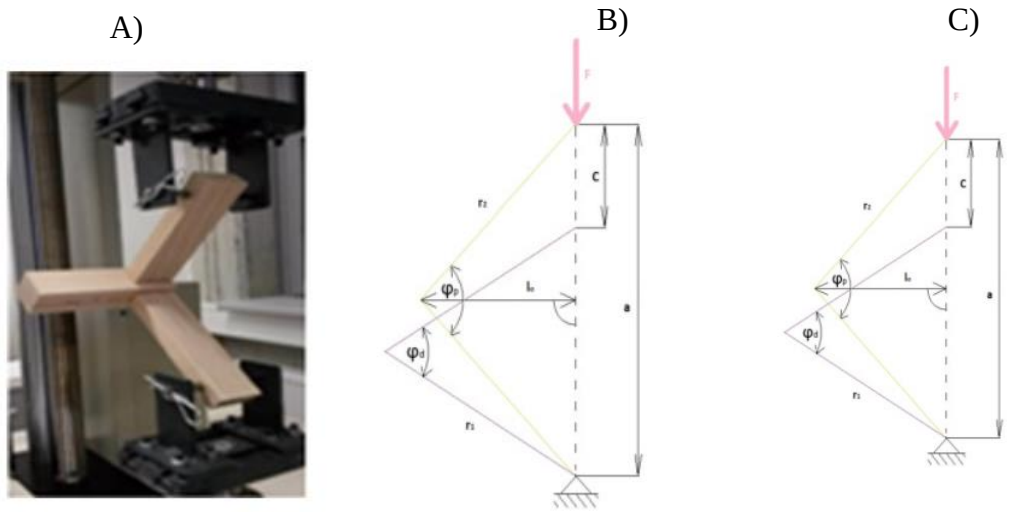

Figure 6 A) Test sample attached to the UTM (Záborský et al. 2018), B) Geometry of joints under compressive load; C) Geometry of joints under tensile load (Kamboj et al. 2020)

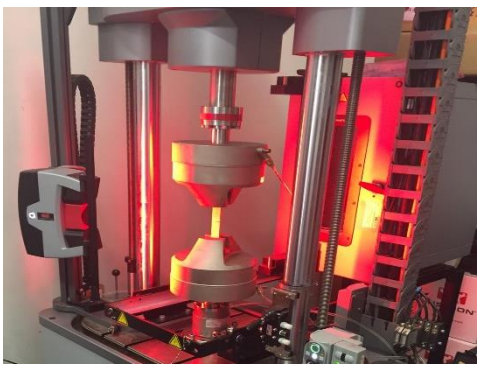

Figure 7 Shear test sample attached to the UTM (Universal testing machine) with video extensometer

Shear lap joint samples were tested under loading according to EN 205-2003. The test specimen was loaded with a video extensometer (INSTRON® 5882, NORWOOD, USA) at a constant speed of 5 ± 0.5 mm/min according to the data for the maximum force acquired by a computer as shown in Fig. 7.

3.1 Calculation of results

The samples were subjected to bending moment under tensile and compressive force perpendicaular to the direction of the moment arm. The effect of the individual factors and their interaction on the elastic stiffness were ascertained with an analysis of variance (ANOVA) and Fischer's F-Test using STATSTISTICA 14 (Statoft Inc; Oklahoma, USA). The elastic stiffness was calculated based on the following equations:

F- force [N], $r_{1,2}$ – arm length (distance of force from the axis of rotation) [m], φ_p- joint angle before loading [rad], φ_d- joint angle after loading [rad], l0- force arm from original shape [m], a- arm spacing [m], c- displacement [m]

The angular deformation φ was calculated according to:

$$\varphi = \varphi_p \pm \varphi_d \tag{1}$$

Deformation limit:

This indicates the maximum angular deformation at the maximum resistance of the joint.

$$\varphi_{max} = \varphi_p \pm \varphi_{dmax} \tag{2}$$

φmax – angular deformation at the ultimate limit [rad]

After the specimens are loaded, a general triangle is formed and its angle φd can be expressed with Kosin's theorem:

$$\begin{aligned} a^2 &= b^2 + c^2 - 2bc\cos\alpha \\ 2bc\cos\alpha &= b^2 + c^2 - a^2 \\ cos\alpha &= \frac{b^2 - c^2 - a^2}{2bc} \end{aligned} \tag{3}$$

The mathematical modification produces the following formula:

$$\alpha = arccos \frac{b^2-c^2-a^2}{2bc} \quad (4)$$

Results value in the form:

$$\varphi_d = arccos \frac{r_1^2+r_2^2-(a-c)^2}{2r_1r_2} \quad (5)$$

The shoulder is defined by the side and content of a general traingle:

$$l_o = \frac{2*S}{a} \quad (6)$$

$$S = \frac{1}{2} r_1 r_2 \sin \varphi\rho \quad (7)$$

The mathematical model produces the following formula:

$$l_o = \frac{r_1 r_2 sin_{\varphi p}}{a} \quad (8)$$

The strength properties were examined for the tested structural joints, and the bearing capacity was calculated according to the following formulas. The size of the arm or the distance between the holes was 195 mm for all the samples. The bending moment was calculated using the following formula:

Bearing capacity up to the elastic limit (ΔM)

$$\Delta M = \Delta F * L_0 \quad (9)$$

Where ΔM - bending moment change [N.m], ΔF- force change [N], L_0 -hole distance [mm]

ΔF is the deviation of the two forces recorded in the stress-strain diagram at values between 10% and 40% of the maximum strength. The resistance of the elastic limit of the joints was calculated for the elastic area. Calculation of the maximum bearing capacity (M):

$$M = F_{max} * x * L_0 \quad (10)$$

M- moment [N × m], F_{max} -maximum force [N], L_0 -hole distance [mm]

We determined the resistance of the structural joint to the external force with the bearing capacity. The bending moment expresses the maximum bearing capacity of the joint.

Elastic stiffness (c_{elast})

$$C_{elast} = \frac{\Delta M}{\Delta \varphi} \tag{11}$$

c_{elast} - elastic stiffness [Nm/rad], ΔM- bending moment [N.m], Δφ- angular deformation

maximum stiffness (c)

$$C = \frac{M_{max}}{\varphi_{max}} \tag{12}$$

c_{elast} - elastic stiffness [Nm/rad], M_{max}- maximum bending moment [N × m], φ_{max}- maximum angular deformation [rad]

Stiffness is indicative of some degree of change induced by the fraction of external force during elastic deformation that affects the entire body.

3.2 Numerical calculation based on the experiment results

The numerical calculation was performed based on experimental results in dovetail joints, which were performed by applying the Abaqus v.6.16 software (Dassault Systems Simulia Corp., Waltham, Ma, USA). In general, a linear hexahedron type C3D8R element was used (about 120000 elements and 90000 nodes per model). The behaviour of the glue line was modelled with the help of the Cohesive Zone Model (CZM) by means of standard COH3D8 cohesive elements shown in table.2. The joint arm was described as an orthotropic body ascerbing its material properties as shown in Table.3. Figure 8 MODEL_FEM presents a mesh model and orientation of fibres in the local coordinate system (X,Y,Z).

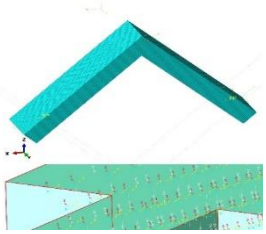

Figure 8 Meshing with fibre orientation in a local coordinate system (Kamboj et al. 2020)

Table 2 Elastic properties of wood (Smardzewski. J 2008)

Elastic Properties/Type of wood (MPa)	Beech	*Spruce
$E_{L(X)}$	14100	16600
$E_{R(Z)}$	2280	1117
$E_{T(Y)}$	1160	583
$\nu_{LR(XZ)}$	0.45	0.42
$\nu_{LT(XY)}$	0.51	0.51
$\nu_{RT(ZY)}$	0.75	0.68
$\nu_{TR(YZ)}$	0.36	0.31
$\nu_{RL(ZX)}$	0.075	0.038
$\nu_{TL(YX)}$	0.044	0.015
$G_{LR(XZ)}$	1645	1181
$G_{LT(XY)}$	1082	693
$G_{RT(ZY)}$	471	70

Where E – Modulus of elasticity (MPa), G – Shear modulus (MPa), and ν – Poisson ratio in the longitudinal (L-X), radial (R-Y) and tangential (T-Z) direction.

*Note – Because the elastic properties of pine wood were not accessible, the elastic properties of spruce wood were used instead for numerical calculation because of their comparable properties.

Table 3 Elastic properties of the glue line (Smardzewski. J. 1998, 2002)

Glue	E (MPa)	Poisson ratio
PVAc	460	0.3
PUR*	820	0.3

*Note – Due to the non-availability of elastic properties for the PUR glue line, the UF value was used for numerical calculation.

3.3 Scanning electron microscopy

Wood samples were attached to cylindrical aluminum mounts with silver paint (SPI Products, West Chester, Pennsylvania, USA) or double-stick carbon tape (Ted Pella, Redding, California, USA). Images were obtained with a MIRA3 LMU (Tescan, a.s., Brno, Czech Republic) scanning electron microscope. An accerlerating voltage of 0.8kV and a beam current of about 6pA were used for visualisation of the results.

3.4 Fourier transform infrared spectroscopy

Fourier transform infrared spectroscopy studies were performed with an FTIR-ATR spectrometer Nicolet (Křelovická, Czech Republic). Before analysis, samples of pure adhesive and nanocellulose reinforced adhesive were dried adequately at room temperature for two days. The obtained samples were analysed in a transmittance range of 4000 - 500 cm^{-1}.

3.5 Statistical evaluation

Duncan‘s test, with a significance level of $\alpha = 0.05$, was chosen to evaluate the results and their interactions. Based on the significance level ‘P’, this test determiens whether the observed factor is statistically significant. According to the value of P, the monitored factor is evaluated.

- P = 0 - the probability that the factor does not act is zero
- P <0.05 - the influence of the factor is statistically significant
- P = 0.05 - the influence of the factor is on the border of statistical significance
- P> 0.05 - the effect of the factor is not statistically significant

4 Synthesis of results

This chapter presents the summary results of the dissertation published in a professional publication during the doctoral study. The PhD dissertation consists of five articles: four first-author aricles and one second author article. Two first author article and one second author article have been published and two first author articles are in the form of manuscript, one is submitted and second in the process of submission. The first part of the results focuses on the effect of geometry, wood species, adhesive type on the elastic stiffness of corner Finger, Dowel, and Dovetail joints (section 4.1). The second part shows the effect of cellulose nanofiber and cellulose nanocrystals reinforcement on the strength and stiffness of PVAc and PUR adhesive bonded joints (section 4.2).

The mechanical properties of wood joints are influenced in various ways, such as by the joint geometry, wood species and wood adhesive. Appropriate selection of geometry, adhesive, and combination with different wood species can allow the change in the properties of wood joints, thereby creating wood joints with specific desired properties.

Article no. 1 (Kamboj et al., 2019) shows that the finger joints used to eliminate wood defects that would cause the weaken the wood joint strength. This research shows that wood species (spruce and beech), adhesive types (PVAc and PUR), and the number of teeth (2 and 5) affect the elastic stiffness of finger joints under compressive and tensile load. The highest elastic stiffness value was obtained in beech wood samples with 5 teeth, which were 30% higher than that of 2 teeth bonded with polyvinyl acetate adhesive (PVAc) under tensile load. The study showed that elastic stiffness increased with the number of teeth in finger joints.

Article no. 2 (Záborský et al., 2018) where we concluded that joints are the critical structure part of furniture. When designing the furniture it is imporatnt to consider the type of joint carefully that can hold the joined elements together under loading condition. In this study, elastic stiffness of spruce (Picea abies L.) wood dowel joints bonded with polyvinyl acetate (PVAc) and polyurethane adhesive (PUR) were investigated. The effects of other selected factors such as loading type (compression and tensile), thickness of dowel (1/2 and 1/3) used, and the annual ring deflection were examined. The impact of annual ring was not a significant factor. The maximum average elastic stiffness was obtained for ½ thickness joints bonded with

PUR adhesive under compressive load and the minimum elastic stiffness was reached in the samples with 1/3 thickness joints bonded with PVAc adhesive. The average elastic stiffness for PUR bonded joints was approximately twice than average value of PVAc bonded joints. The higher glued surface area increases the elastic stiffness of wood joints. It is therefore important to carefully consider the type of joinery used in furniture design.

Article no. 3 (Kamboj et al., 2019) gives an overview of the elastic stiffness of spruce (*Picea abies* L.) and beech (*Fagus Silvatica*) wood dovetail joints bonded with polyvinyl acetate (PVAc) and polyurethane (PUR) adhesive by experimental and numerical calculations. The mechanical properties were determined according to the grain direction loaded under compressive and tensile load. Experimental results are indicated that under compression load beech wood joints bonded with polyvinyl acetate (PVAc) adhesive had maximum elastic stiffness. Further to predict the stiffness of dovetail joints under compressive and tensile load a numerical model using finite element method (FEM) was developed based on the experimental results by the Abaqus program. A cohesive zone was developed with the help of numerical model, which shows stress behavior under compression and tensile load. A positive correlation was found between the numerical model and experimental study. Experimental results shows that beech wood joints bonded with PVAc adhesive had higher elastic stiffness as compared to PUR, on the other side spruce wood joints bonded with PUR had higher elastic stiffness than PVAc. The numerical results also confirmed the similar results as in experimental for beech and spruce wood joints under compression load. However the results are opposite under tensile load. The distribution of stress is very important information which can't be achieved by the experimental studies. The numerical model helps to provide the location of stress in joints and precisely identified that the stress in compression recorded was higher as compared to the tension.

Article no. 4 (Kamboj et al., 2022 manuscript) demonstrates that the effect of cellulose nanofiber (CNF) and cellulose nanocrystals (CNC) reinforced polyvinyl acetate (PVAc) adhesive on the elastic stiffness and shear strength of spruce (*Picea abies* L) and beech (*Fagus sylvatica*) wood joints. This study presents with three different concentration (0.5%, 1%, and 2% w/w) of nanocellulose (CNF and CNC) reinforced with PVAc adhesive. The reinforced adhesive was used to glue spruce

and beech wood joints to determine joint stiffness and shear strength under static load. Samples were tested at 12% moisture content and after one moisture cycle condition (8-19%). The addition of nanocellulose (CNF and CNC) increased the elastic stiffness of joint as well as improve the bond quality. The bond morphology was studied by SEM (scanning electron microscope). The addition of nanocellulose improved the bond line at 12% moisture content and after moisture cycle exposure and thereby improved the mechanical properties. In this study CNF and CNC dispersion in PVAc was achieved by premixing nanocellulose with water and subsequently, mixing the suspension with PVAc, which caused the dilution of PVAc. Despite this, the results are quite encouraging. The optimum elastic stiffness and shear strength value were achieved with 1% addition of nanocellulose.

Article no. 5 (Kamboj et al., 2022 manuscript) shows a comparative study of cellulose nanofiber (CNF) and cellulose nanocrystal (CNC) reinforced 1C-PUR adhesive bonded spruce and beech wood joints. In this study, nanocellulose reinforced adhesive was prepared by mixing the modified cellulose nanofiber (CNF) and cellulose nanocrystals in 1C-PUR adhesive. The chemical modification of cellulose nanofiber (CNF) focused on the compatibilization with PUR adhesive matrices to improve the interfacial adhesion. The reinforcement of nanocellulose in hydrophobic polymer is difficult, therefore the modification of the nanocellulose considered with acetylation method. Three concentration (0.5%, 1%, and 2% w/w) of CNF and CNC were considered in this study. The different concentration of CNF and CNC affected the tensile properties at 12% moisture content and after moisture cycle condition (8-19%) were studied. FTIR (Fourier-transform infrared spectroscopy) and DSC (Differential scanning calorimeter) analyses showed the molecular interaction between nanocellulose and PUR adhesive. DSC analysis shows the glass transition temperature increased for all the nanocomposites compared to the PUR adhesive. Among the three concentration (0.5%, 1%, and 2%) concentration of nanocellulose (CNF and CNC), 1% addition was found the optimum for elastic modulus and shear strength. Further addition of nanocellulose content, will lead to a significant drop in elastic modulus and shear strength. SEM (scanning electron microscope) analyses shows the morphology of bond line, and nanocellulose reinforced adhesive a relative improvement on the bond-line with the good dispersion of CNF and CNC in PUR adhesive.

4.1 Effect of geometry, wood species, adhesive type on the elastic stiffness of corner finger, dowel, and dovetail joints

4.1.1 Influence of Geometry on the Stiffness of Corner Finger Joints

Published as:

Kamboj G, Záborský V, Girl T. Influence of geometry on the stiffness of corner finger joints. BioResources. 2019 Feb 25;14(2):2946-60.

Influence of Geometry on the Stiffness of Corner Finger Joints

Gourav Kamboj,* Vladimír Záborský, and Tomáš Girl

Finger joints enable the full utilization of wood. The finger joint technique is used to eliminate wood defects that would otherwise weaken the wood strength. This research project evaluated how the wood species, adhesive type, and number of teeth affect the elastic stiffness of finger joints. The adhesives used were polyurethane and polyvinyl acetate, and the wood species were beech (*Fagus sylvatica* L.) and spruce (*Picea abies* L.). This study also determined the elastic stiffness of finger joints with 2 teeth and 5 teeth. For this purpose, the samples were loaded *via a* bending moment reaction, with tensile or compression forces in the angular plane. The highest elastic stiffness was obtained from the beech wood samples with 5 teeth bonded with polyvinyl acetate adhesive under tensile stress. Therefore, it was concluded that the elastic stiffness increased when the number of teeth increased. However, further studies on the elastic stiffness of finger joints are necessary in relation to the finger teeth length and surface area of the glue between the finger joint connections.

Keywords: Wooden construction; Finger joint; Mechanical loading; Elastic deformation; Elastic stiffness

*Contact information: Department of Wood Processing, Czech University of Life Sciences in Prague, Kamýcká 1176, Praha 6 - Suchdol, 16521 Czech Republic; *Corresponding author: kamboj@fld.czu.cz*

INTRODUCTION

Joints fulfill important structural, technological, and operational-aesthetic functions in furniture construction. According to the available literature (Eckelman and Lin 1997; Smardzewski and Prekrad 2002; Eckelman 2003), joints in general are the weakest part of a given furniture piece; therefore, furniture durability depends on their quality. Structural design involves choosing the dimensions of load-bearing members and modelling the load-bearing structure according to the requirements set for the material resistance (Bustos *et al*. 2003; Crocetti *et al.* 2011).

Finger joints are commonly used to produce engineered wood products from short pieces of lumber. Such joints must have excellent mechanical performances. This jointing method is said to be an opportunity for mills to upgrade waste lumber and improve the return on low-grade lumber because of the considerably higher dimensional stability that occurs when drying shorter lumber, such as by delivering quasi-deliberate lengths and coping with decreasing log lengths in sawmills. Therefore, finger jointing is an ideal method for improving the efficiency and profitability of sawmills. Additionally, finger joints have been used for many years. In Canada and the USA, finger-jointed lumber is widely used for the fabrication of construction lumber or components of engineered wood products, such as a flange stock for a wood I-joist (Hernández *et al.* 2011). This joint is also used in the automotive industry for wooden steering wheels and wooden wheel

spokes. Foremost, the application of finger jointing allows for the removal of strength-reducing defects.

Several researchers have investigated the effects of the glue line thickness on the strength of finger joints (Groom and Leichti 1994; River 1994). They found that it is necessary to control the glue line thickness to produce a strong joint. Using an increased glue area has produced a product with high engineering properties (Bustos *et al*. 2011). High strength finger joints require a maximized bonding surface area (Franke *et al*. 2014). An increase in the finger length resulted in an increase in bonding or contact with the finger surface. Ayarkwa *et al.* (2000) concluded that the effects of increased glue joint surface area also influenced the modulus of rupture of finger-jointed members. Polyurethane (PUR) adhesives provide interesting characteristics because they produce a high strength bond and cure at ambient conditions. Therefore, it was hypothesized that PUR adhesives are a viable alternative for wood finger joints (Verreault 1999; Chen and Walworth 2001; Lange *et al.* 2001). Murphey and Rishel (1972) explored the possibility of adopting finger jointing technology with polyvinyl acetate (PVAc) adhesive for use in furniture production, and it was found that such joints can replace mortise and tenon or dowel joints in furniture.

Finger joints have been shown to be suitable for use in connection with wood trusses, corner and multiple member furniture joints, laminated beams, and truck decking, as well as a variety of other structural and non-structural applications. Proof loading of end-jointed materials has been implemented in many instances to eliminate substandard joints. One aspect that is critical to the performance of finger joints during service is the overall geometry of the joint.

The purpose of this study was to compare the elastic stiffness of finger-jointed spruce and beech wood with either 2 teeth or 5 teeth and varying adhesive types (PUR or PVAc) under different loads (compression or tension). This study was the initial step to determine the elastic stiffness for different numbers of teeth in the finger jointing process, which will help the beech and spruce wood product industry to optimize their finger jointing methods.

EXPERIMENTAL

Materials

Beech (*Fagus sylvatica* L.) and spruce (*Picea abies* L.) lumber was used to produce test specimens. The lumber came from the woods near Spišska Nová Ves in Slovakia, which was where the basic test specimens were also prepared. The planks were first shortened for machining and then were thickened in a jointer and cut into precise 60-mm (58-mm) × 20-mm cross sections for the test specimens. The planks were then shortened to 215 mm. The basic dimensions of the test specimens were 60 mm (58 mm) × 20 mm × 215 mm, and there were 320 specimens. This was followed by milling of straight fingers using a planer milling machine (Profijoint, Grecon, Kopřivnice, Czech Republic). Either 2 teeth or 5 teeth were milled. Holes with a 10-mm diameter for subsequent fastening to the test machine were created using a rack drill. A diagram of the test specimens before gluing is shown in Fig. 1.

The joints were glued using two different adhesives, (PVAc) AG-COLL(EOC, Oudenaarde, Belgium) 8761/L D3 (EOC, Oudenaarde, Belgium) and (PUR) NEOPUR

2238R (NEOFLEX, Madrid, Spain) . Detailed parameters of these adhesives are shown in Table 1. In both cases, the adhesive was applied to all of the joint surfaces using a brush and followed the curing conditions given in the technical data sheets. To achieve the required pressing pressure, a manual joiner brace was used. The test specimens were then allowed to harden.

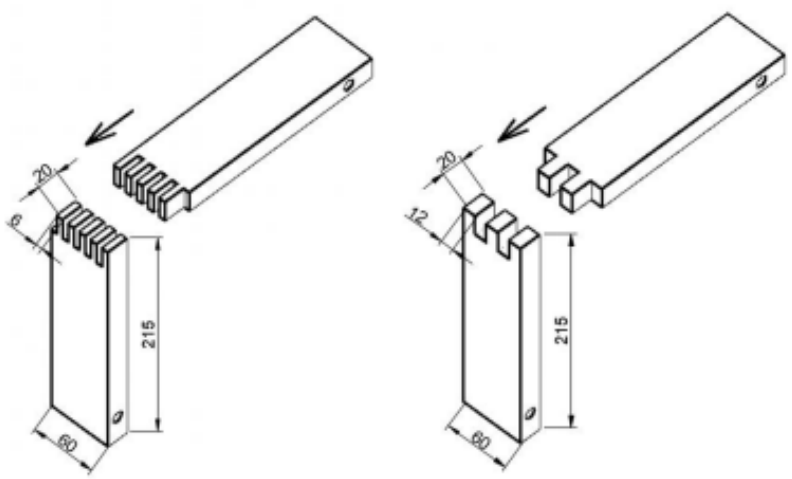

Fig. 1. Dimension of the test specimens

The glued specimens were placed in a climatic chamber that was set to a temperature of 20 °C (± 2 °C) and humidity of 55% (± 5%), so that the final moisture content of the material was 10%, as was established by ČSN EN 942 (2007) for wood used inside heated buildings.

Table 1. Parameters of the PVAc and PUR Adhesives

Technical Data for Adhesive	AG-COLL 8761/L D3	NEOPUR 2238R
Viscosity (mPa)	5000 to 7000 at 23 °C	2000 to 4500 at 25 °C
Working time (min)	15 to 20	60
Density (g/cm3)	0.9 to 1.1 at 23 °C	ca. 1.13
NCO content (%)	-	*ca.* 15.5 to 16.5
Color	White, milky	Brown
Open time (min)	15	*ca.* 20 to 25
Dry matter content (g)	49 to 51	100
pH	to 4.5	-

Methods

The climatized specimens were subjected to strength tests. The specimens were loaded with compression or tensile stress in the angular plane, as is shown in Fig. 2.

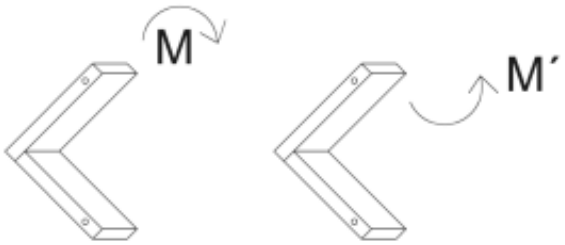

Fig. 2. Test specimen loading

The testing was performed on a UTS 50 universal testing machine (TIRA, Germany), which was designed for testing the mechanical properties of wood and wood-based materials. The values were recorded by the TIRA program (TIRA System GmbH, Schalkau, Germany). This program was also used to set the loading speed so that the test was performed properly according to the 90-s (± 30 s) standard. The loading speed ranged from 9 mm/min to 12 mm/min. The machine recorded the applied force and load head displacement. It also recorded the tests graphically and numerically. To clamp the specimens into the testing machine, a clamping tool was used according to the methodology by Podlena and Borůvka (2016), which they used to test window frames. Each specimen was weighed and recorded with a digital scale after testing.

The monitored factors (F1 through F4) are given in Table 2. The test specimens were divided into 16 sets, according to the individual parameters, and the effects of the individual factors on the stiffness of the joints were monitored. Each set contained 20 test specimens.

Table 2. Categorization of the Observed Factors of the Test Samples

Factor 1 – Wood Species		Factor 2 – Type of Glue	
Beech	Spruce	PVAC	PUR
Factor 3 – Number of Teeth		Factor 4 – Type of Loading	
2	5	Tension (← →)	Compression (→ ←)

A bending moment was generated in a specimen during loading and the test continued until the specimen broke. The bending moment was used to calculate the elastic stiffness, and the stiffness at the maximum load was calculated using the following equations (Eqs. 1 to 3). The output of the test was a stress-strain diagram with data on the dependence between the force and resulting deformation (load head displacement). The force and deformation at 10% and 40% of the yield strength of the joint were also recorded.

The essential characteristics of the wood include the density at a given moisture content, which was determined according to ISO 13061-1 (2014). The density was calculated for the entire specimen together. After testing, the density was immediately determined for the entire specimen at a given moisture content in accordance with ČSN 49 0108 (1993), using Eq. 1,

$$\rho_w = \frac{m_w}{V_w} \quad (1)$$

where ρ_w is the density (kg.m^{-3}) at the given moisture content w (%), m_w is the weight (kg) at the given moisture content w, and V_w is the volume of the specimen (m^3) at the given moisture content w.

The moisture content (w) of the climatized specimens was determined in accordance with ČSN 49 0103 (1979), using Eq. 2,

$$w = \frac{m_w - m_0}{m_0} x\ 100\% \quad (2)$$

where m_0 is the mass (weight) of oven-dry sample (kg).

To calculate the bending moment induced in the test specimen, the length of the arm (Fig. 3) needed to be determined, which was done using Eq. 3,

$$l_0 = a\cos 45 \quad (3)$$

where l_0 is the length of the arm (m) and a is the length of the hypotenuse of the right triangle formed (m).

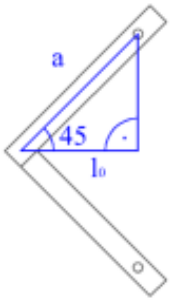

Fig. 3. Scheme of the length calculation

The bending moment induced in the specimen was calculated according to Eqs. 4 and 5,

$$M = Fl_0 \quad (4)$$

$$\Delta M = \Delta F l_0 \quad (5)$$

where F is the maximum applied force (N), M is the maximum bending moment (Nm) at the maximum load F, ΔF is the difference in the forces (N) for the 10% and 40% loads, ΔM is the difference in the moments (Nm) for the 10% and 40% loads, and l_0 represents the force applied to the vertical arm of tested joints.

The force applied to a specimen caused it to deform to L'. Tensile stress causes it to elongate, and compression stress causes the specimen to shorten. Diagrams of the deformation of the specimens are shown in Fig. 4.

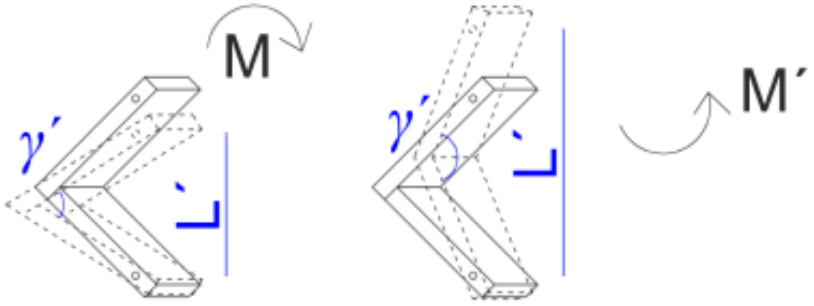

Fig. 4. Deformation of the test samples during loading

If there is a change in angle (γ'), which clasps the arms of the test specimen, this change can be calculated in radians according to Eq. 6,

$$\gamma' = 2arcsin\frac{L'}{2a} \quad (6)$$

where γ' is the size of the angle (rad) that is clasping the arms of the test specimen after loading and L' is as the length of the support span (m) when the force is applied.

The size of this angle was expressed according to Eq. 7,

$$\pi rad = 180° \quad (7)$$

The difference in these angles was used to calculate angular displacement according to Eq. 8,

$$\Delta\gamma = 90 \pm \gamma' \quad (8)$$

Stiffness is the resistance of a structure to deformation (Joščák *et al*. 2015), and it was calculated as the ratio of the bending moment to the angle change caused by this moment, as shown by Eqs. 9 and 10,

$$C_{max} = \frac{M_{max}}{\gamma_{max}} \quad (9)$$

$$C_{elast} = \frac{\Delta M}{\Delta\gamma} \quad (10)$$

where C_{max} is the maximum stiffness of the joint (Nm/rad), M_{max} is the maximum bending moment (Nm), γ_{max} is the angle (rad) caused by M_{max}, C_{elast} is the stiffness of the joint in the elastic region (Nm/rad), ΔM is the difference in the moments (Nm) at the 10% and 40% loads, and $\Delta\gamma$ is the change in the angles (rad) at the 10% and 40% loads.

RESULTS AND DISCUSSION

The highest elastic stiffness was obtained with 5 teeth joint of beech wood (3254 Nm/rad) bonded with PVAc adhesive under tensile load, and the lowest elastic stiffness was found with 2 teeth joint of spruce wood (1279 Nm/rad) bonded with PVAc adhesive under compression load. The data for the beech and spruce wood samples with different numbers of teeth, load types, and adhesive types is shown in Table 3.

Table 3. Density and Stiffness for the Individual Sample Sets

Wood Species	Adhesive Type	Number of Teeth	Type of Loading	Density (g/cm³)	Elastic Stiffness (Nm/rad)	*N*
Spruce	PVAC	2	Compression	378 (7.7)	1279 (15.6)	20
Spruce	PVAC	2	Tension	355 (4.6)	1495 (11.1)	20
Spruce	PVAC	5	Compression	376 (7.8)	2057 (17.4)	20
Spruce	PVAC	5	Tension	376 (5.5)	1863 (19.6)	20
Spruce	PUR	2	Tension	369 (7.3)	1454 (19.3)	20
Spruce	PUR	2	Compression	378 (6.5)	1416 (19.4)	20
Spruce	PUR	5	Compression	394 (7.4)	1977 (13.3)	20
Spruce	PUR	5	Tension	416 (8.6)	2096 (14.5)	20
Beech	PVAC	2	Compression	688 (4.6)	2463 (14.2)	20
Beech	PVAC	2	Tension	678 (3.8)	2511 (17.4)	20
Beech	PVAC	5	Compression	679 (6.2)	3150 (18.2)	20
Beech	PVAC	5	Tension	667 (5.3)	3254 (16.4)	20
Beech	PUR	2	Compression	731 (4.1)	2456 (17.2)	20
Beech	PUR	2	Tension	670 (5.5)	2617 (18.4)	20
Beech	PUR	5	Compression	644 (6.2)	2996 (19.2)	20
Beech	PUR	5	Tension	650 (7.3)	3083 (11.4)	20

Values in parentheses are coefficients of variation (CV) in %.

Table 4 shows the results of the four-factor analysis of variance (ANOVA) and Fisher's F-Test with STATSTICA 12 software (Statsoft Inc; Oklahoma, USA) that evaluated the influence of individual factors on the joint stiffness and the interaction of all of the factors together (F1 through F4). It was clear from the *P*-values that the wood species, number of teeth, and loading type were statistically significant factors for the one-factor analysis. The effect of the adhesive type by itself was not significant, but in combination with the other factors, its effect was significant. The four-factor analysis revealed the statistical significance of the interaction of the monitored characteristics.

Table 4. Statistical Evaluation of the Factors Influencing the Elastic Stiffness

Monitored Factor	Sum of Squares	Degree of Freedom	Variance	Fisher's F-test	Significance *P*-value
Intercept	817521787	1	817521787	18142.56	***
1) Wood Species	49457268	1	49457268	1097.56	***
2) Adhesive Type	329	1	329	0.01	*NS*
3) Number of Teeth	14307412	1	14307412	317.51	***
4) Type of Loading	209710	1	209710	4.65	***
1*2*3*4	242470	1	242470	5.38	***
Error	6488781	144	45061		

The respective model explains roughly 69.9% of the total sum of squares; NS - not significant, *** - significant; significance was accepted at $P < 0.05$

The wood species had an effect on the elastic stiffness, and on average, the beech joint exhibited a 65% greater elastic stiffness than the spruce joint (Fig. 5A). This also demonstrated the higher elasticity obtained from the beech wood samples bonded with the PVAc adhesive (Özçifçi and Yapıcı 2008). The elastic stiffness of the joints bonded with the PUR adhesive was 0.12% higher than that of the joints bonded with the PVAc adhesive (Fig. 5B). Záborský *et al.* (2018) found that there was also a small difference in the bonding factor for dowel joints.

Figure 5C shows the influence of the number of teeth on the elastic stiffness. The 5-tooth joints exhibited a 30.4% higher elastic stiffness than the 2-tooth joints. This meant that the elastic stiffness increased with an increase in the number of teeth in the finger joint. This result corresponded to the results of other researchers (Selbo 1963; Bustos *et al*. 2011; Franke *et al*. 2014). The test specimens subjected to tensile stress exhibited a 3.27% greater elastic stiffness on average than the specimens subjected to compression stress (Fig. 5D).

Figure 6 illustrates the effective interaction of the individual factors on the elastic stiffness with a particular effect from the wood species, adhesive type, number of teeth, and load type. Under compression stress, the elastic stiffness of the spruce wood was 49.7% higher with a 5-tooth joint when compared with a 2-tooth joint (Fig. 6), while a 25% higher elastic stiffness was found for the beech wood. When comparing the elastic stiffness of 5 tooth joint of spruce wood, it was found that the elastic stiffness of joints bonded with PVAc adhesive was 4.04% higher than the elastic stiffness of PUR adhesive with the same type of joints. In contrast, when subjected 2 tooth joints with spruce wood, the type of the joint exhibited higher elastic stiffness bonded with PUR adhesive; the values were 10.7% higher than bonded with PVAc adhesive with the same type of joint.

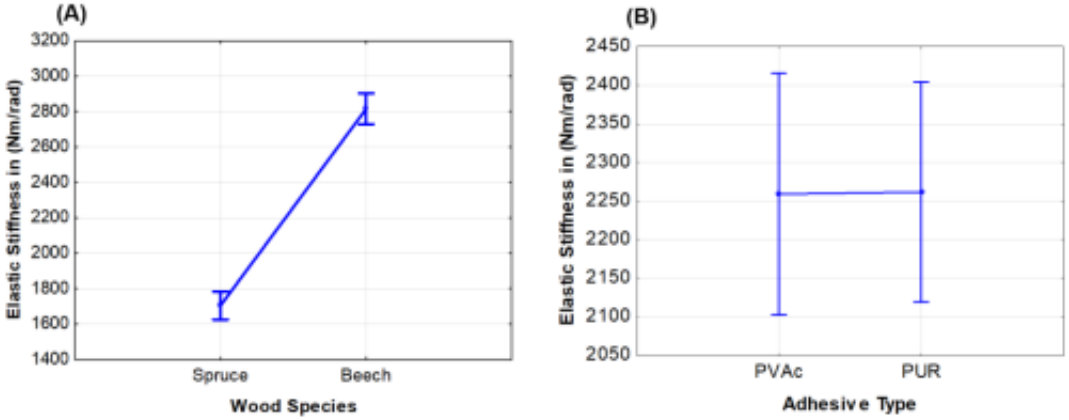

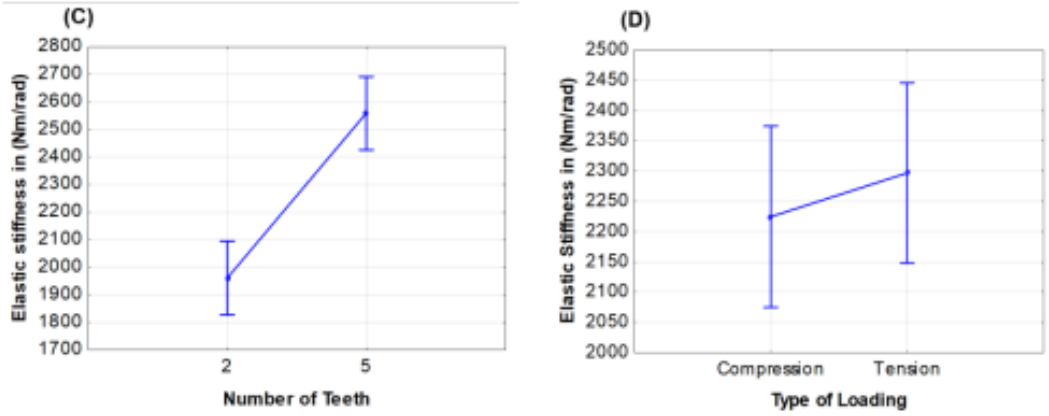

Fig. 5. Graphic visualization of the effect of the wood species (A), adhesive (B), number of teeth (C), and loading (D) on the elastic stiffness

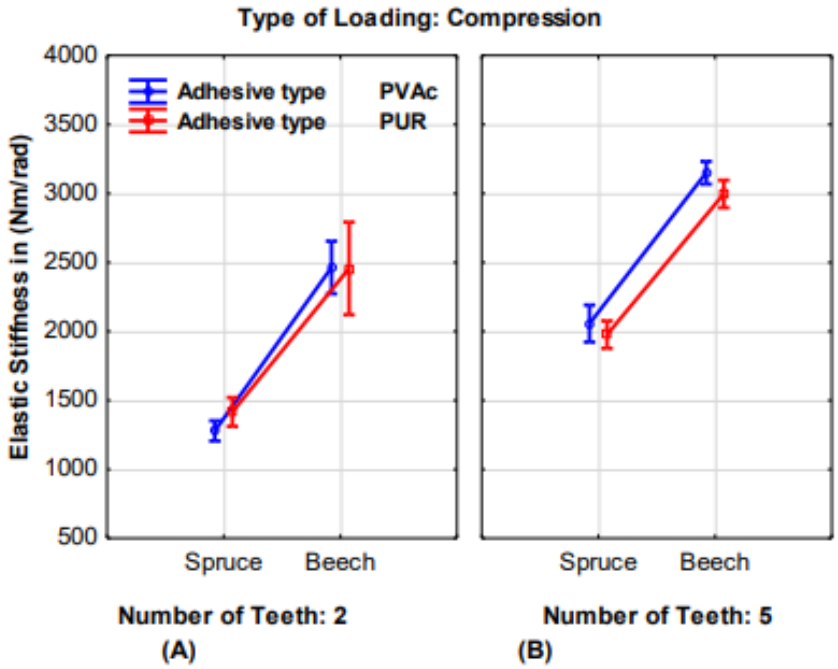

Fig. 6. Graphic visualization of the influence of the wood species and adhesive type on the elastic stiffness while under compression stress for (A) 2 teeth and (B) 5 teeth

Another finding was that the elastic stiffness of beech wood with 5 tooth joints, bonded with PVAc adhesive was 5.14% higher than the elastic stiffness of joint bonded with PUR adhesive with the same type of joints (these results were notably demonstrated in joints subjected to compressive stress).

When placed under tensile stress, the elastic stiffness of the spruce wood was 34.2% higher with 5 teeth than with 2 teeth (Fig. 7). The elastic stiffness of the beech wood was nearly 24% higher with 5 teeth compared with 2 teeth, under both stresses (compression and tensile). The adhesives used in this study had a slight effect on the elastic stiffness. Hemmasi *et al*. (2014) found in previous studies concerning a 10-mm

oak wood finger joint that the PVAc adhesive did not cause any serious change in the studied elastic properties of the beams. Under tensile load, the elastic stiffness of 5 teeth joints have interesting results. In case of spruce wood, the elastic stiffness of joints bonded with PUR was 12% higher than the joints bonded with PVAc adhesive. On the other side, the trend was opposite in beech wood; the elastic stiffness of joints bonded by PVAc adhesive was 5.7% higher value than the joints bonded with PUR adhesive. The elastic stiffness of 2 teeth joints of spruce wood bonded with PVAc obtained 2.8% higher elastic stiffness than joints bonded with PUR adhesive and in beech wood, the results showed that joints bonded with PUR obtained 4.22% higher elastic stiffness than joints bonded with PVAc.

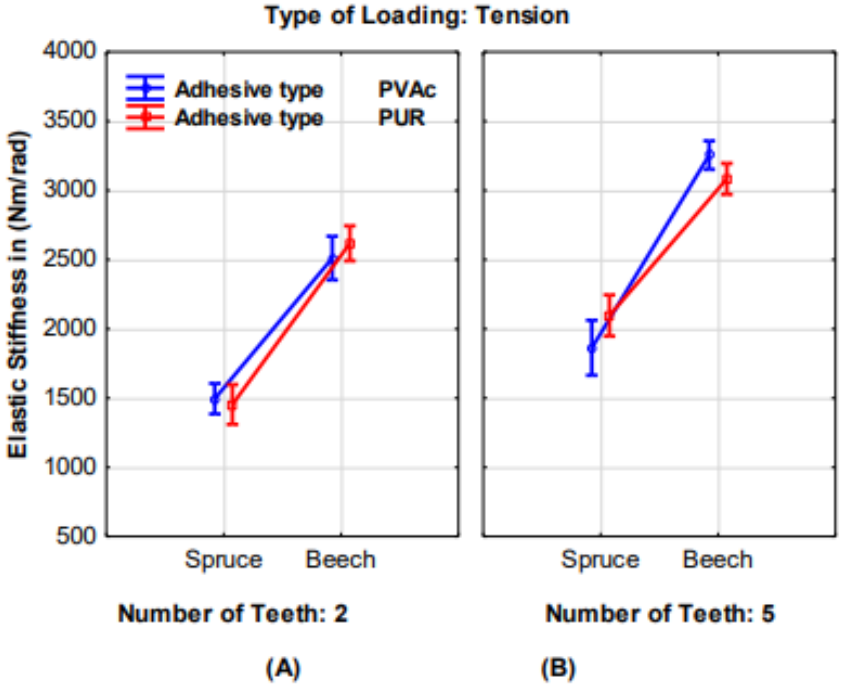

Fig. 7. Graphic visualization of the influence of the wood species and adhesive type on the elastic stiffness while under tensile stress for (A) 2 and (B) 5 teeth

Duncan's test made multiple comparisons of all 16 test sample sets against each other. The results followed the data from the ANOVA test. The results of the tests that were conducted to determine the importance of the difference between the groups are shown in Table 5.

Table 5. Multiple Comparison of the Elastic Stiffness using Duncan's Test

Adhesive Type	No. of Teeth	Type of Loading	(1) 1279	(2) 1495	(3) 2057	(4) 1863	(5) 1415	(6) 1416	(7) 1977	(8) 2095.8	(9) 2463	(10) 2510	(11) 3149	(12) 3254	(13) 2456	(14) 2617	(15) 2996	(16) 3083
PVAC	2	Compression																
PVAC	2	Tension	0.035															
PVAC	5	Compression	0.000	0.000														
PVAC	5	Tension	0.000	0.000	0.052													
PUR	2	Compression	0.149	0.434	0.000	0.000												
PUR	2	Tension	0.081	0.660	0.000	0.000	0.690											
PUR	5	Compression	0.000	0.000	0.397	0.231	0.000	0.000										
PUR	5	Tension	0.000	0.000	0.683	0.023	0.000	0.000	0.239									
PVAC	2	Compression	0.000	0.000	0.000	0.000	0.000	0.000	0.000	0.000								
PVAC	2	Tension	0.000	0.000	0.000	0.000	0.000	0.000	0.000	0.000	0.618							
PVAC	5	Compression	0.000	0.000	0.000	0.000	0.000	0.000	0.000	0.000	0.000	0.000						
PVAC	5	Tension	0.000	0.000	0.000	0.000	0.000	0.000	0.000	0.000	0.000	0.000	0.272					
PUR	2	Compression	0.000	0.000	0.000	0.000	0.000	0.000	0.000	0.000	0.941	0.593	0.000	0.000				
PUR	2	Tension	0.000	0.000	0.000	0.000	0.000	0.000	0.000	0.000	0.126	0.262	0.000	0.000	0.123			
PUR	5	Compression	0.000	0.000	0.000	0.000	0.000	0.000	0.000	0.000	0.000	0.000	0.127	0.011	0.000	0.000		
PUR	5	Tension	0.000	0.000	0.000	0.000	0.000	0.000	0.000	0.000	0.000	0.000	0.484	0.089	0.000	0.000	0.358	

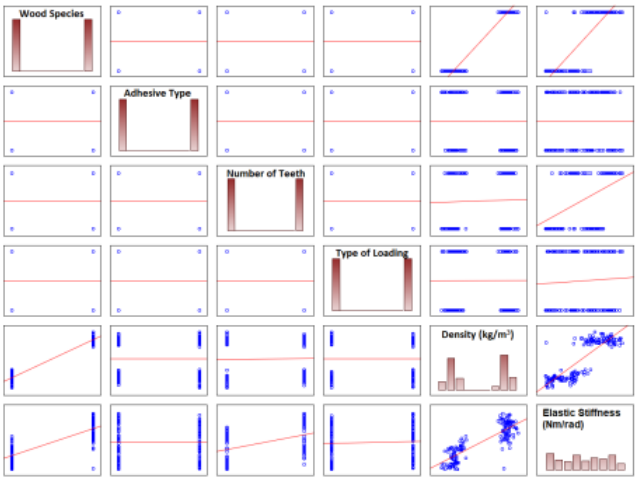

Fig. 8. Graphic visualization of Spearman's rank-correlation test

According to Duncan's test, when considering the interactions between the joint and stress type, the highest elastic stiffness was obtained from the beech wood sample with 5 teeth. Beech wood also has a fine tight grain, large medullary rays, and a small tracheal structure. This may have been a result of the beech wood density because Örs *et al.* (2004) reported that the high density of beech wood (0.67 g/cm^3) increased its mechanical properties

The results of the correlation analysis (Fig. 8) showed how the individual characteristics affected each other. The elastic stiffness was highly correlated with the wood species, wood density, and number of teeth in the finger joints. There was also a slight correlation with the loading type within the experiment.

CONCLUSIONS

1. For the elastic stiffness, the number of teeth in the finger joint played a significant role and increasing the number of teeth increased the elastic stiffness. In general, the elastic stiffness of the 5-tooth joints was 30.4% higher than that of the 2-tooth joints.
2. Comparing the elastic stiffness of the wood species, the spruce wood had a large variation in the elastic stiffness under both stress types with 2 teeth and 5 teeth, while the beech wood had nearly the same difference in the elastic stiffness.
3. Both of the adhesives (PUR and PVAc) proved to be nearly equivalent in finger jointing (2 teeth and 5 teeth) for both wood species (spruce and beech). The elastic stiffness test results suggested that the PUR adhesive formed a high-quality bond.

ACKNOWLEDGMENTS

The authors are grateful for the support of the project "Advanced research supporting the forestry and wood-processing sector's adaptation to global change and the 4th industrial revolution" (No. CZ.02.1.01/0.0/0.0/16_019/0000803) financed by OP RDE and for the support of the University Internal Grant Agency (IGA) of the Faculty of Forestry and Wood Sciences (Project No. 43 230 / 1312 / 3168).

REFERENCE CITED

Ayarkwa, J., Hirashima, Y., and Sasaki, Y. (2000). "Effect of finger geometry and end pressure on the flexural properties of finger-jointed tropical African hardwoods," *Forest Prod. J.* 50(11-12), 53-63.

Bustos, C., Beauregard, R., Mohammad, M., and Hernández, R. E. (2003). "Structural performance of finger-jointed black spruce lumber with different joint configurations," *Forest Prod. J.* 53(9), 72-76.

Bustos, C., Hernández, H., Beauregard, R. E., and Mohammad, M. (2011). "Effect of end-pressure on the finger-joint quality of black spruce lumber: A microscopic analysis," *Maderas-Cienc. Tecnol.* 13(3), 319-328. DOI: 10.4067/S0718-221X2011000300007

Chen, G.-F., and Walworth, G. (2001). "Two-part polyurethane adhesive for structural finger joints," U. S. Patent No. 7655312B2.

Crocetti, R., Johansson, M., Johnsson, H., Kliger, R., Mårtensson, A., Norlin, B., Pousette, A., and Thelandersson, S. (2011). *Design of Timber Structures*, Swedish Wood, Malmö, Sweden.

ČSN EN 942 (2007). "Timber in joinery – General requirements," Czech Office for Standards, Metrology and Testing, Prague, Czech Republic.

ČSN 49 0108 (1993). "Wood – Density detection," Czech Office for Standards, Metrology and Testing, Prague, Czech Republic.

ČSN 49 0103 (1979). "Wood – Moisture detection in physical and mechanical tests," Czech Office for Standards, Metrology and Testing, Prague, Czech Republic.

Eckelman, C. A. (2003). *Textbook of Product Engineering and Strength Design of Furniture*, Purdue University, West Lafayette, Indiana.

Eckelman, C. A., and Lin, F. C. (1997). "Bending strength of corner joints constructed with injection-molded splines," *Forest Prod. J.* 47(4), 89-92.

Franke, B., Schusser, A., and Müller, A. (2014). "Analysis of finger joints from beech wood," in: *World Conference on Timber Engineering*, Quebec, Canada.

Hemmasi, A. H., Khademi-Eslam, H., Roohnia, M., Bazyar, B., and Yavari, A. (2014). "Elastic properties of oak wood finger joints with polyvinyl acetate and isocyanate adhesives," *BioResources* 9(1), 849-860. DOI: 10.15376/biores.9.1.849-860

Hernández, R. E., Coman, R., and Beauregard, R. (2011). "Influence of machining parameters on the tensile strength of finger-jointed high-density black spruce lumber," *Wood Sci. Technol.* 43(1), 2-10.

ISO 13061-1 (2014). "Physical and mechanical properties of wood – Test method for small clear wood specimens – Part 1: Determination of moisture content for physical and mechanical tests," International Organization for Standardization, Geneva, Switzerland.

Joščák, P., Langová, N., and Krasula, P. (2015). *Mechanické Skúšky Nábytku* [*Mechanical Tests of Furniture*], Technical University in Zvolen, Zvolen, Slovakia.

Lange, D. A., Fields, J. T., and Stirn, S. A. (2001). "Finger joint application potentials for one-part polyurethanes," in: *Proceedings of the Wood Adhesives 2000 Symposium*, Madison, WI, pp. 17-18.

Murphey, W. K., and Rishel, L. E. (1972). "Finger joint feasibility in furniture production," *Forest Prod. J.* 22(2), 30-32.

Örs, Y., Atar, M., and Keskin, H. (2004). "Bonding strength of adhesive in wood materials impregnated with Imersol-Aqua," *Int. J. Adhes. Adhes.* 24(4), 287-294. DOI: 10.1016/j.ijadhadh.2003.10.007

Özçifçi, A., and Yapıcı, F. (2008). "Structural performance of the finger-jointed strength of some wood species with different joint configurations," *Constr. Build. Mater.* 22(7), 1543-1550. DOI: 10.1016/j.conbuildmat.2007.03.020

Podlena, M., and Borůvka, V. (2016). "Stiffness coefficients of mortise and tenon joints used on wooden window profile," *BioResources* 11(2), 4677-4687. DOI: 10.15376/biores.11.2.4677-4687

River, B. (1994). "Fracture of adhesive-bonded wood joints," in: *Handbook of Adhesive Technology, Revised and Expanded*, A. Pizzi and K. L. Mittal (eds.), CRC Press, Boca Raton, FL, pp. 325-350.

Selbo, M. L. (1963). "Effect of joint geometry on tensile strength of finger joints," *Forest Prod. J.* 13(9), 390-400.

Smardzewski, J., and Prekrad, S. (2002). "Stress distribution in disconnected furniture joints," *Electronic Journal of Polish Agricultural University* 5(2), 1-7. ISSN: 1505-0297

Verreault, C. (1999). *Performance Evaluation of Green Gluing for Finger Jointing* (Report No. 2295), Forintek Canada Corporation, Quebec, Canada.

Záborský, V., Sikora, A., Gaff, M., Kašíčková, V., and Borůvka, V. (2018). "Effect of selected factors on stiffness of dowel joints," *BioResources* 13(3), 5416-5431. DOI: 10.15376/biores.13.3.5416-5431

Article submitted: October 9, 2018; Peer review completed: January 13, 2019; Revised version received: January 29, 2019; Accepted: February 5, 2019; Published: February 25, 2019.
DOI: 10.15376/biores.14.2.2946-2960

4.1.2 Effect of Selected Factors on Spruce Dowel Joint Stiffness

Published as:

Záborský V, Kamboj G, Sikora A, Borůvka V. Effects of selected factors on Spruce dowel joint stiffness. BioResources. 2019;14(1):1127-40.

Effects of Selected Factors on Spruce Dowel Joint Stiffness

Vladimír Záborský, Gourav Kamboj, Adam Sikora,* and Vlastimil Borůvka

Joints are used to join furniture parts, and they represent a critical part of the structure of furniture. The quality of joints is greatly affected by the accuracy of their execution. When designing furniture, it is important to carefully consider the type of joint used so that it can hold all the joined elements together. Under loading of the joined structures, internal forces develop, which can lead to failure of the joints. This study investigated the elastic stiffness of spruce (*Picea abies* L.) dowel joints. The effects of selected factors such as the type of loading (compressive *versus* tensile), the size of the dowels (one-half *versus* one-third of the thickness of the joined elements), the type of adhesive used (polyvinyl acetate *versus* polyurethane), and annual ring deflection were examined. Spruce dowel joints exhibited the highest elastic stiffness values with a higher-diameter dowel glued with PUR adhesives and subjected to compressive loading. The impact of annual rings was not a significant factor. Finally, the reference type joints were compared with other commonly used types, such as three types of mortise and tenon joints (simple, haunched, and dovetail).

Keywords: Furniture joints; Spruce dowel joints; Elastic stiffness

Contact information: Department of Wood Processing and Biomaterials, Czech University of Life Sciences in Prague, Kamýcká 1176, Prague 6 - Suchdol, 165 21 Czech Republic;
**Corresponding author: sikoraa@fld.czu.cz*

INTRODUCTION

The joints are the most important parts of wooden structures. These elements significantly affect the overall behavior of the structure of the joined components. Joints provide continuity to the member and strength and stability to the structure. Proper joint design is important so that joints can carry a load safely in service conditions without excessive deformation or failure (Eckelman *et al.* 2003). The mechanical strength of a piece of furniture depends mostly on the strength of its joints. One of the main advantages of using wood as a structural material is that each structural element can easily be connected with a wide range of fasteners, and the joints may entirely consist of wooden members (Gaff and Babiak 2017).

The dowel joint is used often in the furniture industry. In this type of joint, a short wooden rod is inserted into a wooden drill hole for the proper connection. In historical timber structures, traditional carpentry joints were used, while wooden dowels fixed the mutual position of the elements. Dowels are often used as primary connectors in furniture frames constructed of both solid wood and wood-based composites (Fukuyama *et al.* 2007). However, because wood is hygroscopic, it is common to see the wood dowel become unfastened in the furniture joint. Drilling dowels uses less energy than milling. Less waste is created, simplifying the production process and making it faster, as the necessary profile and holes for the dowels are formed by one machine. This increases

manufacturing productivity and reduces production costs.

The dowel joints have some advantageous aspects that may compensate for their lower strength. Due to their profile and hole formed by one machine, their production is fast and simple, which increases productivity and reduces production costs. (Efe *et al.* 2005; Hrovatin *et al.* 2013; İmirzi *et al.* 2015). The strength of these joints is somewhat limited relative to the strength of the joint member, so unless they are properly designed, they may be the weakest part of the furniture frame. In a furniture frame, dowel joints may be subjected to axial, shear, tensional, and bending forces (Pizzi *et al.* 2004). The knowledge of the mechanical behavior of these dowel-type connections (the loading distribution, ultimate strength, and failure modes) is important for their intelligent application. The complex behavior is governed by several geometric, material, and load parameters (*e.g.*, wood species, dowel diameter, end and edge distance, space between connectors, clearance, friction, and load configuration) (Vaziri *et al.* 2010). Some techniques have been developed to assess the relationship between the parameters and the mechanical behavior of the connectors and joints in different timber structures (Albin 1989; Eckelman 1989; Eckelmann and Rabiej 1985; Loferski and Gamalath 1989; Ozcifci 1995; Kanazawa *et al.* 2005; Martins *et al.* 2013). Generally, the size of the bending moment and the stiffness of the dowel joints is affected by the dowel spacing, diameter, and the depth of the dowel (Warmbier and Wilczynski 2000). Zhang (1991) stated that the optimal diameter was 8 mm, the optimal depth of dowel embedment in a face member was 16 mm, and the optimal depth of dowel embedment in the edge member of the corner joints was 25.4 mm. Joint stiffness increases when a greater number of dowels is used. Adhesive bonding technology has played an essential role in the development and growth of conservation and the repair of timber structures (Gaff *et al.* 2016). Better joint stiffness is achieved with a thicker joint, but this property is influenced by other factors, particularly the type of adhesive used. Tankut (2007) emphasized the importance of the choosing the right type of adhesive.

The aim of this study was to determine the elastic stiffness of spruce dowel joints under the influence of the selected factors of dowel size (diameters of 8 mm and 12 mm), adhesive used (PVAc and PUR), type of loading (tensile and compressive force in angular plane), and annual ring deflection. The use of the joints was compared with that of the traditional constructional joint.

EXPERIMENTAL

Materials

Spruce wood (*Picea abies* L.) was used in the experiment to make the corner dowel joint (Polana, Slovakia). A diagram of the tested joints is shown in Fig. 1. The cutting was performed at a moisture content of 10%, relative humidity of 55%, and a temperature of 20 °C. According to EN 942 (2007), ČSN 91 0001 (2007), and ČSN 91 0000 (2005), the moisture content corresponds to the equilibrium moisture content of the furniture components intended for indoor environments. The specimens for mechanical testing were made from dried lumber using woodworking machines at a vocational school in Spišská Nová Ves (Slovakia). To connect the joint elements, spruce dowels with a diameter of 8 mm and 12 mm and a length of 50 mm were used.

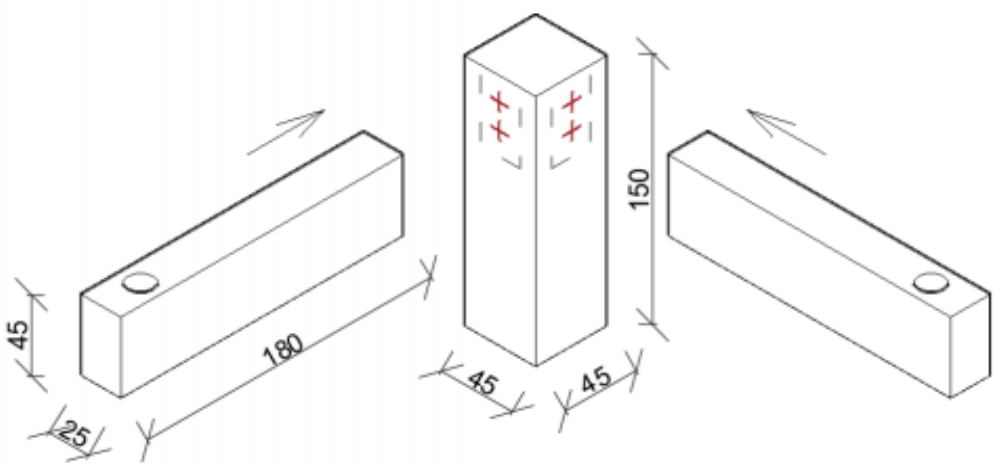

Fig. 1. Structure and dimension of the tested dowel joint

Using 8 mm and 12 mm drill bits, holes were drilled according to the dowel sizes and rails. Joints with 8 mm dowels corresponded to a joint thickness that was 1/3 the thickness of the rail, and 12 mm dowels corresponded with a joint 1/2 the thickness of the rail. The location of the dowels and their dimensions are shown in Fig. 2.

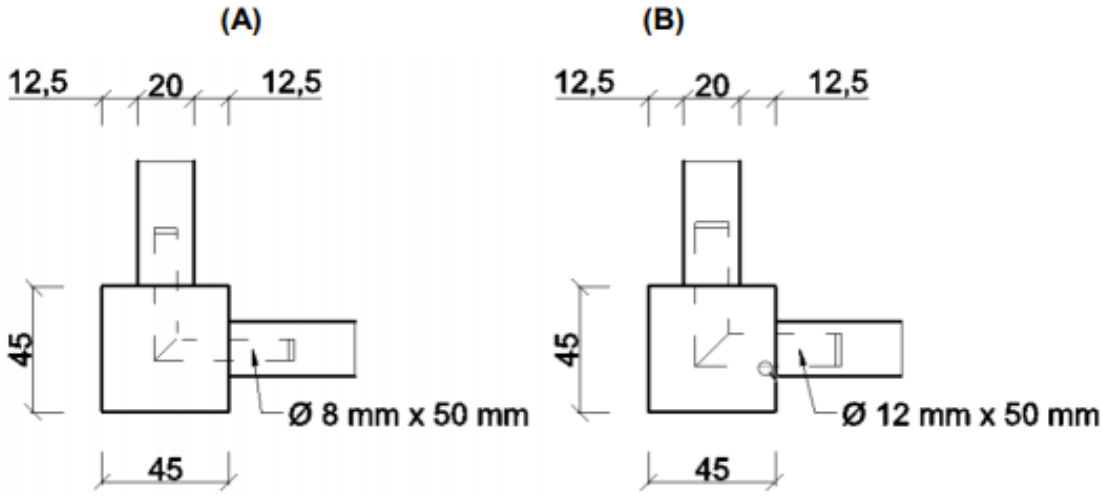

Fig. 2. Geometries of (A) dowel with 8 mm diameter; (B) dowel with 12 mm diameter

Two types of adhesives were used in the joining elements: a single-component, waterproof polyvinyl acetate adhesive (PVAc) AG-COLL (EOC, Oudenaarde, Belgium) 8761/L D3 (EOC, Oudenaarde, Belgium) and a single-component polyurethane adhesive (PUR) NEOPUR 2238R (NEOFLEX, Madrid, Spain). Detailed parameters of these adhesives are shown in Table 1. The adhesives were applied manually to the holes in a single-sided coating of 150 g/m^2 to 180 g/m^2 for PVAc, and 180 g/m^2 to 250 g/m^2 for the PUR adhesive. The test specimens were cold-pressed in manual clamps. After the pressing, the samples were conditioned in a climatic chamber at 20 °C and at a relative humidity of 55%.

Table 1. Parameters of the PVAc and PUR Adhesives

Technical Data for Adhesive	AG-COLL 8761/L D3	NEOPUR 2238R
Viscosity (mPa)	5000 to 7000 at 23 °C	2000 to 4500 at 25 °C
Working time (min)	15 to 20	60
Density (g/cm3)	0.9 to 1.1 at 23 °C	ca. 1.13
NCO content (%)	-	*ca.* 15.5 to 16.5
Color	White, milky	Brown
Open time (min)	15	*ca.* 20 to 25
Dry matter content (g)	49 to 51	100
pH	to 4.5	-

The effects of the annual rings with angles of 45°, 45° to 90°, and 90° were investigated, as shown in Fig. 3. The effect of annual ring deflection was evaluated separately from other monitored factors.

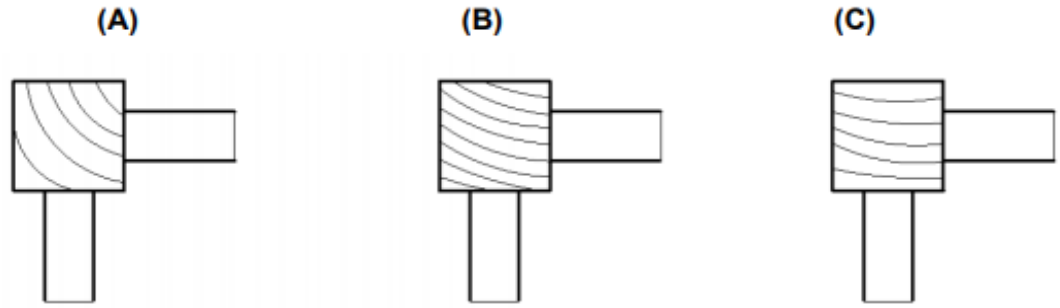

Fig. 3. Schematic of annual ring deflection: (A) 45°; (B) 45 to 90°; (C) 90° (Záborský *et al.* 2018)

A total of 80 joint specimens representing two types of dowel joints were constructed of spruce wood (*Picea abies* L.). The monitored factors affected the elastic stiffness of joints were joint thickness (1/2 and 1/3), type of loading (compressive and tension) and type of adhesive (PUR and PVAc). For each monitored factor, 10 samples were created in each test group. Figure 4 shows the classification of the tested joints.

Methods

All joint samples were conditioned and kept at approximately 12% moisture content before and during the testing time. These calculations were performed according to ISO 13061-1 (2014). The density of the specimens was evaluated per the ISO 13061-2 (2014) standard. The specimens were obtained in oven-dry state according to ISO 13061-1 (2014).

A universal testing machine TIRA 50 (TIRA System GmbH, Schalkau, Germany) for compressive and tensile loads was used to measure the elastic stiffness of the corner joint. This study used the same type of steel clamp that was used in the work of Podlena and Borůvka (2016). Figure 5b shows the experimental testing of the corner joint and its mounting on the device. Figure 5a shows that the testing samples were loaded by the bending moment with the tensile and compressive forces applied in an angular plane.

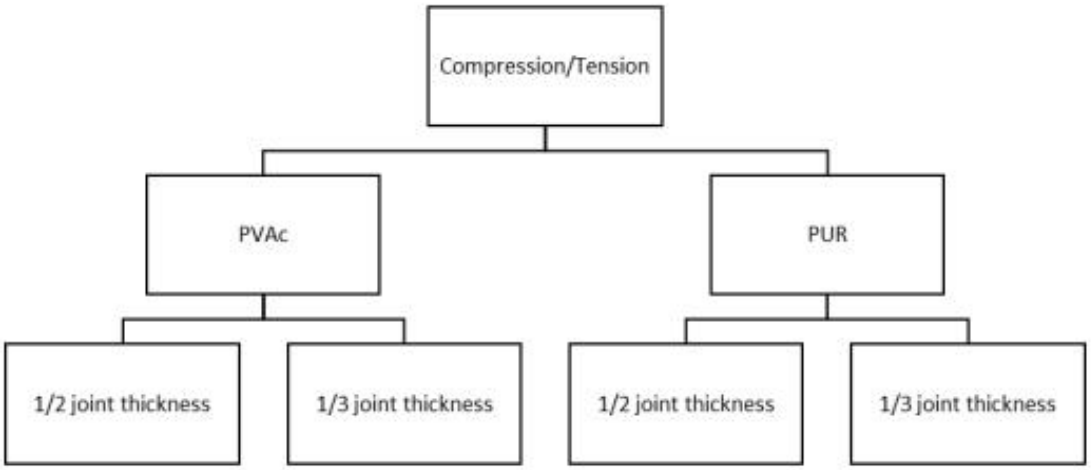

Fig. 4. Classification of the tested half and one third thickness joints

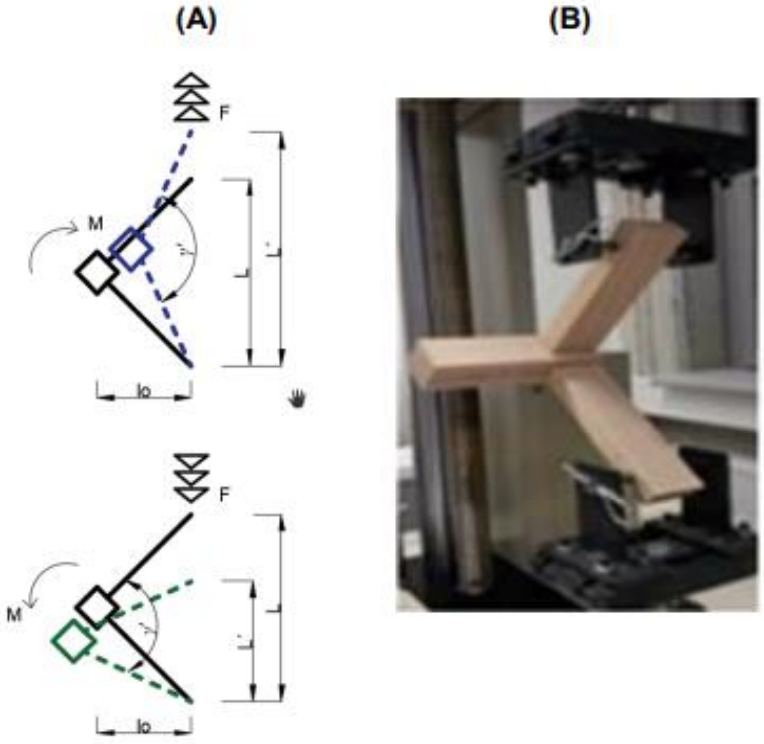

Fig. 5. (A) Diagram showing the bending moment of tension a compressive load; (B) test sample attached to the test device

The change in the distance between the dowels of the device was recorded (L → L′) and used to calculate the angle arc-sin function γ′ (Záborský *et al.* 2018, Warmbier and Wilczynski 2000). Equation 1 was used to calculate the angular displacement $\Delta\gamma$.

$$\Delta\gamma = 90 \pm \gamma' \quad (1)$$

Table 2. Basic Statistical Analysis of Density and Elastic Stiffness of Wood Joints

Type of Loading	Thickness of Joints	Type of Glue	Density (g/cm^3)			Elastic Stiffness (Nm/rad)		
			Mean	Standard Deviation	Coefficient of Variation (%)	Mean	Standard Deviation	Coefficient of Variation (%)
Compressive	Third	PVAc	0.393	0.019	4.8	270	104	38.5
Compressive	Half	PVAc	0.405	0.019	4.8	444	98	22.1
Compressive	Third	PUR	0.403	0.011	2.7	633	156	24.7
Compressive	Half	PUR	0.418	0.028	6.8	921	257	27.9
Tension	Third	PVAc	0.411	0.018	4.3	209	53	25.4
Tension	Half	PVAc	0.409	0.023	5.6	309	79	25.5
Tension	Third	PUR	0.407	0.028	6.9	545	298	54.6
Tension	Half	PUR	0.422	0.022	5.2	779	195	25.0

Equation 2 was used to calculate the change in torque ΔM,

$$\Delta M = \Delta F \times l_0 \quad (2)$$

where ΔF represents the difference between the two forces (N) that was recorded in the stress-strain diagrams at 10% to 40% of the maximum joint strength, and l_0 represents the vertical arm (mm) of the tested joint in the direction of loading force.

The elastic stiffness, c_{elast} (Nm/rad), was calculated according to Eq. 3 as the ratio of the change in torque to the angular displacement in radians.

$$c_{elast} = \frac{\Delta M}{\Delta \gamma} \quad (3)$$

RESULTS AND DISCUSSION

Table 2 shows a statistical analysis of the density and elastic stiffness of spruce wood joints. For spruce specimens, the average density was 0.408 g/cm^3, and the average elastic stiffness was 514 Nm/rad, which is lower than that of the beech dowel joint at 940 Nm/rad (Záborský *et al.* 2018). A relatively large variation coefficient, as was observed, that can be explained by undetected defects in the wood structure. The maximum elastic stiffness was reached in samples with a half-thickness joint bonded with PUR adhesive under compressive loading (Table 2), which is nearly the same result as that obtained by Jivkov (2002) for 25 mm particle board with a half-dowel thickness joint under compressive loading (Derikvand and Ebrahimi 2015). The thickness of the joints also had an important impact on the stiffness of the joint; the stiffness of the joint increased as the diameter of the dowel increased (Záborský *et al.* 2016).

Table 3 presents the results of the four-factor ANOVA test that evaluated the effect of individual factors and their interaction on the elastic stiffness of the joints. It was clear from the significance level *p*-value that the thickness of the joints and type of glue were statistically significant factors for the one-factor analysis.

The effect of the loading type in itself was not shown to be statistically significant, and in interaction with all the other factors its effect was insignificant according to the significance level *p*-value.

The elastic stiffness was affected by the type of loading, thickness of samples (half *versus* one-third joints), and type of adhesive (PVAc or PUR). The samples were tested under a compressive test, which showed 23% greater elastic stiffness (Fig. 6a) than the tensile loading test. As shown in Fig. 6b, the half-thickness joints exhibited approximately 32% higher elastic stiffness than the one-third thickness joints, whereas in the results for the beech wood, the half-thickness dowel joints had 66.6% higher elastic stiffness compared to the joints with one-third thickness (Záborský *et al.* 2018). For adhesive type (Fig. 6c), the elastic stiffness of joints bonded with PUR adhesive and tested with both types of loading (compressive and tensile) and both types of joints (half thickness and one third thickness) was 133% higher than that of joints bonded with PVAc adhesive. Figure 6d shows that the elastic stiffness was affected by the growth ring direction, and higher stiffness was achieved with intermediate annual rings, but we can see that there wasn't statistical significant difference.

Table 3. Multifactor Analysis of Variance for Elastic Stiffness of Wood Joints

Monitored Factor	Sum of Squares	Degree of Freedom	Variance	Fisher´s F-test	Significance Level[1]
Intercept	16532352	1	16532352	530.6927	P < 0.01
1 - Type of loading	172499	1	172499	5.5373	P = 0.02
2 - Thickness joint	553622	1	553622	17.7714	P < 0.01
3 - Type of glue	2594288	1	2594288	83.2773	P < 0.01
4 - Deflection of annual rings	73993	2	36997	1.1876	P = 0.31
1*2	20540	1	20540	0.6593	P = 0.42
1*3	9887	1	9887	0.3174	P = 0.58
2*3	69165	1	69165	2.2202	P = 0.14
1*4	143364	2	71682	2.3010	P = 0.11
2*4	75935	2	37967	1.2188	P = 0.30
3*4	210364	2	105182	3.3764	P = 0.04
1*2*3	9976	1	9976	0.3202	P = 0.57
1*2*4	48363	2	24181	0.7762	P = 0.47
1*3*4	54913	2	27456	0.8814	P = 0.42
2*3*4	44888	2	22444	0.7205	P = 0.49
1*2*3*4	31018	2	15509	0.4978	P = 0.61
Error	1744534	56	31152		

[1] Significance was accepted at P < 0.01

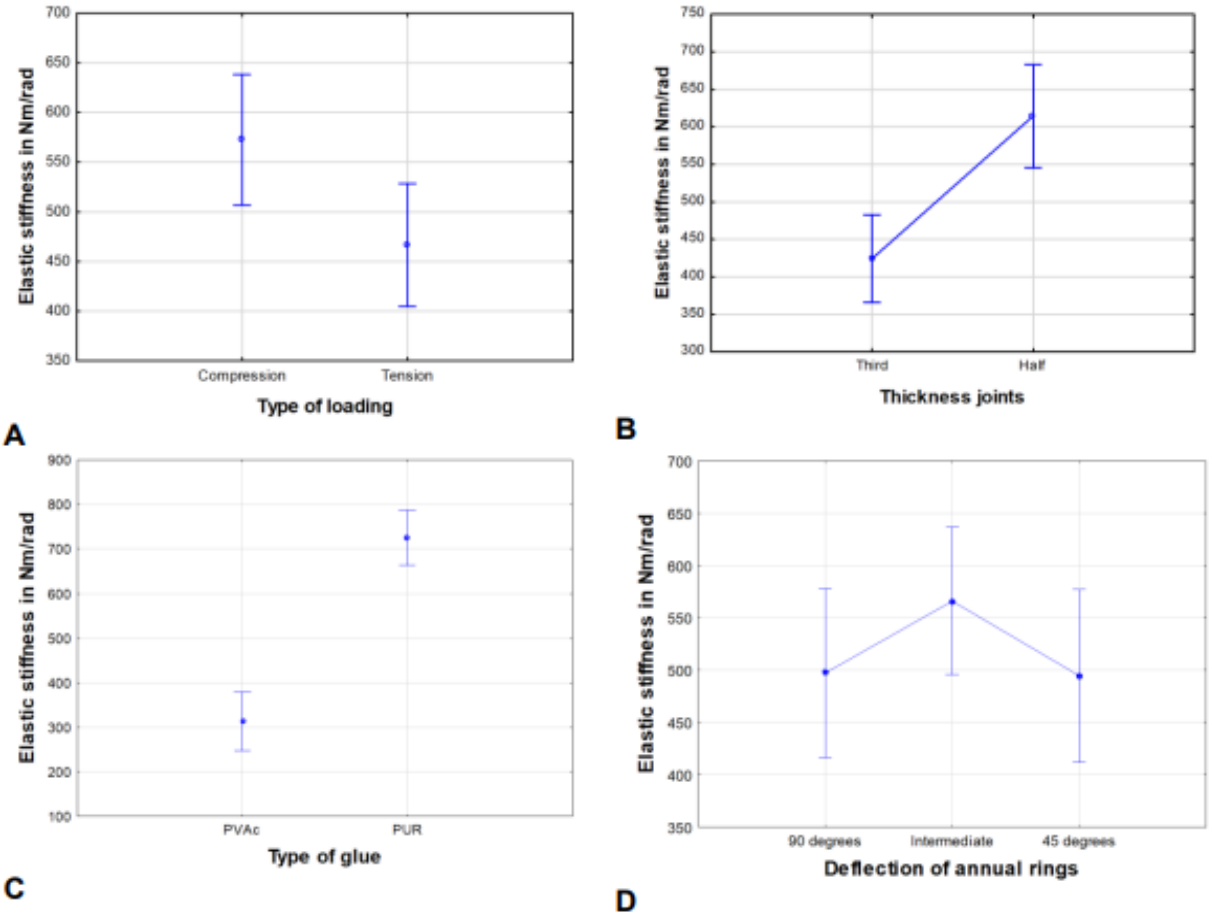

Fig. 6. Graphic visualization of the (A) type of loading; (B) joint thickness; (C) type of glue; and (D) deflection of annual ring on elastic stiffness on mean values of elastic stiffness

Figure 7a shows that with the compressive loading test, the half-thickness joints had approximately 51% higher elastic stiffness than the one-third thickness joints. The effect of the half-thickness joints showed higher elastic stiffness under both types of loading. The elastic stiffness of the joints bonded with PUR and PVAc adhesive (Fig. 7b) was lower under tensile loading as compared to compressive loading. The elastic stiffness of the PVAc adhesive under compressive loading was 38% higher than that under tensile loading, and in the case of PUR adhesive, the elastic stiffness under compressive loading reached a 17% higher value compared with tensile loading. Therefore, the elastic stiffness of joints (half joints and one-third thickness joints) bonded with PVAc and PUR adhesive was higher under compressive loading than under tensile loading.

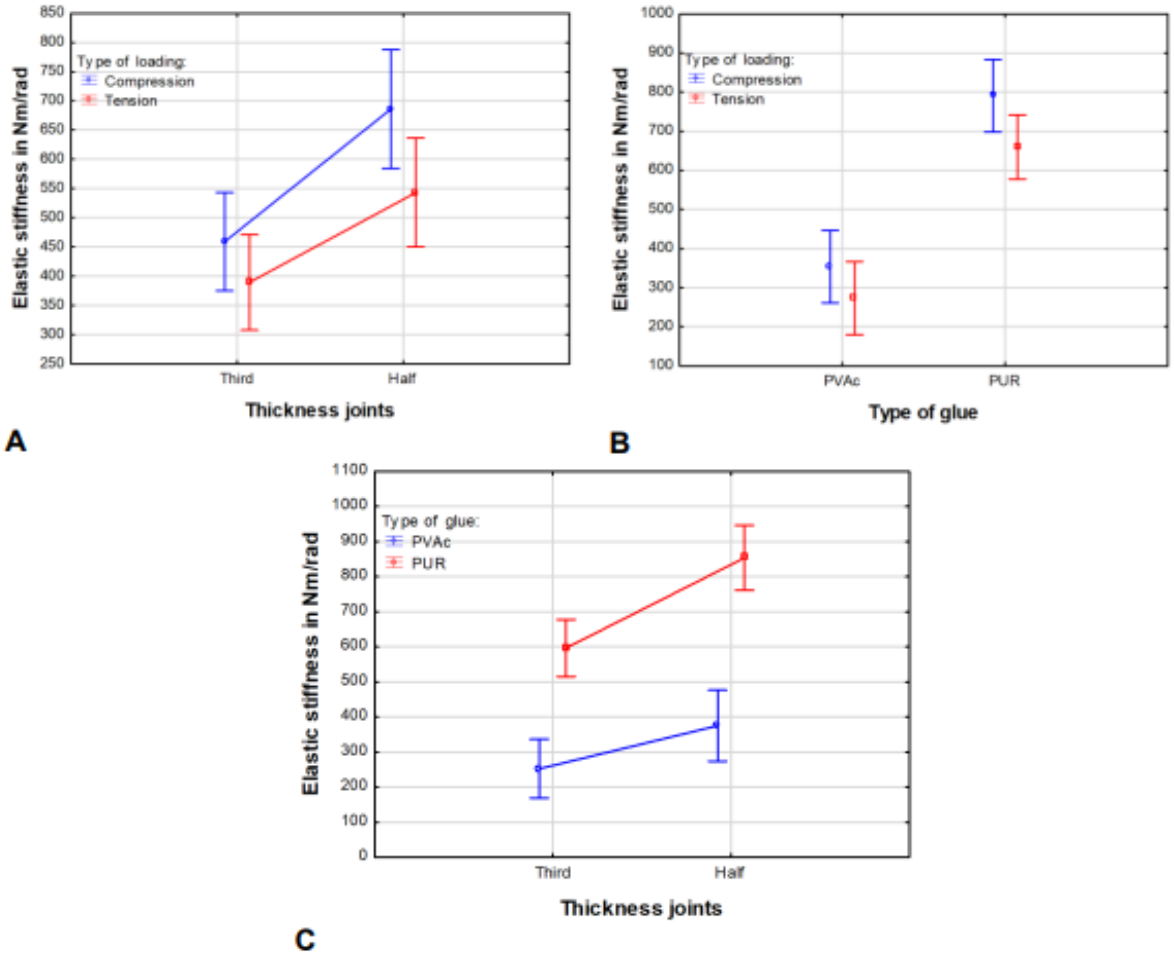

Fig. 7. The effect of (A) joint thickness and type of loading; (B) type of glue and type of loading; (C) joint thickness and type of glue on mean values of elastic stiffness

Figure 7c shows the interaction of the elastic stiffness of joints bonded with PVAc and PUR adhesives with one third and half joint thickness. The elastic stiffness of the one-third joints bonded with PVAc was 46% lower than the PUR adhesive with the one third joint. The elastic stiffness of the half joints with PUR adhesive was 126% higher compared to the joint bonded with PVAc, and similar results were found with tenon joints (Gaff *et al*. 2018). Thus, in both cases (the half joint and one third thickness joints), the PUR

adhesive showed higher values of elastic stiffness compared with the PVAc adhesive.

The elastic stiffness of joints bonded with PVAc (half and one-third thickness joint) under compressive loading (Fig. 8) was 38% higher compared to those under tensile loading, while with PUR adhesive the elastic stiffness was 17% higher for compressive loading. The elastic stiffness of the one-third thickness joints bonded with PUR adhesive under compressive loading was approximately 134% higher compared to that of PVAc, and under tensile loading it was 273% higher. In the case of the half thickness joints bonded with PUR under compressive loading, it was 107% higher compared to PVAc, and with tensile loading that with PUR was 152% higher compared to PVAc. The elastic stiffness of the PUR adhesive bonded with half and one-third thickness joints under both types of loading (compressive and tensile) was 134% higher compared to that for PVAc.

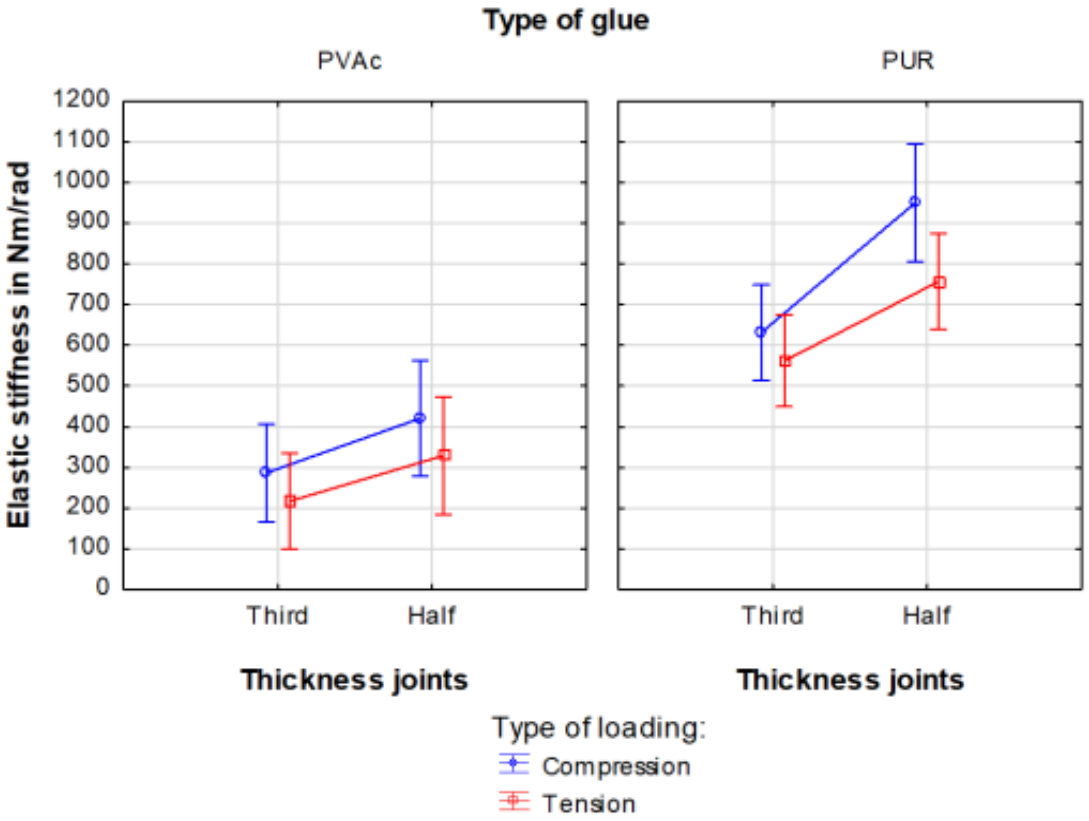

Fig. 8. Synergistic effect of the type of glue, joint thickness, and type of loading on the mean values elastic stiffness

Figure 9 shows correlation between the elastic stiffness and density of wood (r = 0.21), which indicates that the elastic stiffness of dowel joints can be poorly predicted based on the density of wood.

Figure 10 shows that there was a linear dependence between the elastic stiffness and the stiffness at the maximum load. This dependence is expressed by the correlation coefficient r = 0.84, which means that the maximum stiffness of the joint can be predicted based on the elastic stiffness.

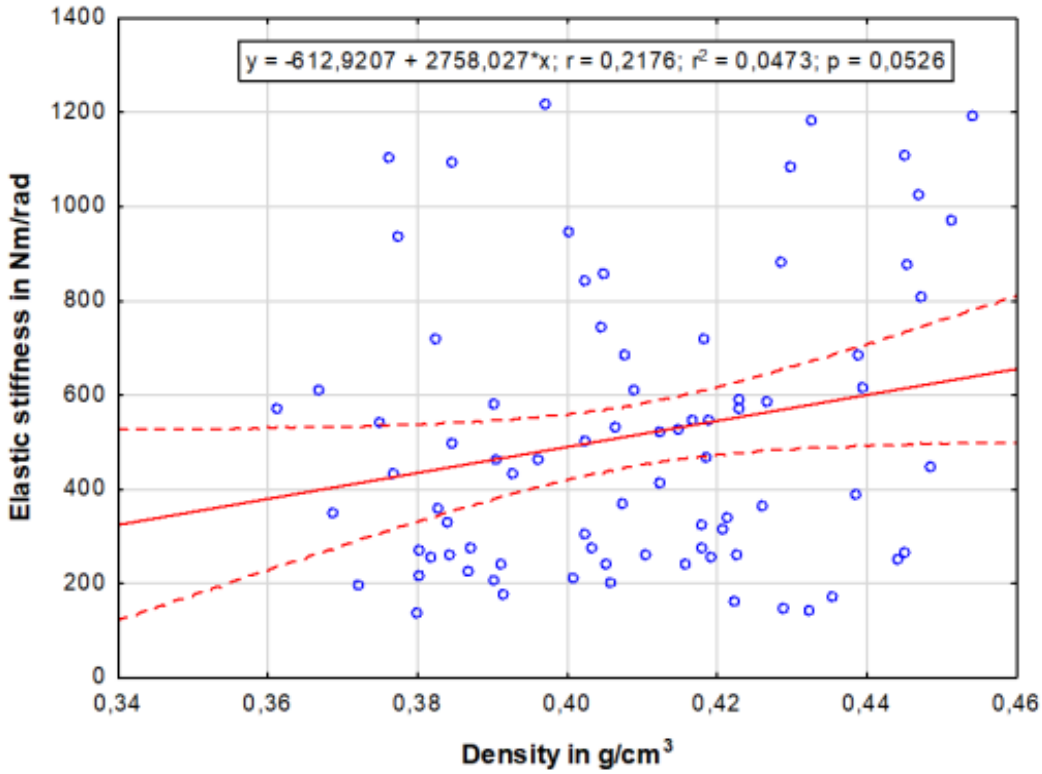

Fig. 9. Dependence of elastic stiffness on density for wood joints

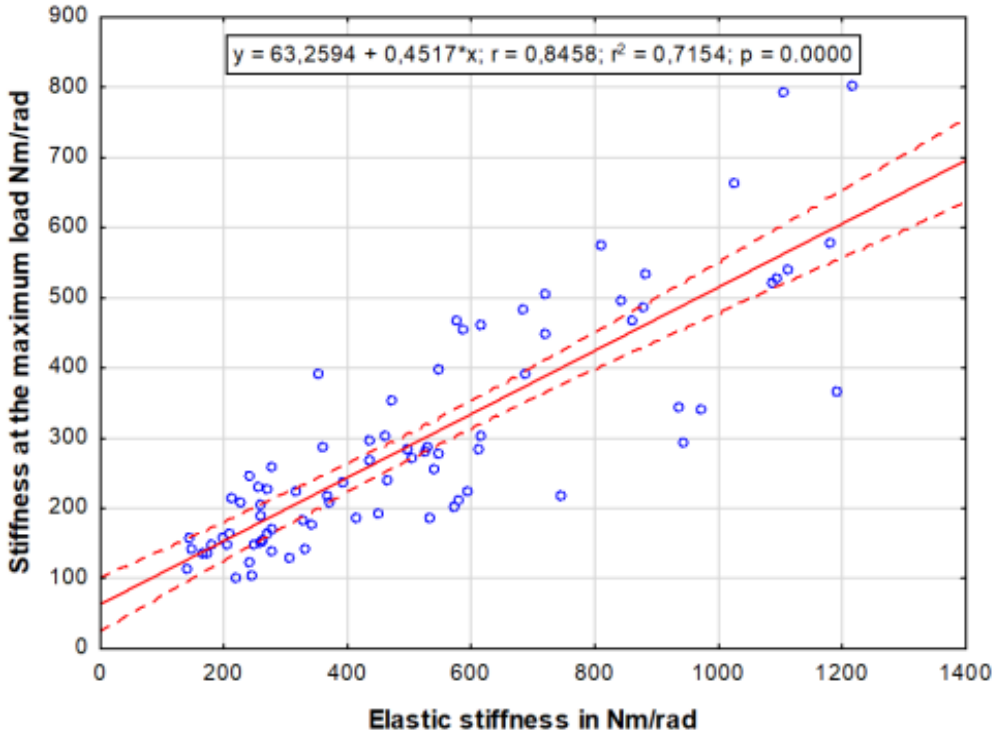

Fig. 10. Dependence of stiffness at the maximum load on elastic stiffness in wood joints

CONCLUSIONS

1. Spruce dowel joints had higher elastic stiffness with PUR adhesive than PVAc, with respect to compressive and tensile loading, with half and one-third joint thickness. The test results revealed that half thickness joints had a higher elastic stiffness than one-third thickness joints.
2. In spite of this result, there were significant differences between the average elastic stiffness of joints glued with PVAc and those glued with PUR; the average elastic stiffness for PUR was approximately twice that of the average value for PVAc.
3. The maximum average elastic stiffness was obtained for half-thickness joints bonded with PUR adhesive under compressive loading, which was 921 Nm/rad, and the minimum average value of elastic stiffness, 209 Nm/rad, was reached in samples with one third thickness joints bonded with PVAc adhesive under tensile loading.
4. Although elastic stiffness varies from joint to joint, the size of the dowel should be standardized. Future studies will have to investigate the elastic stiffness of different species of dowel with different loads (compressive and tensile) and different adhesives.

ACKNOWLEDGMENTS

The authors are grateful for the support of project Advanced Research Supporting the Forestry and Wood-processing Sector's Adaptation to Global Change and the 4th Industrial Revolution, No. CZ.02.1.01/0.0/0.0/16_019/0000803, financed by OP RDE. The authors are also grateful for the support of the University-wide Internal Grant Agency (CIGA) of the Faculty of Forestry and Wood Sciences, project No. 2016 - 4311.

REFERENCES CITED

Albin, R. (1989). "Durchbiegung und Lastannahmen im Korpusmöbelbau," *Holz als Roh- und Werkstoff* 47, 7-10. DOI: 10.1007/BF02612342

ČSN 91 0001 (2007). "Furniture – Technical requirement," Czech Office for Standards: Metrology and Testing, Prague, Czech Republic.

ČSN 91 0000 (2005). "Furniture – Nomenclature," Czech Technical Standard, Prague, Czech Republic.

Derikvand, M., and Ebrahimi, G. (2015). "Rotational stiffness of L-shaped joints," in: *The XXVIITH International Conference Research for Furniture Industry*, Karaj, Iran, pp 19-26.

Eckelman, C. A. (1989) "Strength of furniture joints constructed through-bolts and dowel-nuts," *Forest Products Journal* 39, 41-48.

Eckelman, C.A., Rabiej, R. (1985). "A comprehensive method of analyze of case furniture," *Forest Product Journal* 35, 41-48.

Eckelman, C. A., Zhang, J., and Erdil, Y. Z. (2003). "Withdrawal and bending strength of dowel-nuts in plywood and oriented strand board," *Forest Products Journal* 53(6), 54-57.

Efe, H., Zhang, J., Erdil, Y. Z., and Kasal, A. (2005). "Moment capacity of traditional

and alternative T-type end-to-side-grain furniture joints," *Forest Products Journal* 55(5), 69-73.

EN 942 (2007). "Timber in joinery - General requirements," European Committee for Standardization, Brussels, Belgium.

Fukuyama, H., Ando, N., Inayama, M., Takemura, M., and Inoue, M. (2007). "Proposal of analytical model of wooden dowel shear joint: Single shear joint with slender-type round dowel," *Journal of Structural and Construction Engineering* 72(622), 129-136, DOI: 10.3130/aijs.72.129_4

Gaff, M., and Babiak, M. (2017). "Methods for determining the plastic work in bending and impact of selected factors on its value," *Composite Structures* 163(1), 410-422. DOI: 10.1016/j.compstruct.2017.11.036

Gaff, M., Vokatý, V., Babiak, M., and Bal, B. (2016). "Coefficient of wood bendability as a function of selected factors," *Construction and Building Materials* 126, 632-640. DOI: 10.1016/j.conbuildmat.2016.09.085

Gaff, M., Záborský, V., Kasickova, V., and Borůvka, V. (2018). "The effect of selected factors on domino joint stiffness," *BioResources* 13, 2424-2439. DOI: 10.15376/biores.13.2.2424-2439

Hrovatin, J., Zupančič, A., Sernek, M., and Oblak, L. (2013). "The fracture moment of corner joint bonded by different glues," *Drvna Industrija* 64(4), 335-340. DOI: 10.5552/drind.2013.1248

İmirzi, H. Ö., Smardzewski, J., and Dongel, N. (2015). "Method for substitute modulus determination of furniture frame construction joints," *Turkish Journal of Agriculture and Forestry* 39(5), 775-785. DOI: 10.3906/tar-1406-92

ISO 13061-1 (2014). "Physical and mechanical properties of wood—Test methods for small clear wood samples—Part 1: Determination of moisture content for physical and mechanical tests," International Organization for Standardization, Geneva, Switzerland.

ISO 13061-2 (2014). "Physical and mechanical properties of wood—Test methods for small clear wood samples—Part 2: Determination of density for physical and mechanical tests," International Organization for Standardization, Geneva, Switzerland.

Jivkov, V. (2002). "Bending strength and stiffness of some end corner joints from 25 mm laminated particleboard," in: *Nabytok Conference*, Slovakia, Zvolen, ISBN 80-228-1193-9.

Kanazawa, F., Pizzi, A. P., Properzi, M., Delmotte, L., and Pichelin, F. (2005) "Parameters influencing wood-dowel welding by high-speed rotation," *Journal of Adhesion Science and Technology* 19(12), 1025-1038. DOI: 10.1163/156856105774382444

Loferski, J. R., and Gamalath, S. (1989). "Predicting rotational stiffness and nail joints," *Forest Product Journal* 39(7-8), 8-16. ISSN: 0015-7473

Martins, S. A., Menezzi, C. H. S. D., Ferraz, J. M., and Souza, M. R. (2013). "Bonding behavior of *Eucalyptus benthamii* wood to manufacture edge glued panels," *Maderas. Ciencia y Tecnología* 15, 79-92. DOI: 10.4067/S0718-221X2013005000008

Ozcifci, A. (1995). *A Study about Resistance Features to Corner Points of Furniture made by Particleboard*, M.Sc. Thesis, Gazi University, Institute of Science and Technology, Ankara, Turkey.

Pizzi, A. P., Leban, J. M., Kanazawa, F., Properzi, M., and Pichelin, F. (2004). "Wood dowel bonding by high-speed rotation welding," *Journal of Adhesion Science and*

Technology 18(11), 1263-1278. DOI: 10.1163/1568561041588192

Podlena, M., and Borůvka, V. (2016). "Stiffness coefficients of mortise and tenon joints used on wood window profile," *BioResources* 11(2), 4647-4687. DOI: 10.15376/biores.11.2.4677-4687

Tankut, N. (2007). "The effect of glue and glueline thickness on strength of mortise and tenon joints," *Wood Research* 54(4), 69-78.

Vaziri, M., Lindgren, O., Pizzi, A. P., and Mansouri, H. R. (2010). "Moisture sensitivity of Scots pine joints produced by linear frictional welding," *Journal of Adhesion Science and Technology* 24(8-10), 1515-1527. DOI: 10.1163/016942410X501098

Warmbier, K., and Wilczynski, A. (2000). "Strength and stiffness of dowel corner joints: Effect of joint dimension," *Folia Forestalia Polonica* 31, 29-4. ISSN 0208-5704

Záborský, V., Borůvka, V., Ruman, D., and Gaff, M. (2016). "Effect of geometric parameters of structural elements on joint stiffness," *BioResources* 12, 932-946. DOI: .10.15376/biores.12.1.932-946

Záborský, V., Sikora, A., Gaff, M., Kasickova, V., and Borůvka, V. (2018) "Effect of selected factors on stiffness of dowel joint," *BioResources* 13(3), 5416-5431. DOI: 10.15376/biores.13.3.5416-5431

Zhang, J. L. (1991). *Rational Design of Dowel Joint in Case Construction*, Master's Thesis, Purdue University, West Lafayette, IN, USA.

Article submitted: September 11, 2018; Peer review completed: October 28, 2018; Revised version received: November 13, 2018; Accepted: November 22, 2018; Published: December 14, 2018.
DOI: 10.15376/biores.14.1.1127-1140

4.1.3 Numerical and experimental investigation on the elastic stiffness of glued dovetail joints

Published as:

Kamboj G, Gaff M, Smardzewski J, Haviarová E, Borůvka V, Sethy AK. Numerical and experimental investigation on the elastic stiffness of glued dovetail joints. Construction and Building Materials. 2020 Dec 10;263:120613.

Construction and Building Materials 263 (2020) 120613

Contents lists available at ScienceDirect

Construction and Building Materials

journal homepage: www.elsevier.com/locate/conbuildmat

Numerical and experimental investigation on the elastic stiffness of glued dovetail joints

Gourav Kamboj [a], Milan Gaff [a,*], Jerzy Smardzewski [b], Eva Haviarová [c], Vlastimil Borůvka [a], Anil Kumar Sethy [a]

[a] Department of Wood Processing and Biomaterials, Faculty of Forestry and Wood Sciences, Czech University of Life Sciences Prague, Kamýcká 1176, Praha 6 – Suchdol 16521, Czech Republic
[b] Poznan University of Life Sciences, Faculty of Wood Technology, Department of Furniture Design, Wojska Polskiego 28, 60-637 Poznan, Poland
[c] Purdue University, Department of Forestry and Natural Resources, West Lafayette, IN 47907-2033, USA

HIGHLIGHTS

- Spruce and beech wood dovetail joints bonded with PVAc and PUR adhesive were tested.
- Joint stiffness was analyzed by both, experimental and numerical methods.
- Numerical model provided information on stress distribution in the joints.
- Numerical and experimental results are well aligned, with exception of tension load in beech wood.

ARTICLE INFO

Article history:
Received 3 March 2020
Received in revised form 4 August 2020
Accepted 16 August 2020
Available online 30 August 2020

Keywords:
Wooden construction
Dovetail joints
Mechanical loading
Elastic stiffness
Finite element method

ABSTRACT

This study investigates the stiffness of dovetail joints by both numerical and experimental methods. Test specimens were made of Spruce (*Picea abies* L) and Beech (*Fagus Silvatica* L) wood, which were bonded with polyurethane (PUR) and polyvinyl acetate (PVAc) adhesives into dovetail joints. To determine the mechanical behavior, the joints were loaded according to grain direction under compressive and tensile load. The results of the experiment indicated that, under compression load, beech wood bonded with polyvinyl acetate (PVAc) adhesive had maximum elastic stiffness. Based on the experimental results, a numerical model using the finite element method (FEM) was developed by the Abaqus program to predict the stiffness of dovetail joints under compressive and tensile load. For numerical analysis, the assumption was made that arm deflection was caused by a displacement in the supports. The value of deflection corresponds to the limit of linear elasticity and the value of the force reduced stresses, which was determined on the basis of deflections. A cohesive zone was developed, which shows stress behavior under compressive and tensile load. A positive correlation was found between the numerical model and experimental study.

1. Introduction

Furniture products are subjected to different kinds of load during their use. Various factors are considered while designing furniture so that the final product is not only strong enough to resist various kinds of load, but also to save material and time. Joints are integral elements of furniture, and they are considered to be the weakest link. The majority of furniture failures occur due to the failure of joints. The dovetail joint is a classic furniture joint where two wood pieces are interlocked. The self-locking character gives the joint outstanding strength properties. The strength of the joints depends on the mechanical properties of materials used, geometry of the joint and reinforcement of joints with adhesive [1,2].

Joints highly resistive to bending under compressive and tensile forces are most important for the construction of chairs [3]. The resistance of a dovetail joint under bending forces could offer an alternative to the mortise and tenon joint [4,5]. Asomani [6] determined the performance of a dovetail halving joint in leg and rail application, finding that chairs constructed with dovetail joints were 70% stronger than those made with mortise-tenon joints. Su and Wang [7] observed greater strength in dovetail joints than mortise-tenon and dowel joints.

* Corresponding author.
E-mail address: gaff@fld.czu.cz (M. Gaff).

https://doi.org/10.1016/j.conbuildmat.2020.120613
0950-0618/

The stiffness of the whole furniture depends on the rigidity of the furniture joints. Knowledge of the mechanical behavior of joints is of prime importance for their rational application. Stiffness is one of the most important criteria to obtain high-quality furniture and cabinets, [8–13]. While the stiffness of the joint depends on materials, joint geometry and loading parameters, reinforcement of the joint with adhesive can improve the joint's stiffness [14]. Load transfer in adhesive-reinforced joints is very complex if there is a mismatch in stiffness. Hence, additional strength can only be realized with properly designed combinations [15].

Testing of furniture joints is mostly carried out by experimental as well as numerical simulation methods. Experimental testing has been extensively reported to assess mechanical properties of various wooden joints [16–18]. While the experimental method is a precise method of assessing mechanical behavior of joints, numerical simulation provides an opportunity to assess the distribution of stress in the joint. Numerical models also give us information about the post elastic behavior, which is most important to reduce damage in the experiment and optimize furniture design [19–21]. Numerical models provide information based on the deformations and internal forces acting on a piece of furniture being used. To calculate furniture stiffness, numerical models have been developed by various researchers [8,11,14]. Various forms of parametric models of joints using FEM analysis have been reported by Mihăilescu [22]. Stress distribution in furniture corner joints has been reported using experimental testing and numerical simulation [23]. A round dovetail beam-to-beam connection was investigated under shear loading with a numerical model, and it was found that failure is mainly caused by changes in the stress of the used material which is subjected to load [21,24].

Many studies compared joint stiffness obtained by experiment and numerical models, and most of the comparisons reported lower experimental values than those obtained by models. The reasons for such discrepancy in joint stiffness could be attributed to simplified numerical models. Therefore, many researchers focused on the stiffness and strength of joints and how it influences the rigidity of the entire furniture [4,19,21,24–35]. The aim of this work was to investigate the elastic stiffness of dovetail joints reinforced with PVAc and PUR adhesives (Fig. 1), by numerical simulation and an experimental method. The effect of compressive and tensile loading on the elastic stiffness was also considered.

2. Experiment

2.1. Material

Two types of wood species were used in this study: Spruce (*Picea abies*. L), representing softwood, and Beech (*Fagus Silvatica* L), representing hardwood. The wood was sourced from the region of Presov in the Eastern Slovakia. The lumber was conditioned at a temperature of 20 °C and a relative humidity of 65% to achieve 12% moisture content according to the European standard [36]. Straight grained and defect-free lumber was used for the test specimens. Samples with dimensions of 214 × 60 × 24 mm (L × W × H) were prepared. In total, 80 samples were prepared and divided randomly into 4 groups. The configuration of test samples is shown in Fig. 1.

Polyvinyl acetate (PVAc) and polyurethane (PUR) adhesive were used for dovetail joint assembly. PVAc is very easy to apply and does not damage the tools during the cutting process. PVAc (Ag-Coll 8761/L D3) with a viscosity ranging from 7000 to 13,000 mPa.s at 23 °C and a density ranging between 0.9 and 1.1 g/cm^3 was used. A glue spreading rate of 150–180 g/m^2 was used. The adhesive was applied on both members of dovetail joints. A pressing time of 60 min was applied based on the adhesive application instructions. PUR adhesives tend to be very flexible and durable and provide good impact resistance. They vary in the degree of resistance to heat and chemicals, as well as in the level of their bulk flexibility. PUR (Neopur 2238R) with a viscosity ranging from 2000 to 4500 mPa.s at 23 °C and a density of approx. 1.13 g/cm^3 was used with a glue spreading rate of 180–250 g/m^2. Bonding surfaces were clean, dry and free of dust and oil.

2.2. Method

The stiffness value was determined based on the change of angle between arms of the L-shape joint with an annual ring orientation of 0^0, 45^0 and 90^0 (represented as 0, M and 90 respectively) while applying an external load. To calculate the strength of the joint, the bending moment under compression and tension was calculated. The configuration described in Figs. 2 and 3 was used for testing joint strength in compression and tension constructed on climatized L-shaped joints described in the material section.

The configuration and dimensions of test specimens are shown in Fig. 1. Ten replicate samples for each adhesive, species, and load

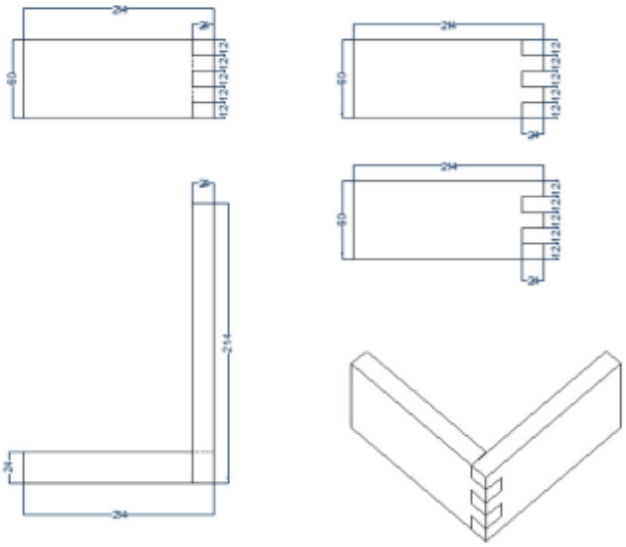

Fig. 1. Geometry of dovetail joints.

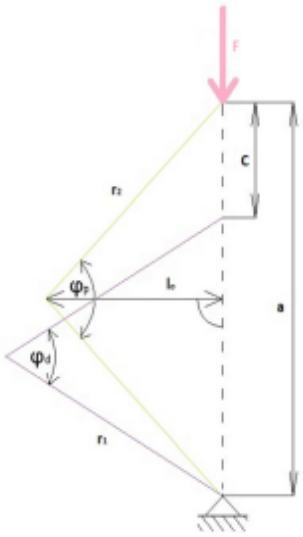

Fig. 2. Geometry of joints under compression load.

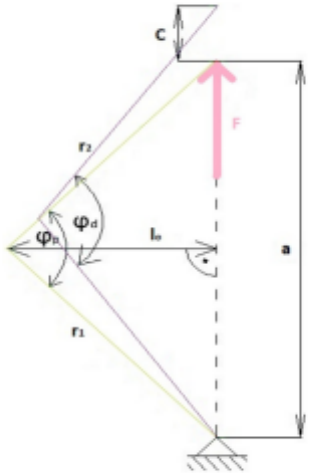

Fig. 3. Geometry of joint under tensile load.

type were tested. Tests were performed on a TIRA 50 universal testing machine (TIRA system, GmbH, Schalkau, Germany). The samples were subjected to bending moment under tensile and compressive forces applied perpendicular to the direction of the moment arm. Sample's moisture content [37], as well as density [38], were measured before the test. The effect of individual factors and their interaction on the elastic stiffness were ascertained with an analysis of variance (ANOVA) and Fischer's F-Test using STATSTISTICA 14 (Statoft Inc; Oklahoma, USA).

F – force [N], r_1 and r_2 – arm length (distance of force from the axis of rotation) [m], φ_p – joint angle before loading [rad], φ_d – joint angle after loading [rad], l_0 – moment arm from original shape [m], a – arm spacing [m], c – displacement [m]

The angular deformation φ was calculated according to the following equation [39]:

$$\varphi = \varphi_P \pm \varphi_d \quad (1)$$

φ_{max} – angular deformation at the ultimate limit [rad] indicates the maximum angular deformation created at the maximum resistance of the joint, with the following equation:

$$\varphi_{max} = \varphi_P \pm \varphi_{dmax} \quad (2)$$

After the specimens are under load, a general triangle is formed between the joint arms and its angle φ_d, which can be expressed using Kosin's theorem:

$$(a-c)^2 = r_1^2 + r_2^2 - 2\, r_1 r_2 \cos(\varphi_d)$$

$$\cos(\varphi_d) = \left(r_1^2 + r_2^2 - (a-c)^2\right)/2\, r_1 r_2 \quad (3)$$

The mathematical derivation of the formula can be expressed as:

$$\varphi_d = \arccos\left(r_1^2 + r_2^2 - (a-c)^2\right)/2\, r_1 r_2 \quad (4)$$

The moment arm (lo) is defined by the side and content of general triangle:

$$lo = (a-c)/\left(2tg\left(\varphi_d/2\right)\right) \quad (5)$$

The joints were tested and bending moment capacities were calculated for each joint. The bending moment expresses the maximum bearing capacity of the joint.

The distance between the attachment holes was 195 mm for all samples. Bending moment capacity was calculated by the following formula:

Bending moment capacity up to the elastic limit (ΔM) is expressed as:

$$\Delta M = \Delta F \times lo \quad (6)$$

where ΔM is change in bending moment [N.m], ΔF – change in force [N], l_0 – moment arm [mm].

ΔF is the deviation of the two forces recorded in the stress-strain diagram at values between 10% and 40% of the maximum strength. The elastic limit of the joints was calculated in the elastic area.

The maximum bending moment capacity (M) was calculated using equation (7).

$$M = F_{max} \times lo \quad (7)$$

M – moment [N × m], F_{max} – maximum force [N], lo – moment arm [mm]

Elastic stiffness (C_{elast}) was derived with the following equation:

$$C_{elast} = \Delta M/\Delta\varphi \quad (8)$$

C_{elast} – elastic stiffness [Nm/rad], ΔM – bending moment [N.m], Δφ – angular deformation

Maximum stiffness (C) was calculated as:

$$C = M_{max}/\varphi_{max} \quad (9)$$

C – Maximum stiffness [Nm/rad], Mmax – maximum bending moment [N × m], φ_{max} – maximum angular deformation [rad]

2.3. Numerical model

Numerical calculations were performed applying the Abaqus v.6.16 program (Dassault Systems Simulia Corp., Waltham, Ma, USA). Geometry, support and loading conditions of joints are presented in Fig. 4a and are consistent with the methodology descried earlier. Joint arms were described as an orthotropic body ascribing their material properties as in Table 1 and Fig. 4b. In general, a linear hexahedron type C3D8R element was used (about 120,000 elements and 90,000 nodes per model). Between the joints, the bonded interaction and glue lines (0.1 mm in thick) were applied. The behavior of glue lines has been modelled with the help of Cohesive Zone Model (CZM) by means of standard COH3D8 cohesive elements (Table 2). Fig. 5 presents a mesh model and orientation of fiber in a local coordinate system (X, Y, Z).

3. Results

3.1. Experimental results

Results pertaining to stiffness, as well as the maximum bending moment, are shown in Table 3. Elastic stiffness was higher in compression loading than tensile loading, and the effect of adhesive was found to be specific to different wood species. Similar results have been reported in previous studies [43–45]. It is evident that beech wood joints exhibited significantly higher elastic stiffness with PVAc adhesive under compression load (1880 Nm/rad) as compared to joints bonded with PUR adhesive (1,324 Nm/rad). The elastic stiffness of beech wood joints was significantly higher compared to spruce wood joints. Under compression loading, beech wood bonded with PVAc exhibited 57% higher elastic stiffness, as compared to spruce wood, while under tensile load it was 39% higher. In the case of PUR bonding, joints of beech wood loaded under compression had 31% higher elastic stiffness than spruce wood, while under tensile load the results were almost the same. Higher elastic stiffness of joints in beech wood is due to its higher density. The average wood density of beech is 0.723 g/cm^3, while that of spruce is 0.389 g/cm^3. These results

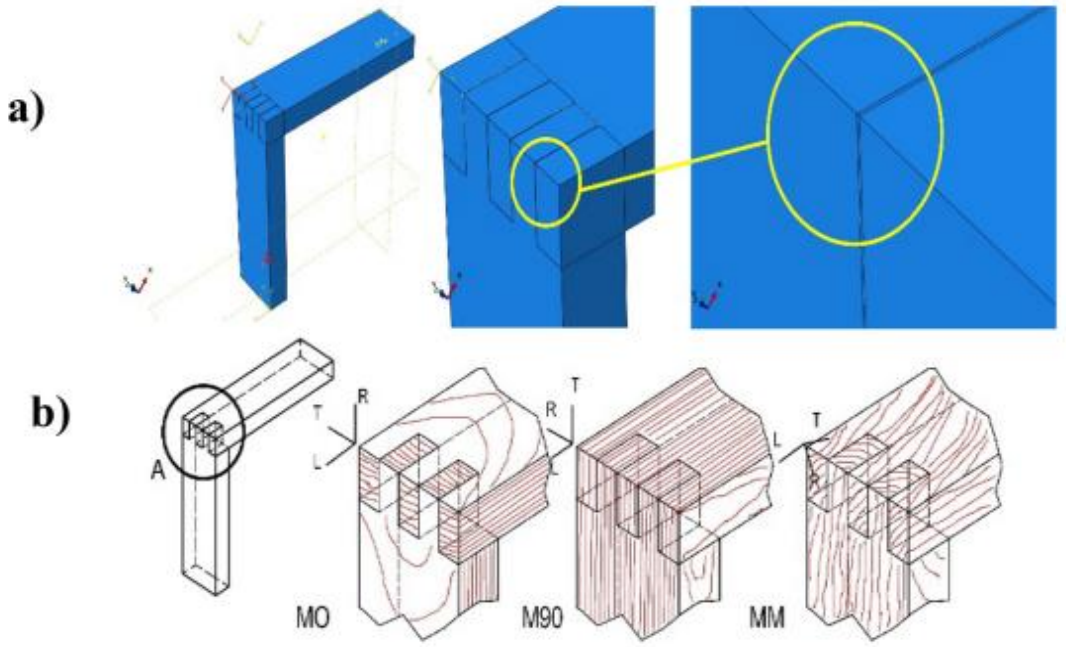

Fig. 4. Finite element model of dovetail joint: a) glue line, b) bonded interaction with annual rings.

Table 1
Elastic properties of wood [40].

Elastic properties/Type of wood (MPa)	Values used for Beech	Values used for *Spruce
Density(g/cm^3)	0.725	0.389
$E_{L(X)}$	14,100	16,600
$E_{R(Y)}$	2280	1117
$E_{T(Z)}$	1160	583
$\nu_{LR(XY)}$	0.45	0.42
$\nu_{LT(XZ)}$	0.51	0.51
$\nu_{RT(YZ)}$	0.75	0.68
$\nu_{TR(ZY)}$	0.36	0.31
$\nu_{RL(YX)}$	0.075	0.038
$\nu_{TL(ZX)}$	0.044	0.015
$G_{LR(XY)}$	1645	1181
$G_{LT(XZ)}$	1082	693
$G_{RT(YZ)}$	471	70

Where E – Modulus of elasticity (MPa), G – Shear modulus (MPa), and ν – Poisson ratio in longitudinal (L-X), radial (R-Y) and tangential (T-Z) direction.
*Note – As elastic properties of pine wood was not accessible, therefore the elastic properties of spruce wood was used instead for numerical calculation because of their comparable properties.

Table 2
Elastic properties of glue line [41,42].

Glue	E (MPa)	Poisson ratio
Value used for PVAc	460	0.3
Value used for PUR*	820	0.3

*Note – Due to non-availability of elastic properties for PUR glue line, UF value was used for numerical calculation.

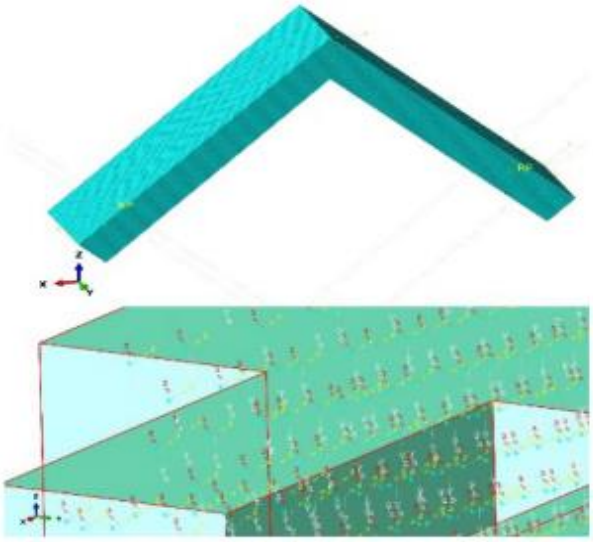

Fig. 5. Meshing with orientation of fiber in local coordinate system.

are in line with the results reported by Zaborsky *et al.* (2017) [18]. The authors have reported higher elastic stiffness in PVAc bonded mortise and tenon joints as compared to PUR bonded joints, and higher values for beech wood as compared to spruce wood.

As can be seen in Table 3, under compression load, beech wood joints glued with PVAc had the highest bending moment capacity of 87.31 Nm, and spruce wood joints glued with PVAc had the lowest bending moment capacity of 37.89 Nm. Similarly, under tensile load, beech wood joints glued with PVAc had the highest bending moment capacity of 51.32 Nm, and spruce wood joints glued with PVAc had the lowest bending moment capacity of 22.33 Nm. On average, the bending moment capacity of joints bonded with PVAc was 28% higher than that of joints bonded with PUR.

A statistical analysis was carried out to ascertain the effect of monitored factors and their interactions on the elastic stiffness of the joints, and the result is shown in Table 4. The results show that all the monitored factors, such as adhesive type and loading type within both species (spruce and beech), significantly influenced the elastic stiffness of the joints. As far as the interaction of factors concerned, only the combination of wood species with adhesive, as well as with the type of loading, was found to have a significant effect on the elastic stiffness of the joints.

Table 3
Elastic stiffness and bending moment of joints with interaction of wood species, adhesive and load.

Wood species	Adhesive type	Loading type	Density (g/cm³)		Elastic stiffness (Nm/rad)		Maximum Bending moment (Nm)	
			Mean	Coefficient of variation (%)	Mean	Coefficient of variation (%)	Mean	Coefficient of variation (%)
Spruce	PVAc	Compression	0.379	3.9	800	20.9	37.89	7.91
Spruce	PVAc	Tension	0.396	3.3	800	39.5	22.33	12.88
Spruce	PUR	Compression	0.389	4.5	909	25.3	39.65	18.12
Spruce	PUR	Tension	0.395	4.9	997	29.2	28.90	18.23
Beech	PVAc	Compression	0.706	2.8	1880	14.6	87.31	8.99
Beech	PVAc	Tension	0.742	2.4	1322	31.7	51.32	11.27
Beech	PUR	Compression	0.702	2.6	1324	35.5	42.90	12.08
Beech	PUR	Tension	0.743	2.5	969	29.4	30.69	17.40

Table 4
Statistical evaluation of selected factors and their interaction. DoF – Degree of freedom NS – not significant, *** – significant, P < 0.05.

The effect of selected factor on Elastic stiffness in Nm/rad					
Monitored factor	Sum of squares	DoF	Variance	Fisher's F-test	Significance Level. P
Intercept	101,293,029	1	101,293,029	890.36	***
Wood species (1)	4,945,087	1	4,945,087	43.46	***
Adhesive type (2)	453,192	1	453,192	3.98	***
Loading type (3)	851,775	1	851,775	7.48	***
1 * 2	1,845,629	1	1,845,629	16.22	***
1 * 3	1,250,587	1	1,250,587	10.99	***
2 * 3	106,222	1	106,222	0.93	NS
1 * 2 * 3	16,702	1	16,702	0.14	NS
Error	8,191,147	72	113,766		

The respective model explains roughly 53.6% of the total sum of squares.
NS – not significant, *** – significant, P < 0.05.

The effect of wood species on the value of elastic stiffness of joints is shown in Fig. 6. The results indicate the average of the adhesive and both type of loads. This graph clearly shows that spruce wood joints have significantly lower (36%) elastic stiffness than beech wood joints; this is because of the lower density of spruce wood compared to beech wood [46–49].

Adhesives can have varying effects on wood bonding strength [50]. The values of elastic stiffness of both types of loads were averaged for each species and each adhesive type, and the results are presented in Fig. 7. In spruce wood, the joints bonded with PUR adhesive have 16% higher elastic stiffness than joints bonded with PVAc adhesive, though the difference was not statistically significant (P < 0.05). This is expected due to the higher stiffness of PUR adhesive. However, the results were opposites in case of beech wood. Elastic stiffness of joint bonded with PVAc adhesive were significantly higher (28%) as compared to PUR adhesive. Such difference in the elastic stiffness can be due to the differences in the penetration behavior of both the adhesives in these wood species. The penetration ability of PUR is very fast as compared to PVAc. Further, penetration of adhesive is also influenced by the permeability of wood [51]. As beech wood is more permeable than spruce wood, the penetration of PUR is very fast as compared to PVAc. Hence, the lower elastic stiffness of PUR bonding in beech wood could be attributed to the starved bond line due to deeper penetration of PUR resin in to the wood. On the other hand, the bond line of PVAc in beech wood will be rather distinct due to its limited penetration [51]. With its high content of acetate groups and flexible backbone, PVAc can form many hydrogen bonds with wood for good interfacial adhesion [52]. Although, beech wood bonded with PUR showed higher elastic stiffness than spruce wood, the values were comparable without any significant difference (P < 0.05).

Fig. 6. The effect of wood species on elastic stiffness.

Fig. 7. The effect of adhesive type on spruce and beech wood elastic stiffness.

The values of elastic stiffness obtained for both types of loading (compression and tension) were compared and the results are shown in Fig. 8. Average elastic stiffness of joints under tensile load was 16.7% lower than under compression loading, when data for both species and both adhesives were pooled together. Similar results have been reported by various authors in case of corner joints [53,54]. The difference was pronounced in case of beech wood, irrespective of adhesive used. However, the values were also most comparable without any significant difference in case of spruce wood. Properties of wood, length of moment arm (due to change in pivot point), geometry of the dovetail, glue line thickness and stiffness of the glue are the important parameters responsible for the differential stiffness in compression and tension load. Wood is stronger in compression than tension perpendicular to grain (load on the tails is nearly perpendicular to grain direction). Length of moment arm under tensile load is relatively longer than compressive load due to the position of pivot points. Longer arm can cause higher bending moment than shorter arm, even for same level of applied force. During compressive loading, maximum stress is exerted on the outer edge (tip of the tails) while under tensile loading, maximum stress is exerted in the inner edge (towards base of the tail). Due to the relatively bigger bonding surface area towards the tip of the tails compared to the base, the deformation is expected to be less under compression than in tension for similar load, thereby resulting in higher stiffness in compression. Cumulatively all these factors could contribute towards higher stiffness in compression than in tension. Glue line in beech wood is expected to be thinner due to its higher permeability. The differential result in spruce wood might be due to the distinct glue line (poor permeability of spruce wood to adhesive penetration) and its inherent stiffness. Furniture joints are more sensitive under tensile stress compared to compressive stress and almost all failure occurs in tensile zones.

Orientation of annual rings in wood used for test specimens also affects the elastic stiffness of the joints. The results pertaining to the effect of annual ring orientation on elastic stiffness of joints are shown in Fig. 9. The highest value of the elastic stiffness was obtained at 90–90 orientation, because the annual rings are perpendicular to the force of loading and corresponds to radial loading.

To determine the difference between all the variables, Duncan test was performed and results are shown in Table 5–8 reflecting interaction between wood species, adhesive and load.

3.2. Numerical results

Fig. 10 shows the distribution of reduced stresses in joints. It should be noted that under the compression loading (10a) the greatest stresses are concentrated in the glue line. These stresses are located in the corners of glue line. The stresses concentrated in the upper corner above the pivot point have the highest value of 5.18 MPa. At the pivot point, the stresses have the value of 3.02 MPa, while on the opposite side, the value of these stresses is close to zero. A different distribution of stresses is observed during tension loading (10b). The highest stress (12.65 MPa) was developed below the pivot point in the place of joint opening. In other places, the adhesive end has a value close to zero. This explains why the joints subjected to tension have less stiffness compared to those in compression.

In the case of structure joints, the reduced stress slightly exceeds the stresses in L-type joints. The highest stresses recorded in the compression test are 13.8 MPa, while in the tension test it was 12.1 MPa (Fig. 11). As we can see, these are stresses at the base of the wedges subjected to bending. In the linear elastic range, these stresses do not affect the strength of the joint; this is why they transfer much greater loads than glued joints.

The effect of wood species and type of adhesive on the load bearing capacity of joints bonded with annual rings M0 is shown in Fig. 12. The deflection under compression and tension load was calculated for beech and spruce wood joints with annual ring M0 bonded with PUR and PVAc adhesive. In spruce wood joints under compression load, the load bearing capacity for a similar

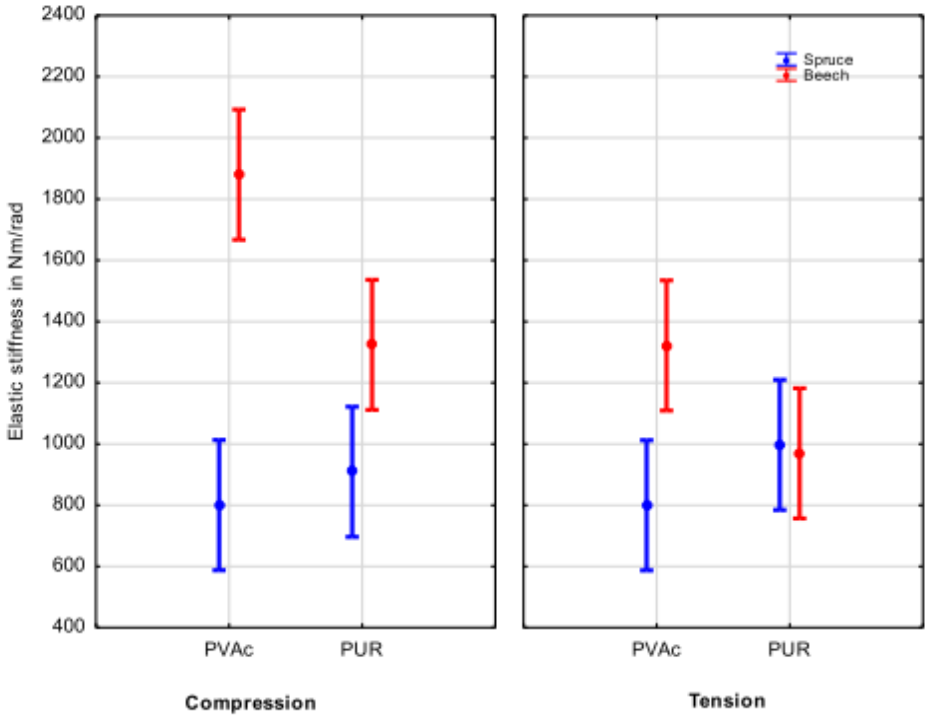

Fig. 8. Influence of loading type on elastic stiffness.

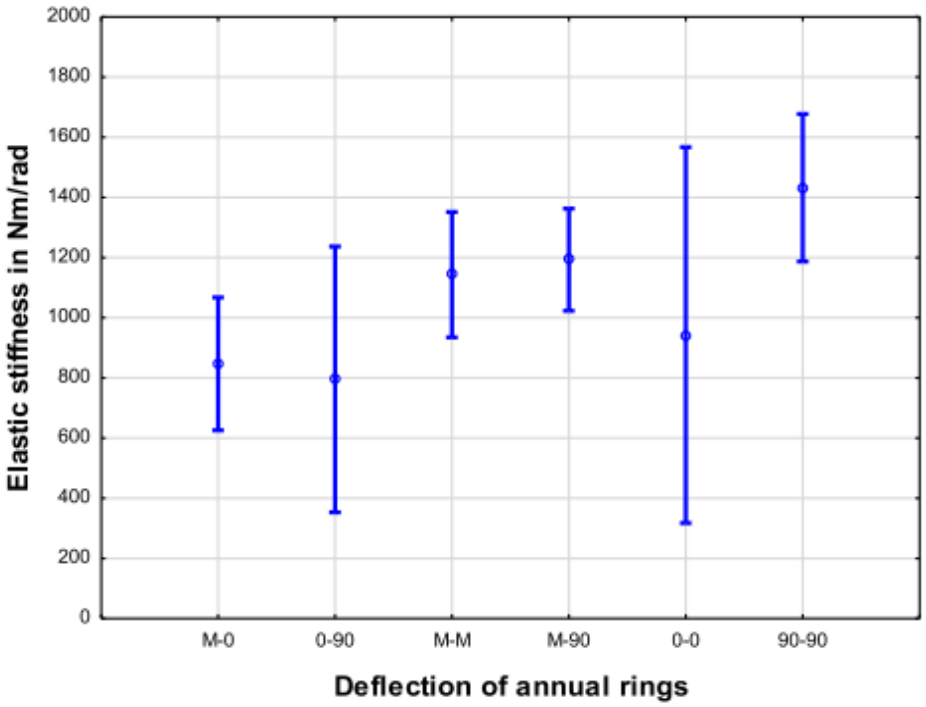

Fig. 9. Influence of annual rings on stiffness of Dovetail Joint.

Table 5
The effects of wood species and adhesive on the elastic stiffness (Nm/rad) using Duncan test.

Cell No.	Wood species	Adhesive type	(1) 799	(2) 953	(3) 1601	(4) 1146
1	Spruce	PVAc		0.155	0.000	0.003
2	Spruce	PUR	0.155		0.000	0.074
3	Beech	PVAc	0.000	0.000		0.000
4	Beech	PUR	0.003	0.074	0.000	

Table 6
The effects of wood species and load on the elastic stiffness (Nm/rad) using Duncan test.

Cell No.	Wood species	Loading type	(1) 854	(2) 898	(3) 1602	(4) 1145
1	Spruce	Compression		0.683	0.000	0.011
2	Spruce	Tension	0.683		0.000	0.023
3	Beech	Compression	0.000	0.000		0.000
4	Beech	Tension	0.011	0.023	0.000	

Table 7
The effects of adhesive and load on the elastic stiffness (Nm/rad) using Duncan test.

Cell No.	Adhesive type	Loading type	(1) 1340	(2) 1060	(3) 1116	(4) 983
1	PVAc	Compression		0.015	0.040	0.002
2	PVAc	Tension	0.015		0.602	0.469
3	PUR	Compression	0.040	0.602		0.243
4	PUR	Tension	0.002	0.469	0.243	

Table 8
The effects of wood, adhesive and load on the elastic stiffness (Nm/rad) using Duncan test.

Cell No.	Wood species	Adhesive type	Loading type	(1) 800	(2) 799	(3) 909	(4) 997	(5) 1880	(6) 1321	(7) 1324	(8) 969
1	Spruce	PVAc	Compression		0.999	0.471	0.241	0.000	0.002	0.002	0.296
2	Spruce	PVAc	Tension	0.999		0.499	0.252	0.000	0.002	0.002	0.313
3	Spruce	PUR	Compression	0.471	0.499		0.588	0.000	0.013	0.014	0.692
4	Spruce	PUR	Tension	0.241	0.252	0.588		0.000	0.035	0.043	0.855
5	Beech	PVAc	Compression	0.000	0.000	0.000	0.000		0.001	0.001	0.000
6	Beech	PVAc	Tension	0.002	0.002	0.013	0.035	0.001		0.989	0.029
7	Beech	PUR	Compression	0.002	0.002	0.014	0.043	0.001	0.989		0.033
8	Beech	PUR	Tension	0.296	0.313	0.692	0.855	0.000	0.029	0.033	

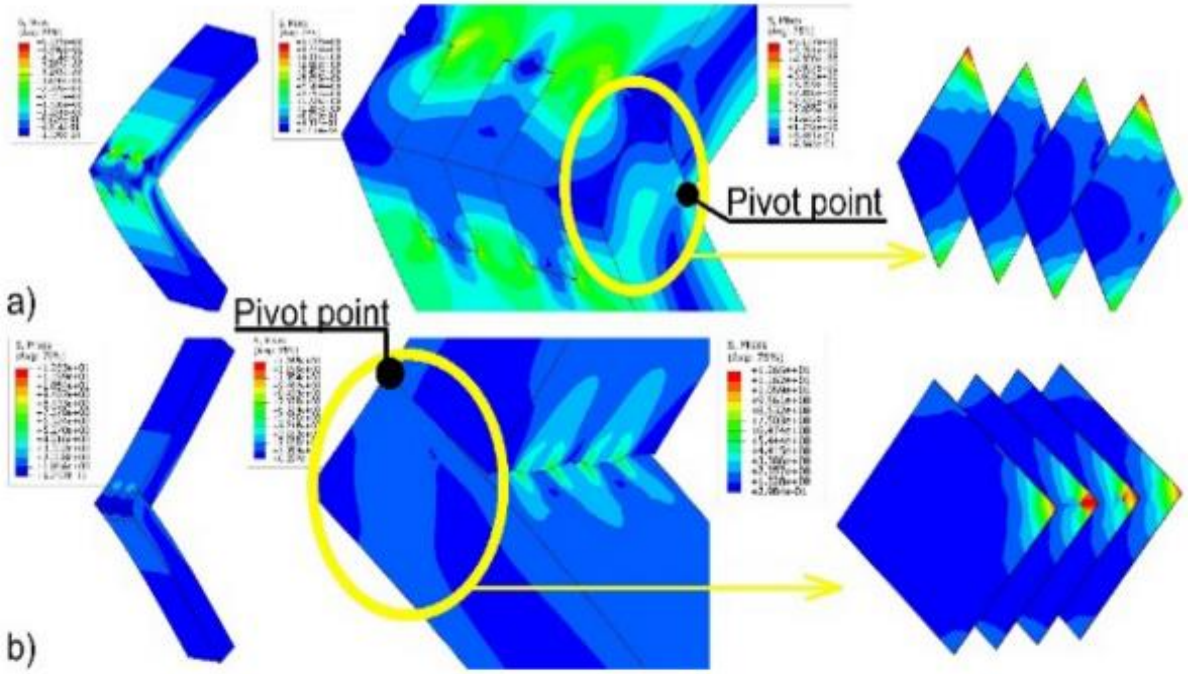

Fig. 10. Distribution of reduced stresses (Mises) in L-type joint: Loaded in a) compression, b) tension.

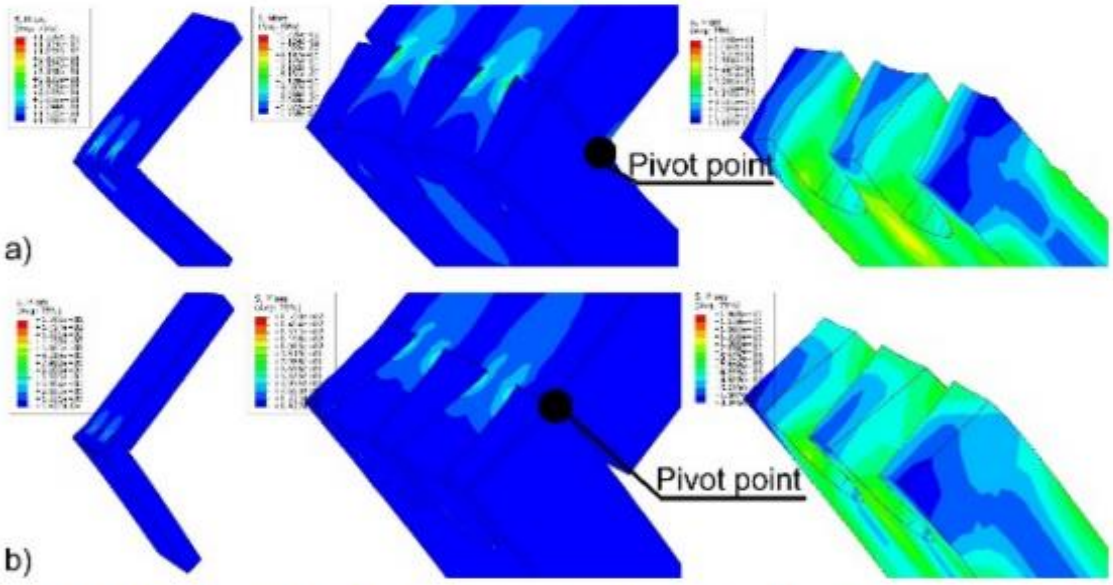

Fig. 11. Distribution of reduced stresses in dovetail joint with inclination angle of tenon's surfaces angles: loaded in a) compression, and b) tension.

deflection was found to be 20.5% higher with PUR than PVAc, while under tensile load it was 14% higher. In beech wood joints, PVAc had 26.4% higher load bearing capacity than PUR under compression load. Under tensile load, the obtained results were the opposite: joints bonded with PUR had 55.7% higher load bearing capacity than those bonded with PVAc. It was expected that the use of PUR adhesive with a higher modulus of linear elasticity than PVAc adhesive would result in smaller joint deflections for each type of wood and load. However, in the case of compression of beech wood joints, numerical calculations provided results indicating higher stiffness with the use of PVAc adhesive. In addition, this relationship has been confirmed experimentally for beech samples subjected to tension. Considering the interaction of beech wood and adhesive, joints bonded with PVAc should be more rigid. This regularity is justified by literature [51]. However, the chemical interactions between adherent parts in a glued joint were not included in the numerical models. The opposite results of beech samples subjected to shorting, indicate only a different nature of energy dissipation, especially in the adhesive joint. After all, in a glued joint subjected to compression, almost half the amount of tangential stress is concentrated compared to tension. This is also influenced by the direction of fiber orientation in the parts of the joints. To determine which factor decided such relations, it would be necessary to conduct experimental research and numerical calculations of the stiffness of joints in the plastic range and considering the cyclic heterogeneity of wood.

Fig. 13 shows the effect of wood species and type of adhesive on the load bearing capacity of bonded joints with the annual rings

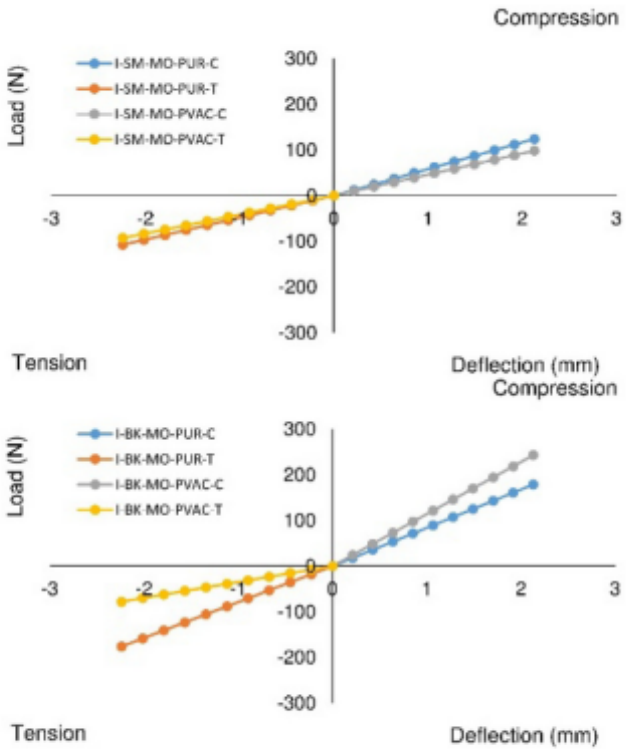

Fig. 12. The impact of the wood species and type of glue on the stiffness of the L-type joint bonded with the annual ring M0.

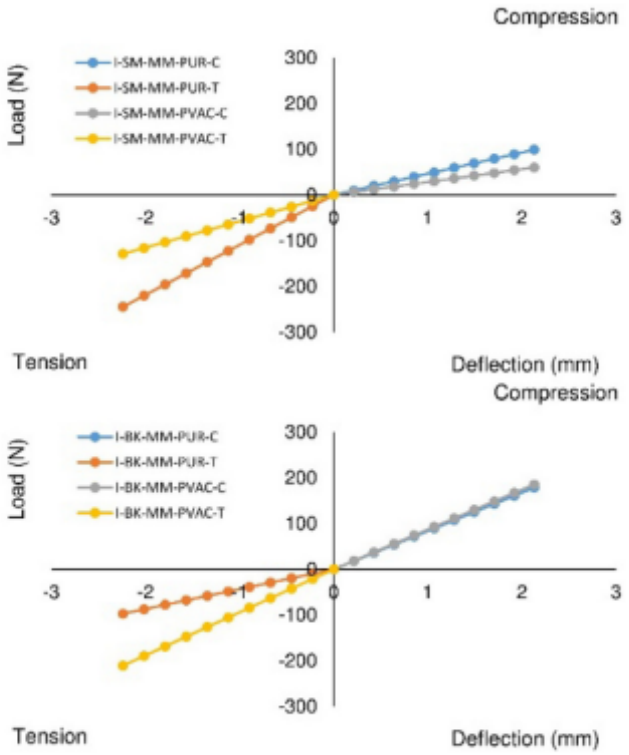

Fig. 13. The impact of the wood species and type of glue on the stiffness of the L-type joint bonded with the annual ring MM.

MM (45° orientation in both tail and pins). Under compression load in spruce wood, joints bonded with PUR had 39% higher load bearing capacity than those bonded with PVAc for a similar deflection. Under tensile load, joints bonded with PUR had 47% higher load bearing capacity than those bonded with PVAc. In the case of beech wood, there was not much difference in the load bearing capacity of joints bonded by both adhesives under compressive load. Under compressive load with a similar deflection, joints bonded with PVAc had 3.7% higher load bearing capacity than those bonded with PUR. On the other hand, under tensile load, the difference was very high; joints bonded with PVAc had 53.8% higher load bearing capacity than those bonded with PUR.

The effect of wood species and type of adhesive on the load bearing capacity of joints bonded with annual rings M90 (45° orientation in tail and 90° orientation in pins) is shown in Fig. 14. Under compression load with a similar deflection, the load bearing capacity in spruce wood joints bonded with PUR was 5.6% higher than with PVAc, while under tensile load joints bonded with PVAc had 2.9% higher load bearing capacity than those bonded with PUR. In beech wood under compression load for a similar deflection, joints bonded with PVAc had a higher load bearing capacity than those bonded with PUR, which was 45% higher. On the other hand, under tensile load PUR had 13.9% higher load bearing capacity than PVAc.

Fig. 15 shows the impact of wood species and the orientation of annual rings on the load carrying capacity of joints bonded with PUR glue under compression and tension load. In spruce wood under compression load, for similar deflection, the joints with annual rings M0 had higher load carrying capacity than joints with annual ring M90 and MM, which was 14% and 20.5% higher respectively. On the other hand, under tensile load, the highest load carrying capacity, having similar deflection, was obtained in joints with annual ring orientation MM, as compare to M90 and M0, which was 26% and 52% higher, respectively. In beech wood joints, under compression load, the higher load carrying capacity for similar deflection was found with annual rings orientation M0 and MM, compare to M90, which was 34% higher. On the other hand, under tensile load, the higher load carrying capacity was in M90

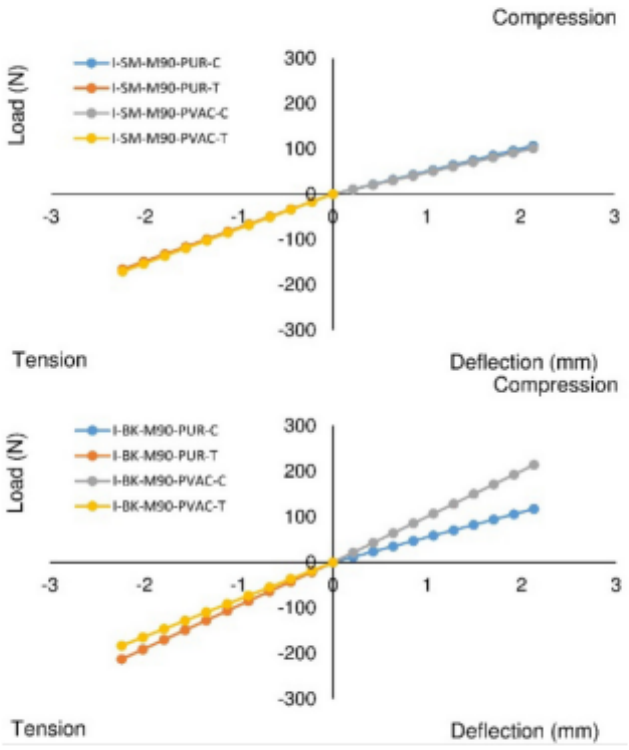

Fig. 14. The effect of wood species and type of adhesive on the stiffness of an L-type joint bonded with the annual rings M90.

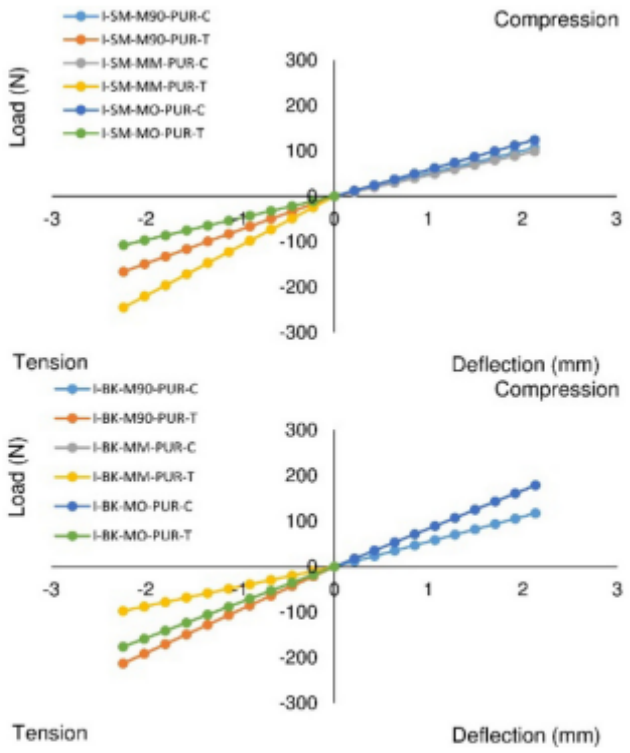

Fig. 15. The effect of wood species and the angle of annual rings (M0, MM and M90) on the stiffness of L-type joints bonded with PUR adhesive.

annual rings than M0 and MM, which was 17% and 54% higher respectively. As most of the joint failure occurs under tension load, it will be more appropriate to decide the annual ring orientation, which offers maximum load carrying capacity against tension load. From the results, it is advisable to prepare dovetail joint with M0 orientation in spruce wood and M90 orientation in beech wood.

Fig. 16 shows that effect of annual rings on the stiffness of dovetail joints with an inclined angle of the tenon's surfaces bonded with PUR. The maximum load (775.1 N) was obtained with annual rings M0 under compression load for a similar deflection, which was 7.4% and 17.55% higher than MM and M90 respectively. On the other hand, under tensile load, the maximum load (599 N) was obtained by M0, which was 6.1% and 17.2% higher than MM and M90 respectively.

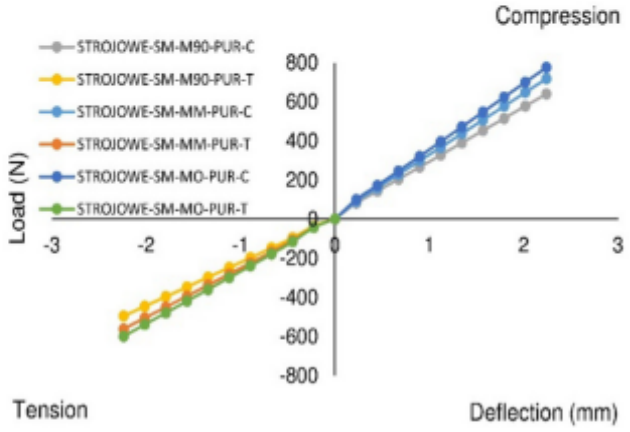

Fig. 16. The impact of wood species and the angle of annual rings on the stiffness of dovetail joint with inclination angle of tenon's surfaces bonded with PUR glue.

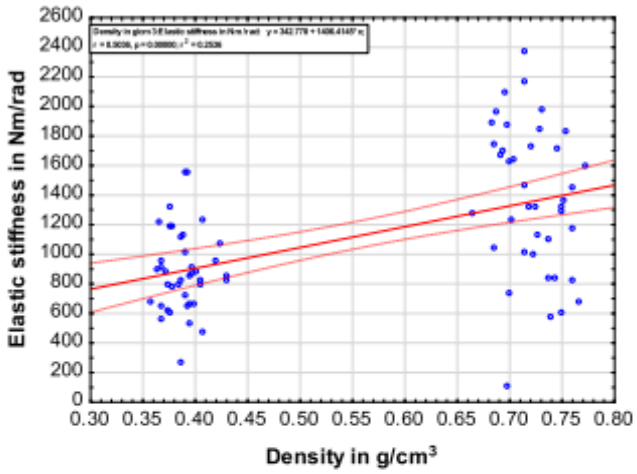

Fig. 17. Dependence of elastic stiffness on density of beech and spruce wood.

The results on elastic stiffness obtained by numerical method were compare with experimental results. In case of spruce wood, both, experimental and numerical results proves higher elastic stiffness with PUR bonding than PVAc under both, tensile and compression loading. Similarly, in case of beech wood, the higher stiffness of PVAc bonding over PUR was also ascertained by both, experimental and numerical methods under compression load. However, the results differed in case of tensile loading with experimental method, giving higher elastic stiffness values for PVAc bonding and numerical methods, giving higher elastic stiffness values for PUR bonding.

To determine the mechanical properties of wood, stiffness is one of the most important factors. For this reason, we wanted to know how wood density correlates with elastic stiffness of wood joints. The results are shown in Fig. 17. Wood density has a moderate correlation with elastic stiffness of the joint with r^2 values of 0.25 respectively.

4. Conclusions

- This paper presents the elastic stiffness of dovetail joints made of beech and spruce wood, bonded with PVAc and PUR adhesives, under compression and tension load. Effect of annual ring orientations (0, 45°, 90°) were also considered.
- Experimental results showed that beech wood dovetail joints bonded with PVAc had 28% higher elastic stiffness as compared to PUR, while spruce wood joints bonded with PUR had 16% higher elastic stiffness than PVAc.
- Annual ring orientation had a significant effect on the elastic stiffness; load applied perpendicular to the rings had highest elastic stiffness.
- Beech wood joints bonded with PVAc had greater bending moment capacity. However, spruce wood joints bonded with PUR had greater bending moment capacity.
- Numerical calculations confirmed similar results as in experimental for beech and spruce wood joints under compression loading. However, the results are opposite under tension load.
- In the case of spruce wood, both experimental and numerical results are similar with higher stiffness in PUR bonded adhesive under both type of loading. In the case of beech wood, experimental results gave higher stiffness in PVAc glued joint under both type of loading. Numerical results coincided with experimental results under compression load. Even under tensile loading, both experimental and numerical results were also similar in spruce wood, however, the results are opposite under tension load.

- Moreover, numerical model provided important information about the distribution of reduced stresses in joints, which can't be achieved by experimental studies. This model helps to provide the location of stress in joints and precisely identified that the stress in compression was recorded to be higher as compare to tension.

CRediT authorship contribution statement

Gourav Kamboj: Conceptualization, Formal analysis, Investigation, Writing - original draft, Funding acquisition. **Milan Gaff:** Resources, Supervision, Project administration, Methodology, Formal analysis, Funding acquisition. **Jerzy Smardzewski:** Formal analysis, Supervision, Formal analysis, Methodology. **Eva Haviarová:** Supervision. **Vlastimil Borůvka:** Formal analysis. **Anil Kumar Sethy:** Supervision, Formal analysis.

Declaration of Competing Interest

The authors declare that they have no known competing financial interests or personal relationships that could have appeared to influence the work reported in this paper.

Acknowledgements

The authors are grateful for the support of "Advanced research supporting the forestry and wood-processing sector's adaptation to global change and the 4th industrial revolution", No. CZ.02.1.01/0.0/0.0/16_019/0000803 financed by OP RDE" and by the International Grant Agency (IGA) of the Faculty of Forestry and Wood Science at Czech University of Life Science (C_07_18).

References

[1] T. Tannert, F. Lam, T. Vallée, Strength prediction for rounded dovetail connections considering size effects, J. Eng. Mech. 136 (3) (2010) 358–366.
[2] T. Tannert, F. Lam, T. Vallée, Structural performance of rounded dovetail connections: Experimental and numerical investigations, Eur. J. Wood Wood Prod. 69 (3) (2011) 471–482.
[3] J. Smardzewski, Furniture Design, Springer, 2015, p. 649.
[4] J.L. Zhang, C.A. Eckelman, The bending moment resistance of single-dowel corner joints in case construction, Forest Prod J. 43 (6) (1993) 19–24.
[5] R.B. Hoadley, Understanding Wood: A Craftsman's Guide to Wood Technology, Taunton Press, 2000, p. 280.
[6] J. Asomani, The performance of dovetail halving joint in Leg-and rail construction using Chrysophyllum albidum. Case study: the working chair M. Phil Thesis, Kwame Nkrumah University of Science and Technology, Kumasi, 2009, p. 71.
[7] W.C. Su, Y. Wang, Withdrawal properties of single dovetail joints, Taiwan J. Forestry Sci. 22 (3) (2007) 321–328.
[8] C.A. Eckelman, K. Kwiatkowski, Experimental testing of the theory of deformations of cabinet designs, Ilolztechnologie 19 (4) (1978) 202–206.
[9] C.A. Eckelman, R.A. Rabiej, A comprehensive method of analysis of case furniture, Forest Prod. J. 35 (4) (1985) 62–68.
[10] T. Kotaš, Sztywność. mebli skrzyniowych. Przemysł Drzewny, 1957, vol. 10, pp. 15–18.
[11] T. Kotaš, Sztywność mebli skrzyniowych (cz. II), Przemysł Drzewny 11 (1957) 10–14.
[12] R. Ganowicz, T. Dziuba, B. Ozarska-Bergandy, Theorie der verformungen von schrankkonstruktionen, Holztechnologie 19 (2) (1978) 100–107.
[13] R. Ganowicz, K. Kwiatkowski, Experimentelle prüfung der theorie der verformungen von schrankkonstruktionen, Holztechnologie 19 (4) (1978) 202–206.
[14] J. Estévez, D. Otero, E. Martín, J.A. Vázquez, The use of adhesive bulbs in the inner end of drills in order to improve the axial strength of steel threaded bars glued in timber, in: World conference of timber engineering (WCTE), Riva del Garda (Vol. 2024), 2010.
[15] J.R. Weitzenböck, D. McGeorge, Science and technology of bolt-adhesive joints, in: Hybrid Adhesive Joints, Springer, Berlin, Heidelberg, 2011, pp. 177–199.
[16] A. Nandanwar, M.V. Naidu, C.N. Pandey, Development of test methods for wooden furniture joints, Wood Mat. Sci. Eng. 8 (3) (2013) 188–197.
[17] T. Tannert, Improved performance of reinforced rounded dovetail joints, Constr. Build. Mater. 118 (2016) 262–267.
[18] V. Záborský, V. Borůvka, V. Kašičková, D. Ruman, Effect of wood species, adhesive type, and annual ring directions on the stiffness of rail to leg mortise and tenon furniture joints, BioResources 12 (4) (2017) 7016–7031.
[19] D.Y.E. Chuan, M. Fragiacomo, P. Aldi, M. Mazzilli, U. Kuhlmann, Performance of notched coach screw connection for timber–concrete composite floor system, NZ Timber Design J 17 (2008) 4–10.
[20] A. Ceccotti, J.-W. van de Kuilen, The WCTE 2010 conference proceedings, June 20–24, 2010, Riva del Garda, Italy.
[21] T. Tannert, H. Prion, F. Lam, Structural performance of rounded dovetail connections under different loading conditions, Can. J. Civ. Eng. 34 (12) (2007) 1600–1605.
[22] T. Mihăilescu, Finite Element Analysis of Mortise and Tenon Joints in Parametric Form, Editura Universitatii, Transilvania, 2003.
[23] J. Smardzewski, P. Silvana, Stress distribution in disconnected furniture joints, Electr. J. Polish Agric. Univ. 5 (2) (2002) 1–20.
[24] B.H. Xu, A. Bouchaïr, M. Taazount, E.J. Vega, Numerical and experimental analyses of multipledowel steel-to-timber joints in tension perpendicular to grain, Eng. Struct. 31 (10) (2009) 2357–2367.
[25] W.Q. Liu, C.A. Eckelman, Effect of number of fasteners on the strength of corner joints for cases, For. Prod. J. 48 (1) (1998) 93–95.
[26] A.N. Tankut, N. Tankut, Effect of some factors on the strength of furniture corner joints constructed with wood biscuits, Turk. J. Agric. For. 28 (2004) 301–309.
[27] V. Norvydas, I. Juodeikiene, D. Minelga, The Influence of glued dowel joints construction on the bending moment resistance, Mater. Sci. (Medziagotyra) 11 (1) (2005) 36–39.
[28] A.N. Tankut, Optimum dowel spacing for corner joints in 32 mm cabinet construction, For. Prod. J. 55 (12) (2005) 100–104.
[29] V. Vassiliou, I. Barboutis, Screw withdrawal capacity used in the eccentric joints of cabinet furniture connectors in particleboard and MDF, J. Wood. Sci. 51 (2005) 572–576.
[30] A. Kasal, S. Sener, Ç.M. Belgin, H. Efe, Bending strength of screwed corner joints with different materials, Gazi. Univ. J. Sci. 19 (3) (2006) 155–161.
[31] M. Atar, A. Ozcifci, The effects of screw and back panels on the strength of corner joints in case furniture, Mater. Des. 29 (2008) 519–525.
[32] A. Kasal, Y.Z. Erdi, J. Zhang, H. Efe, E. Avci, Estimation equations for moment resistances of L-type screw corner joints in case goods furniture, For. Prod. J. 58 (9) (2008) 21–27.
[33] I. Kureli, M. Altinok, Determination of mechanical performances of the portable fasteners used on case furniture joints, Afr. J. Agric. Res. 6 (21) (2011) 4893–4901.
[34] N.Ç. Yerlikaya, Effects of glass–fiber composite, dowel, and minifix fasteners on the failure load of corner joints in particleboard case-type furniture, Mater. Des. 39 (2012) 63–71.
[35] N.Ç. Yerlikaya, A. Aktas, Enhancement of load-carrying capacity of corner joints in case-type furniture, Mater. Des. 37 (2012) 393–401.
[36] ČSN EN 942, Timber in joinery – General requirements. Czech Office for Standards, Metrology and Testing, Prague, Czech Republic, 2007.
[37] ISO 13061–1, Physical and Mechanical Properties of Wood – Test Method for Small Clear Wood Specimens – Part 1: Determination of Moisture Content for Physical and Mechanical Tests, International Organization for Standardization, Geneva, Switzerland, 2014.
[38] ISO 13061–2, Physical and Mechanical Properties of Wood – Test Method for Small Clear Wood Specimens – Part 2: Determination of Density for Physical and Mechanical Tests, International Organization for Standardization, Geneva, Switzerland, 2014.
[39] P. Joščák, N. Langová, P. Krasula, Mechanické Skúšky Nábytku [Mechanical Tests of Furniture]. Technical University in Zvolen, Zvolen, Slovakia, 2015.
[40] J. Smardzewski, Furniture design. Springer, ISBN 978-3-319-19532-2 ISBN 978-3-319-19533-9 (eBook), 2008, DOI 10.1007/978-3-319-19533-9.
[41] J. Smardzewski, Influence of wood and glue-line heterogeneity on the distribution of tangential stress in furniture joints. Book, Roczniki Akademii Rolniczej w Poznaniu, Rozprawy Naukowe, 1998, ISBN 8371601182 9788371601187.
[42] J. Smardzewski, Technological heterogeneity of adhesive bonds in wood joints, Wood Sci. Technol. 36 (2002) 213–227.
[43] S. Maleki, M. Derikvand, M. Dalvand, G. Ebrahimi, Load carrying capacity of mitered furniture corner joints with dovetail keys under diagonal tension load, Turk. J. Agric. For. 36 (2012) 636–643.
[44] M. Dalvand, G. Ebrahimi, A.R. Haftkhani, S. Maleki, Analysis of factors affecting diagonal tension and compression capacity of corner joints in furniture frames fabricated with dovetail key, J Forest Res 24 (2013) 155–168.
[45] M. Derikvand, G. Ebrahimi, C.A. Eckelman, Bending moment capacity of mortise and loose-tenon joints, Wood Fiber Sci. 46 (2014) 1–8.
[46] A. Požgaj, D. Chovanec, S. Kurjatko, M. Babiak, Štruktúra a Vlastnosti Dreva (Structure and Properties of Wood). 2. ed., Príroda a. s.: Bratislava, , 1997, Slovakia 485 p., ISBN: 80-07-00960-4 (in Slovak).
[47] A. Wagenführ, B. Buchelt, A. Pfriem, Material behaviour of veneer during multidimensional molding, Holz als Roh-und Werkstoff 64 (2) (2006) 83–89, https://doi.org/10.1007/s00107-005-0008-5.
[48] M. Frese, H.J. Blaß, Characteristic bending strength of beech glulam, Mater. Struct. 40 (1) (2006) 3–13, https://doi.org/10.1617/s11527-006-9117-9.
[49] Z. Bao, C. Eckelman, H. Gibson, Fatigue strength and allowable design stresses for some wood composites used in furniture, Holz als Roh- und Werkstoff 54 (6) (1996) 377–382, https://doi.org/10.1007/s001070050204.
[50] C.R. Frihart, C.G. Hunt, Adhesives with wood materials: bond formation and performance. In: Wood Handbook: Wood as an Engineering Material, Chapter 10. Madison, WI: U.S. Department of Agriculture, Forest Service, Forest Products Laboratory, 2010.

[51] P. Hass, F.K. Wittel, M. Mendoza, H.J. Herrmann, P. Niemz, Adhesive penetration in beech wood: experiments, Wood Sci. Technol. 46 (1–3) (2012) 243–256.
[52] Roger, M. Rowell, Handbook of wood chemistry and wood composites, Carb. Polym. (2006).
[53] S. Altun, E. Burdurlu, M. Kılıç, Effect of adhesive type on the bending moment capacity of miter frame corner joints, BioResources 5 (3) (2010) 1473–1483.
[54] M. Dalvand, G. Ebrahimi, A.R. Haftkhani, S. Maleki, Analysis of factors affecting diagonal tension and compression capacity of corner joints in furniture frames fabricated with dovetail key, J. For. Res. 24 (1) (2013) 155–168.

4.2 Effect of cellulose nanofiber and cellulose nanocrystals reinforcement on the strength and stiffness of PVAc and PUR adhesive bonded joints

4.2.1 Effect of Cellulose Nanofiber and Cellulose Nanocrystals Reinforcement on the Strength and Stiffness of PVAc bonded Joints

Submited Manuscript:

Kamboj G, Gaff M, Smardzewski J, Haviarová E, Hui D, Rezaei F, Sethy A.K. (2022). Effect of Cellulose Nanofiber and Cellulose Nanocrystals Reinforcement on the Strength and Stiffness of PVAc Bonded Joints. *Composite Structure*

Effect of Cellulose Nanofiber and Cellulose Nanocrystals Reinforcement on the Strength and Stiffness of PVAc Bonded Joints

Gourav Kamboj[1], Milan Gaff[1,2], Jerzy Smardzewski[3], Eva Haviarová[4], David Hui[5], Fatemeh Rezaei[1], Anil Kumar Sethy[1,6]

[1]*Department of Wood Processing and Biomaterials, Czech University of Life Sciences in Prague, Kamýcká 1176, Prague 6 - Suchdol, 16521 Czech Republic*

[2]*Department of Furniture, Design, and Habitat (FFWT), Mendel University in Brno, Zemědělská 1665, 613 00 Brno-sever-Černá Pole, Czech Republic*

[3]*Poznan University of Life Sciences, Faculty of Wood Technology, Department of Furniture Design, WojskaPolskiego 28, 60-637 Poznan, Poland*

[4]*Purdue University, Department of Forestry and Natural Resources, West Lafayette, IN 47907-2033, USA*

[5]*Deptartment of Mechanical Engineering, University of New Orleans, New Orleans, LA 70124, USA*

[6]*Institute of Wood Science and Technology, 18th Cross, Malleswaram, Bangalore-560003, India*

ABSTRACT

Cellulose nanofiber (CNF) and cellulose nanocrystals (CNC) are strong bio-based materials and have great potential in a reinforcement of the polymeric matrix. This study presents the effect of nanocellulose (CNF and CNC) reinforcement of polyvinyl acetate (PVAc) adhesive. Adhesive formulations with three different concentrations (0.5%, 1%, and 2% w/w) of nanocellulose were prepared by dispersing them in water and mixing the suspension with PVAc adhesive; the other percentages are omitted due to obvious adverse effect. The reinforced adhesive was then used to glue spruce (*Picea abies* L) and beech (*Fagus sylvatica*) wood joints to determine joint stiffness and shear strength under static load. Samples were tested at 12% moisture content and after cyclic moisture exposure. Bond line morphology was studied by SEM. FTIR analysis was performed to see the molecular interaction between nanocellulose and PVAc. The addition of nanocellulose to PVAc adhesive significantly improved the elastic stiffness and shear strength of the joints. Optimum elastic stiffness and shear strength values were achieved with a 1% addition of nanocellulose. The general trends are found to be valid for various kind of CNF and CNC.

Keywords: cellulose nanofiber, cellulose nanocrystal, PVAc adhesive

Abbreviations

PVAc-N-B, Pure PVAc beech wood joint (at 12%);
PVAc-C-B, Pure PVAc beech wood joint (cycling 8-19-8%);
PVAc-W-N-B, PVAc with water beech wood joint (at 12%);
PVAc-W-C-B, PVAc with water beech wood joint (cycling 8-19-8%);
PVAc-0.5%-N-B, PVAc reinforced 0.5% nanocellulose beech wood joint (at 12%);
PVAc-0.5%-C-B, PVAc reinforced 0.5% nanocellulose beech wood joint (8-19-8%);
PVAc-1%-N-B, PVAc reinforced 1% nanocellulose beech wood joint (at 12%);
PVAc-1%-C-B, PVAc reinforced 1% nanocellulose beech wood joint (8-19-8%);
PVAc-2%-N-B, PVAc reinforced 2% nanocellulose beech wood joint (12%);
PVAc-2%-C-B, PVAc reinforced 2% nanocellulose beech wood joint (8-19-8%);
PVAc-N-S, Pure PVAc spruce wood joint (at 12%);
PVAc-C-S, Pure PVAc spruce wood joint (cycling 8-19-8%);
PVAc-W-N-S, PVAc with water spruce wood joint (at 12%);
PVAc-W-C-S, PVAc with water spruce wood joint (cycling 8-19-8%);
PVAc-0.5%-N-S, PVAc reinforced 0.5% nanocellulose spruce wood joint (at 12%);
PVAc-0.5%-C-S, PVAc reinforced 0.5% nanocellulose spruce wood joint (8-19-8%);
PVAc-1%-N-S, PVAc reinforced 1% nanocellulose spruce wood joint (at 12%);
PVAc-1%-C-S, PVAc reinforced 1% nanocellulose spruce wood joint (8-19-8%);
PVAc-2%-N-S, PVAc reinforced 2% nanocellulose spruce wood joint (12%);
PVAc-2%-C-S, PVAc reinforced 2% nanocellulose spruce wood joint (8-19-8%);

1 INTRODUCTION

With the evolving environmental movement, the furniture industry also has a grooving mission to utilize environmentally sound materials in its production and the products it supplies to customers. This trend is forcing the industry to look for renewable materials with a minimum environmental impact. Wood and wood-based materials, with their vital sustainability attributes, can offer endless opportunities for this mission. Wood is a renewable, recyclable, and biodegradable material with many unique properties such as high specific strength, flexibility, durability, reasonable fire performance, etc. These properties make wood the most acceptable of construction materials [1 - 3].

However, the performance of existing wood products and the development of new engineered wood products are highly dependent on the performance of wood adhesives. Adhesives play an essential role in the wood product industry. Formaldehyde-based adhesives are predominantly used in wood-based industries because of their high bonding strength and low cost. But, formaldehyde-based adhesives are not environmentally friendly because of the emission of formaldehyde [4]. Industries, especially producers of interior wood products, are under pressure to reduce formaldehyde emissions. PVAc-based adhesives are an excellent alternative to some formaldehyde-based adhesives. Waterborne PVAc adhesive is the most common and has been used in the wood products industry for over five decades [5]. It offers numerous advantages, such as good adhesion to wood, easy processing with a simple mixing method, excellent stability, and low dispersion cost [6]. PVAc has a low degree of toxicity and does not have an adverse effect on human health.

Despite these advantages, there has been some limitation to using PVAc in humid conditions and at higher temperatures. Moreover, some acidic additives can damage the wood substrate and affect the overall performance of wood joints. So far, two approaches have been used to increase the performance of PVAc: copolymerizing vinyl acetate with

more hydrophobic monomer or functional monomer [7] and blending PVAc with other adhesive or hardeners [8, 9]. These methods can improve specific properties of PVAc, but they reduce certain other properties like thermal stability. For instance, the water resistance and toughness of the adhesive can be improved by copolymerizing vinyl acetate with butyl acrylate and ethylene; however, copolymerization reduces its tensile modulus, especially at elevated temperatures [8]. Another alternative to alleviate the shortcoming of PVAc adhesive is the use of nanoparticles such as carbon nanotube [10] on physciomechanical properties of PVAc, nano-aluminum oxide [11] to improve bonding strength of PVAc, graphene [12] to improve PVAc strength and toughness, cellulose nanocrystals [13, 14] to see the effects of filler on thermal stability, or nanoclays [11] to improve the performance of PVAc at elevated temperature and humid condition. These particles were shown to have a beneficial effect on the properties of PVAc adhesives. The use of inorganic nanoparticles, as additives, for modifying wood adhesives has been studied, but the use of the inorganic nanoparticle introduced certain environmental and sustainability issues [15, 16].

Bio-based materials have excellent potential for producing high-value (low cost and low durability), low (environmental friendly) environmental impact products. Cellulose is one of the most abundant bio-based material available on earth. It is composed of a linear polysaccharide chain consisting of repeated β-(1→4)-D-glucopyranose units [17]. The production of cellulose in nanoscale is known as nanocellulose (NC). Both cellulose nanocrystals (CNC) and cellulose nanofiber (CNF) are the nanoforms of cellulose. CNC is produced by hydrolysis of various sources of cellulose, such as wood pulp, cotton, tunicin, etc. with the use of strong acids. The acid treatment removes most of the amorphous regions of cellulose and produces crystalline cellulose of 10-20nm in width and several hundred nanometers in length. CNF is produced by TEMPO oxidation (2,2,6,6-tetramethylpiperidine-1-oxyl radical) and high-pressure homogenization [18]. The crystallinity of CNF is lower due to the presence of amorphous regions. The hydroxyl group on these nanomaterials allows potential hydrogen bonding and surface modification. Their application in composite materials has gained attention due to their specific properties such as high strength, high stiffness, low weight, and biodegradability [3].

There has been great interest in bio-based binders and various cellulosic materials for application in the adhesive field [19-27]. Recent studies have focused on the reinforcement of adhesive with NC to improve their mechanical properties. These studies have found that stronger reinforcement occurred with fibers of smaller diameter and longer length. Several recent studies have investigated NC applications in composites, but only a few reports bonding with wood. Many researchers have focused on the reinforcement of urea-formaldehyde (UF), melamine-formaldehyde (MF), phenol-formaldehyde (PF), and polyvinyl acetate (PVAc) adhesives with nanocellulose. López-Suevos et al. [23] prepared lap-shear specimens with chemically modified, mechanically disintegrated, and chemical modification followed by mechanically disintegrated CNF reinforced PVAc (3% CNF). The results showed that chemically modified fibers added to PVAc adhesive improved wood bonding and heat resistance. Richter et al. (2009) [28] reported improved rheological behavior and bonding properties of 1C-PUR and water-based PVAc adhesive with the addition of CNF.

PVAc adhesive was reinforced with CNC at different concentrations (1%, 2%, and 3%) and then block shear tests were conducted under different loading [11]. The CNC improved the bonding strength of polyvinyl acetate adhesive in all conditions. The improvement was measured in terms of wood failure percentage in dry conditions and shear strength in wet conditions at elevated temperatures. Kawalerczyk et al. (2020) [29] investigated the effect of NC reinforcement in UF adhesive on the properties of plywood.

The studies have shown that CNC reinforcement led to significant improvement in the bonding quality of plywood. Rigg-Aguilar et al., (2020) [30] used micro and nano-fibrillated cellulose (MNFC) obtained from pineapple to reinforce PVAc and UF adhesive. The shear strength showed significant improvement with the addition of 0.5% MNFC to PVAc and 1% MNFC to the UF.

The stiffness of PVAc adhesive, widely used in wood products, can be improved by reinforcement with nanocellulose, a high stiffness material of plant origin. In this study, PVAc adhesive was reinforced separately with CNF and CNC with an aim to assess the comparative performance of CNC and CNF as reinforcing material. The performance of reinforced PVAc adhesives was analyzed by testing the shear strength of wood joints bonded with these adhesives. Two wood species such as beech, a hardwood and spruce, a softwood, were used to produce glued joint specimens. The effect of moisture cycling on the glue shear strength was also ascertained.

2 MATERIALS AND METHODS

2.1.Material

Defect-free beech (*Fagus sylvatica*) and spruce (*Picea abies* L) wood samples measuring 150 × 20 × 5 mm (l × b × h) and as per the standard [31] were used. The average density of the beech wood was 0.725 g/cm^3 and that of spruce wood was 0.389 g/cm^3. All samples were conditioned at a temperature of 20±2°C and RH of 65 ± 3% to an equilibrium moisture content of 12%. PVAc (Ag-Coll 8761/L D3) with a viscosity of 7000 to 13000 mPas at 23°C and density ranging between 0.9 to 1.1 g/cm^3 was used as the adhesive. Cellulose nanofiber (CNF) in dry form (5-200 nm width and 130 nm-225 µm length) was sourced from the University of Maine, and cellulose nanocrystals (CNC) in dry form (20 ± 5 nm width and 150 ± 39 nm length) was sourced from CelluForce, Windsor, Quebec, Canada.

2.2.Method

Three different concentrations (0.5%, 1.0%, and 2.0% w/w) of CNF and CNC were prepared separately by dispersing them with 50mL of water at room temperature. Nanocellulose was dispersed using a high-speed homogenizer (T 18 digital ULTRA - TURRAX® IKA-Werke, Staufen, Germany) followed by sonication (SONOPLUS HD 3100, Berlin, Germany). One part of NC (CNF or CNC) suspension was added to two parts of PVAc adhesive and mixed again thoroughly using the high-speed homogenizer followed by sonication. For comparison, reference samples were prepared with pure PVAc adhesive and diluted PVAc adhesive (2part PVAc with 1-part water). The details of the proportion of PVAc and NC used in this study are shown in Table 1.

2.2.1.Preparation of wood joints and shear test

Lap joints were prepared as per European standard [31] with NC (CNF/CNC) reinforced PVAc, diluted PVAc and PVAc adhesive. The adhesive was applied to the wood samples with a brush at a rate of 150 - 180g/m^2. Assembled samples were pressed with a hydraulic press (SCM-Villa, Verucchio, Rimini – Italy) with a specific pressure of 2.45 kg/cm^2 for 90 min at ambient temperature. The average thickness of the glue line was about 0.1 mm. The glued samples were conditioned at 20 ±2 °C and 65±3% RH for two weeks before testing. The moisture content of the samples was determined according to the standard procedure [32] and the wood density was determined according to the international standard [33]. The average modulus of elasticity of the beech and spruce wood were13549 MPa and 10057 MP a respectively.

Ten replicate samples were prepared for each concentration of CNF and CNC. The effect of moisture cycling on the strength of the glue bond was studied by subjecting the glued samples to moisture cycles at a constant temperature of 30 ± 2°C. The conditioned samples with 12% moisture content were first exposed to 30 ± 2 °C and 43 ± 2 RH (relative humidity) to arrive at 8% EMC (equilibrium moisture content), followed by exposure to 30 ± 2 °C and 86 ± 2 RH to reach 19% EMC. Then the samples were brought down to 8% EMC by exposing them to 30 ± 2°C and 43 ± 2 RH, and finally conditioned back to 12% moisture content by exposing them to 20 ± 2 °C and 65 ± 3% RH. Only one cycle was followed in this study. Samples were exposed at each temperature and RH combination until the weights stabilized in that condition.

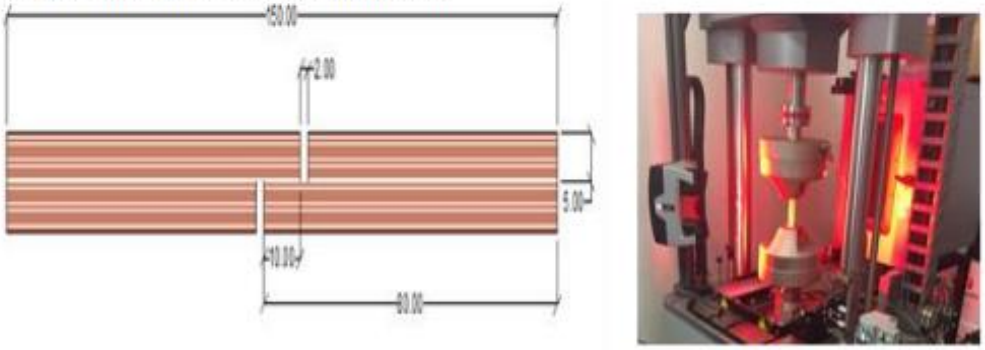

a) b)

Fig 1a). Dimensions (mm) of the shear test specimen, and **b)** Sample being tested in UTM.

Table 1 Summary of the used nanocellulose (CNF and CNC) reinforced adhesives and their concentrations (0.5%, 1%, and 2%).

	PVAc %	W%	0.5%	1%	2%
PVAc	100	-	-	-	-
PVAc+W	66.66	33.33	-	-	-
PVAc+ 0.5%CNF	66.66	-	33.33	-	-
PVAc+ 1% CNF	66.66	-	-	33.33	-
PVAc+ 2% CNF	66.66	-	-	-	33.33
PVAc+ 0.5%CNC	66.66	-	33.33	-	-
PVAc+ 1% CNC	66.66	-	-	33.33	-
PVAc+ 2% CNC	66.66	-	-	-	33.33

Abbreviations: CNF - Cellulose Nanofiber; CNC - Cellulose Nanocrystal, W- Water

The shear strength of wood joints was assessed as per European standard [31] with a universal testing machine equipped with a video extensometer (INSTRON® 5882, NORWOOD, USA). The test was performed at a constant speed of 5 ± 0.5 mm/min. The proportion of wood failure was also recorded for each test sample.

2.2.2.Scanning electron microscopy

The morphology of the bond line and penetration of the adhesive into the wood were observed with a scanning electron microscope (SEM) MIRA3 LMU (Tescan, a.s., Brno, Czech Republic). An accelerating voltage of 0.8 kV at a beam current of 6 pA was used to obtain high-quality SEM images.

2.2.3.Fourier transform infrared spectroscopy (FTIR-ATR)

Fourier transform infrared spectroscopy studies were performed with an FTIR spectrometer, (Nicolet, Křelovická, Czech Republic). Before analysis, the reinforced CNF/CNC samples were properly dried at room temperature for two days. The obtained samples were analyzed in a transmittance range of 4000 - 500 cm^{-1}.

2.2.4.Calculation of results

The tensile shear strength was calculated as per the equation 1:

$$\tau = \frac{F_{max}}{l \times b} \quad (1)$$

Where τ represents the tensile-shear strength along the fibers (MPa), F_{max} is the maximum force at breaking point (N), l is the length of overlap (mm), and b is the width of the specimen (mm).

The elastic stiffness of wood joints was determined using the equation 2.

$$E = \frac{\sigma 2 - \sigma 1}{\varepsilon 2 - \varepsilon 1} \times \frac{A}{L} \quad (2)$$

Where σ_1 and σ_2 are the stresses at 10% and 40% of maximum load and ε_1 and ε_2 are the corresponding strains at those stresses. The stress strain relationships are quite linear from 10% to 40% as observed from experiments. A is bonded area cross-section and L is length of sample between holding clamp.

2.2.5.Statistical analysis

STATISTICA 13 software (TIBCO Inc., USA) was used to analyze the data. Data were analyzed witha one-way analysis of variance (ANOVA). Duncan's test was performed to verify the results with a 95% confidence level. A correlation analysis was performed to ascertain the interaction between the individual characteristics.

3. RESULTS AND DISCUSSION:

An FTIR (Fourier-transform infrared spectroscopy) analysis was carried out to reveal the interaction of cellulose nanofiber with PVAc adhesive and the result is shown in Fig 2. FTIR spectra did not show any new peak after the addition of cellulose nanofiber to the PVAc adhesive. The FTIR peaks occur at 1725, 1430, 1377, and 1245 - 1275 cm^{-1} in PVAc adhesive represent carbonyl, methyl, methylene, and ester groups respectively [34]. As shown in Fig.2, an increase in the band intensity occupying the range from 3000 to 3500 cm^{-1} was observed with the addition of 1% CNF as compared to pure PVAc adhesive. This wide band is due to the -OH vibrations in cellulose nanofibers. The band at 2924 cm^{-1} is associated with asymmetric stretching CH_2 of cellulose. For pure PVAc, the band (region) at 3300 cm^{-1} is attributed to -OH stretching vibrations, while the 1425 cm^{-1} is associated with C-H bending of methyl group. The peak at 1433 cm^{-1} is mainly associated with crystalline cellulose, which is substantial for crystalline and weak for amorphous cellulose [35 - 37]. In the FTIR spectra of cellulose nanofiber, both crystalline and amorphous cellulose are present. According to Poletto et al. 2014 [35], the signals at 1053 cm^{-1} and 896 cm^{-1} indicate the presence of amorphous cellulose. In 1% CNF reinforced PVAc adhesive spectra, the intensity of the relevant peak at 1640 cm^{-1} increased, which was mostly due to the higher content of cellulose nanofiber.

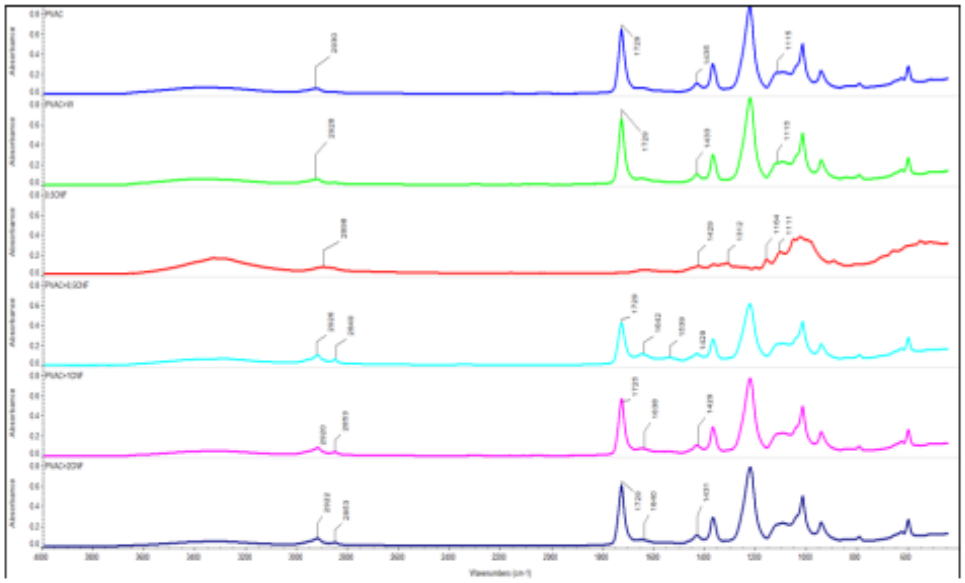

Fig.2 FTIR analysis of PVAc, CNF suspension and CNF reinforced PVAc adhesive

Fig. 3 shows the FTIR spectra of PVAc and CNC reinforced PVAc adhesive with different contents of CNC (0.5%, 1%, and 2%). At 3200-3400 cm^{-1}, the intensity of the band increased as the content of cellulose nanocrystalline (CNC) increases. The absorption peaks at 3392 cm^{-1}, 3339 cm^{-1}, and 1642 cm^{-1} are attributed to the hydroxyl group of free water molecules adsorbed onto the CNC surface. The peak at 3300 and 1650 cm^{-1} was found to increase with higher content of CNC. The peak intensity at 2924 cm^{-1} also increased as CNC increased in the PVAc matrix, which shows the stretching of C-H of cellulose. The band at 2874 cm^{-1} and 1427 cm^{-1} was attributed to the stretching of CH_2 and C-H groups in crystalline cellulose. This adsorption band corresponds to the -OH stretching vibration between PVAc and CNC. The PVAc adhesive signal presented at 1730, 1433, 1370, 1245-1275 cm^{-1} shows carbonyls, methyl, methylene, and an ester group respectively. The band at 1028 cm^{-1} and 1058 cm^{-1} shows C-O bonding on the cellulose ring at positions 3 and 6, and at 1166 cm^{-1} there is a bond stretching C-O-C in xylose chains, which is one of the cellulose components.

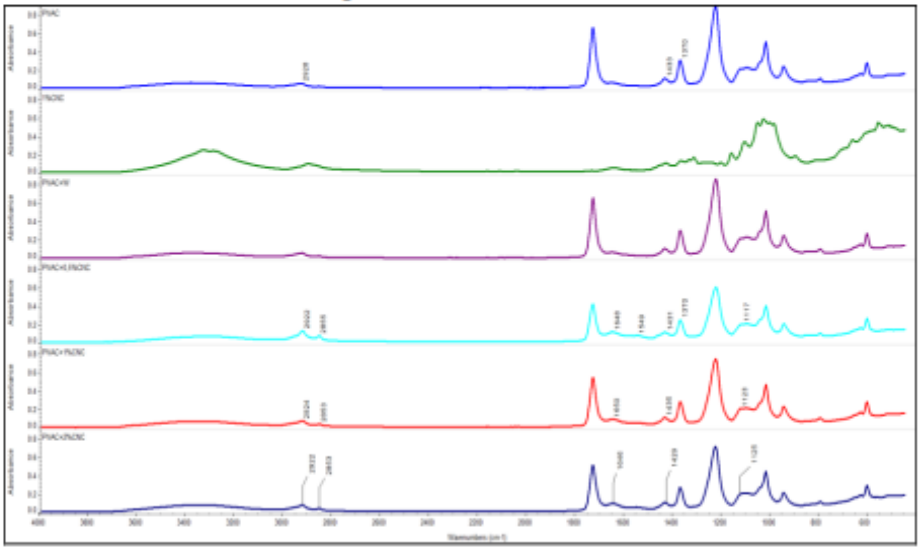

Fig.3 FTIR analysis of pure PVAc and CNC reinforced PVAc adhesive

Fig. 4 shows the elastic stiffness of beech wood joints bonded with pure PVAc, PVAc with water, CNC and CNF reinforced PVAc adhesive. Direct dispersion of nanocellulose with pure PVAc adhesive was very difficult; hence CNC and CNF were first dispersed in water and then added to PVAc adhesive. The addition of CNC and CNF dramatically improved the elastic stiffness of the adhesive joints. Fig. 4 shows that the joints bonded with PVAc exhibited an average elastic stiffness of 2200 N/m in beech wood. Dilution of PVAc with water caused a significant decrease in the joint stiffness (1600 N/m). However, reinforcement of PVAc with CNC and CNF improved the joint stiffness. The improvement was more significant in CNC reinforced adhesive as compared to CNF reinforced adhesive at 12% MC. In the case of CNC, the improvement in the elastic stiffness of beech wood joints was in the range of 39% to 65%, as compared to pure PVAc bonded joints and 48-119% as compared to diluted PVAc bonded joints depending on CNC concentration. Among the 3 concentrations tried, 1% CNC loading gave the best results in terms of improvement in elastic stiffness. The results are in line with the results reported by [11]. The authors used CNC reinforced PVAc adhesive and found that average values of MOE were affected significantly by the addition of CNC; the addition of 1% of CNC to PVAc adhesive increased the average MOE by 48% and further, addition did not change the MOE. In the formulation of CNC reinforced PVAc, the added CNC seems to positively affect the mean value of elastic stiffness, which is supposed to be an interlocking effect due to increased cross-linking of a methylene group from PVAc and hydroxyl groups from CNF as well as cellulose in the wood. Besides, the inherent stiffness of CNC (~ 160 GPa) also contributes to the stiffness of the joints. The increase in the elastic stiffness could also be attributed to the high-stress transfer efficiency because of the larger surface area of CNC. The improvement in the elastic stiffness, as compared to joints bonded with pure PVAc, is almost negligible when CNF was added as a reinforcing material. In fact, the elastic stiffness marginally decreased with the increase in the CNF concentrations. The negative impact of the bound moisture at CNF-PVAc interfaces is considered to be responsible for the limited improvement. However, the values were higher when compared with joints bonded with diluted PVAc. This suggests that the polymer chain segments in the vicinity of the CNF are rather free to move as the stiffness of CNF is comparatively less concerning CNC.

Effect of moisture cycling condition on beech wood joints bonded with PVAc, diluted PVAc, CNC and CNF reinforced PVAc adhesive have shown Fig. 4. After cyclic moisture exposure, beech wood joints bonded with PVAc and diluted PVAc had an elastic stiffness of 2100 N/m and 1250 N/m respectively. Pure PVAc adhesive exhibited satisfactory performance against cyclic moisture exposure as the elastic stiffness values, before and after cyclic moisture exposure, were almost the same without any significant difference. But the joints bonded with diluted PVAc suffered the most deterioration in elastic stiffness following cyclic moisture exposure. However, it is interesting to note that the addition of CNC and CNF significantly improved the elastic stiffness of PVAc adhesive joints following cyclic moisture exposure. The improvement was substantial in the case of CNF reinforcement compared to CNC reinforcement. For instance, cyclic moisture exposure of CNC reinforced PVAc adhesive bonded joints exhibited 6% to 14% higher elastic stiffness, while CNF reinforced adhesive exhibited 49% to 78% higher elastic stiffness as compared to CNC/CNF reinforced adhesive before cyclic moisture exposure. The addition of nanocellulose reduces the ability of water absorption and the diffusion coefficient of polymers. The lower water absorption and decreased diffusion coefficient of the material reduce the movement of atoms within a material which reduce the activation energy and a low practicle temperature range which might be due to the high crystallinity

of CNC. The reason accounting for the lower sensitivity of PVAc-CNF adhesive to water could be the stronger reinforcing effect of CNF when the polymer matrix is ductile. Since the water diffusion inside the adhesive joint film has a plasticizing effect, the adhesive joints in the rubbery state and the presence of CNF would lead to a strong increase in elastic stiffness. These results are in line with the results reported by [38], where the authors found that the inclusion of CNF within the PVAc adhesive matrix led to a decrease in the moisture absorption by PVAc adhesive.

Spruce wood joints bonded with PVAc, diluted PVAc, CNC and CNF reinforced PVAc adhesive are shown in Fig. 5. There was no significant difference in the elastic stiffness of CNC and CNF (0.5%, 1%, and 2%) reinforced PVAc at 12% MC and after moisture cycling conditioning, while it was 2 times higher compared to diluted PVAc adhesive. Penetration of PVAc adhesive itself into spruce wood is as such limited as spruce is a nonporous wood with very poor liquid permeability [39]. The addition of NC to PVAc further increases the viscosity of the adhesive and this, in turn, might be affecting the penetration of the NC reinforced adhesive into the wood. Limited penetration with poor interlocking might be the cause for poor improvement in the elastic stiffness of NC reinforced joints in spruce wood.

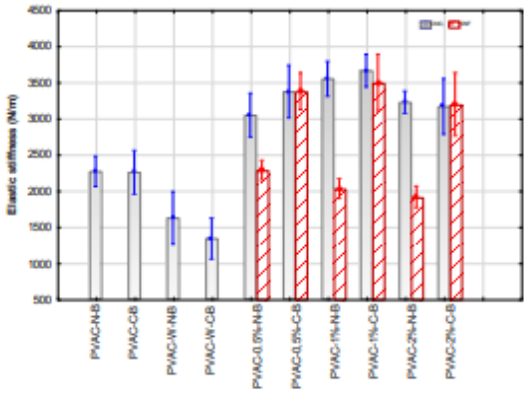

Fig.4 Elastic stiffness of beech wood joints bonded with PVAc and varying contents of CNC, CNF reinforced adhesive

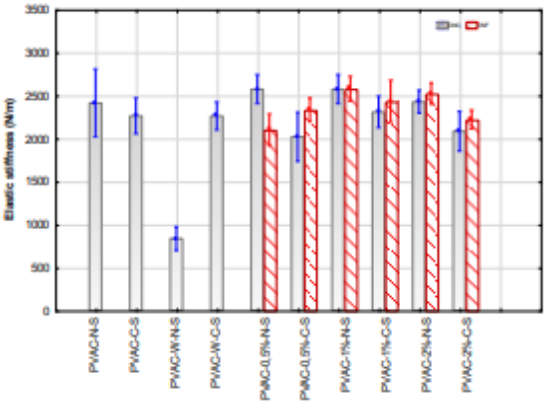

Fig.5 Elastic stiffness of spruce wood joints bonded with PVAc and varying contents of CNC, CNF reinforced adhesive

Fig.6 shows the shear strength of beech wood joints bonded with PVAc, diluted PVAc, CNC and CNF reinforced PVAc adhesive conditioned at 12% moisture content as well as exposed to cyclic moisture conditions. The average shear strength of pure PVAc adhesive bonded beech wood joints was 10 MPa and cyclic moisture exposure did not affect the shear strength. However, the addition of water to PVAc caused a significant decrease in the shear strength. It is interesting to note that the addition of CNF could able to restore the loss in shear strength to a larger extent, while reinforcement with CNC failed to compensate for the strength loss. The differential effect of CNC and CNF on the shear strength can be attributed to their chemical composition and morphology. CNF is comparatively longer than CNC and contains both amorphous and crystalline regions. However, CNC mostly contains crystalline regions. Due to the presence of an amorphous region, the number of hydroxyl groups available on the surface of CNF is manyfold higher than that available on the surface of CNC. This makes CNF more hygroscopic than CNC. Hydroxyl molecules, readily available on CNF, easily form hydrogen bonding with accessible water molecules available in the diluted PVAc thereby minimizing the effect of

dilution on shear strength. On the other hand, CNC has limited availability of hydroxyl molecules on its surface and might not be absorbing much of the available water in the diluted PVAc, leaving the excess water in the system to interfere with the bond and affect the shear strength.

As highlighted earlier, cyclic moisture exposure did not cause any significant variation in the bond strength of pure PVAc bonded joints. However, joints bonded with diluted PVAc and NC reinforced PVAc showed variation in the shear strength and the variations were not consistent. For instance, 0.5% and 2% CNC loading caused a marginal reduction in the bond strength, while 1% CNC significantly improved the bond strength following cyclic moisture exposure. Similarly, 0.5% CNF reinforcement improved the shear strength significantly, while CNF loading of 1% and 2% caused a reduction in the shear strength in the samples exposed to cyclic moisture variation. Despite all these variations, it is quite apparent that CNF reinforcement has the potential of improving the shear strength of PVAc joints and the results could have been better realized if the NC could have been added to PVAc without dilution with water.

Fig.7 shows the shear strength of spruce wood joints bonded with PVAc, diluted PVAc, CNC and CNF reinforced PVAc adhesive conditioned at 12% moisture content as well as exposed to cyclic moisture conditions. The average shear strength of pure PVAc adhesive bonded spruce wood joints was about 4.1 MPa and following cyclic moisture exposure the average shear strength reduced to 3.4 MPa. However, the dilution of PVAc with water caused a significant decrease (~ 80%) in the shear strength. Strength reduction was surprisingly restored with the addition of NC and both the CNC and CNF showed the comparable effect. The trend of results of spruce wood was almost similar to that of beech wood through the shear strength values were significantly less for spruce as compared to beech wood. Lower glue shear strength in spruce wood can be attributed to its lower inherent strength and lower permeability as compared to beech wood. Lower permeability can hinder glue penetration and interlocking. The highest shear strength was obtained at 1% CNF reinforced PVAc adhesive. Joints bonded with 1% CNF reinforced PVAc adhesive showed comparable shear strength to that of pure PVAc adhesive, while it was almost 8 times higher as compared to pure PVAc adhesive.

From the foregoing discussion, it is apparent that nanocellulose reinforced PVAc has the potential to improve joint stiffness and joint strength even after cyclic moisture exposure conditions. Considering the strong reinforcing potential of nanocellulose, it is certain that the inclusion of CNF and CNC in PVAc adhesive can improve the performance of wood joints bonded with PVAc. However, research results on the application of nanocellulose for PVAc wood adhesive reinforcement have been very meager [23].

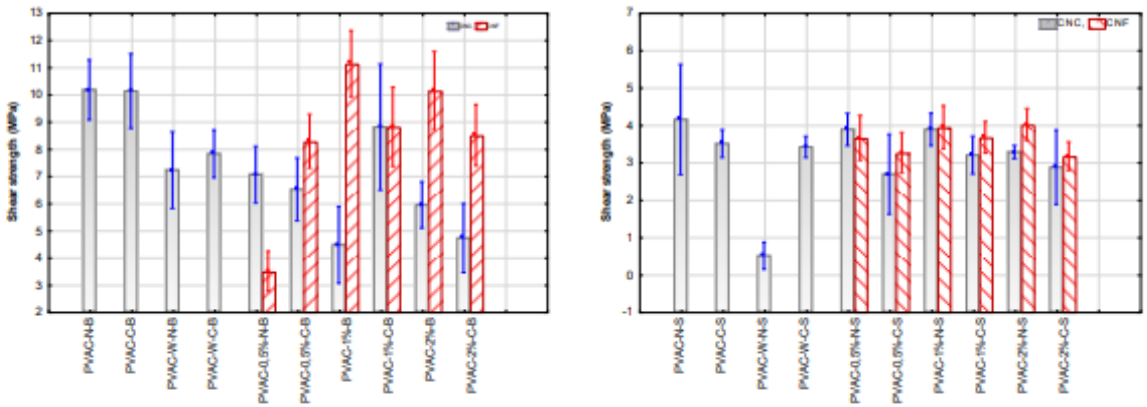

Fig.6 Shear strength of beech wood joints bonded with PVAc and varying contents of CNC and CNF reinforced adhesive

Fig.7 Shear strength of spruce wood joints bonded with PVAc and varying contents of CNC and CNF reinforced adhesive

Fig. 8 shows the wood failure percentage of beech wood joints bonded with PVAc, diluted PVAc, CNC and CNF reinforced PVAc adhesive. Higher wood failure indicates better bonding quality of the glue. Joints bonded with pure PVAc adhesive exhibited 90% wood failure. However, the dilution of PVAc adhesive created a weaker bond line, resulting in lower wood failure. Reinforcement of PVAc with CNC as well as CNF could be able to restore the glue quality which was apparent from the increased wood failure percentage, not only in the 12% moisture conditioned samples but also in the samples exposed to cyclic moisture conditions. All three levels of reinforcement gave comparable results with a wood failure between 90-100%.

Fig. 9 shows the average wood failure percentage of spruce wood joints bonded with PVAc, diluted PVAc, CNC and CNF reinforced PVAc adhesive. The results are almost similar to those of beech wood joints bonded with reinforced adhesive, except for the fact that CNC gave corporately better results than CNF with a wood failure in the range of 85-95%. Cycling moisture exposure had no significant detrimental effect on the bond quality as ascertained from the wood failure percentage. The increase in the proportion of wood failure with the addition of CNF and CNC to the PVAc adhesive suggests that CNF and CNC made the bond line of PVAc stronger. Several researchers reported a strong reinforcing effect of CNC on the formation of the network structure due to hydrogen bonding [40].

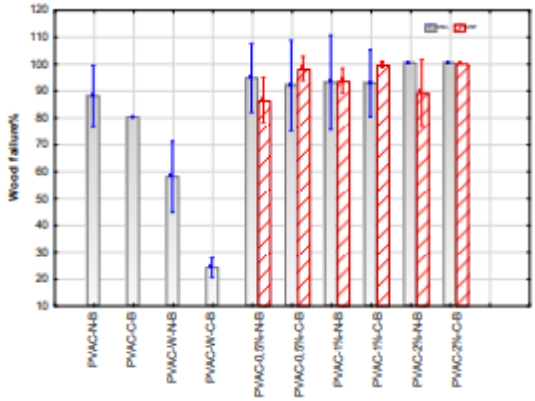

Fig.8 Wood failure % of beech wood joints bonded with PVAc and varying contents of CNC, CNF reinforcement

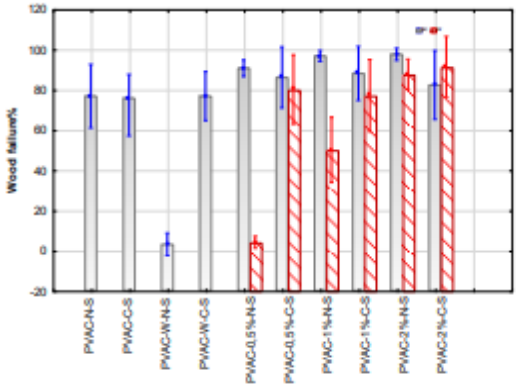

Fig.9 Wood failure % of spruce wood joints bonded with PVAc and varying contents of CNC, CNF reinforcement

SEM (scanning electron microscope) images of beech and spruce wood joints glued with PVAc and PVAc reinforced with 1% CNF/CNC are shown in Fig.10. Figure 10a-c shows the bond line of beech wood glued joints with pure PVAc, 1% CNF reinforced PVAc, and 1% CNC reinforced PVAc respectively. Adhesive penetration into the vessel lumens can be seen with pure PVAc adhesive, resulting in a thinner bond line (Fig 10a), whereas thicker bond lines were observed in PVAc adhesive reinforced with CNF and CNC (Fig. 10 b-c). Similarly, adhesive penetration can also be seen into the tracheid lumens in spruce wood joints bonded with pure PVAc adhesive (Fig. 10d), resulting in a thinner bond line, whereas a thicker bond line has been observed with CNF and CNC reinforced adhesive (Fig. 10 e-f). PVAc is a gap-filling adhesive and a proper bond line is necessary for better load transfer. The morphology of the bond line indicates that the addition of

nanocellulose, in addition to reinforcing the adhesive, works as a filler and arrests excessive penetration of adhesive into the wood by preventing starved joints. As a result, an improved bond line of wood joints forms and the improved bond line is propitious to load transfer. This may be one of the reasons why nanocellulose reinforcement improved the stiffness of adhesive joints. Another reason may be that the local bridging of nanocellulose (CNF or CNC) considerably restrains the plastic deformation in PVAc adhesive.

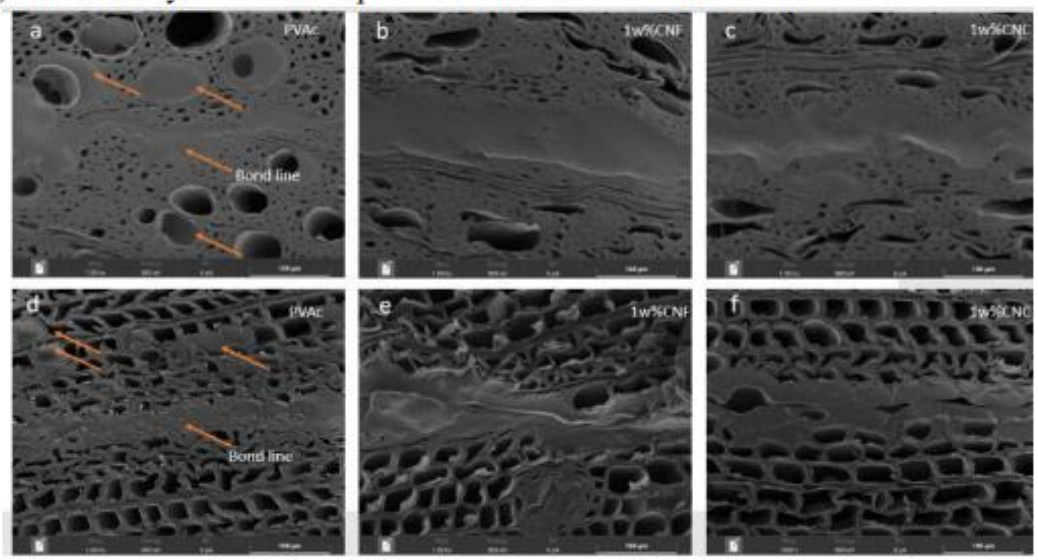

Fig.10 SEM images of beech wood joint: a) PVAc b) 1% CNF reinforced PVAc c)1% CNC reinforced PVAc; spruce wood joint: d) PVAc e) 1% CNF reinforced PVAc f) 1% CNC reinforced PVAc, at 12% of moisture content

The effect of cyclic moisture exposure on the morphology of the bond line is shown in Fig. 11 (a-f). The SEM images show that cyclic exposure causes the development of microcracks in pure PVAc bonded joints in both species. However, the bond line appears to be very intact in nanocellulose reinforced PVAc bonded joints. This suggests that reinforcement of PVAc with nanocellulose increases the stiffness of the bond line to withstand the stresses developed during shrinkage and swelling of the wood during cyclic moisture exposure. The improvement of the bond line's morphological stability can also be explained by the interaction of CNF and CNC in the PVAc matrix. Availability of the large number of hydroxyl groups with CNF/CNC, might be making hydrogen-bond network with the PVAc adhesive.

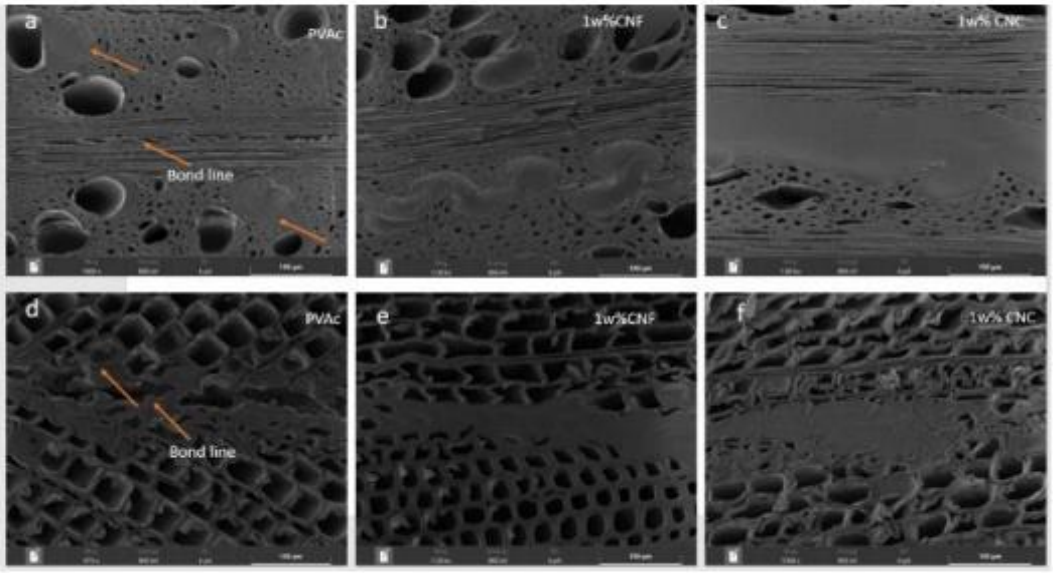

Fig.11 SEM images of beech wood joint: a) PVAc b) 1% CNF reinforced PVAc c)1% CNC reinforced PVAc; spruce wood joint: d) PVAc e) 1% CNF reinforced PVAc f) 1% CNC reinforced PVAc after moisture cycling

CONCLUSIONS

Nanocellulose (CNF and CNC) reinforced adhesives were prepared by mixing CNF and CNC suspension in PVAc adhesive. The addition of nanocellulose (CNF and CNC) to PVAc adhesive improved the elastic stiffness of the joints as well as the bond quality. The addition of nanocellulose stabilized the bond line against cyclic moisture exposure and thereby improved the mechanical properties. The bonding ability of CNF and CNC reinforced PVAc adhesives is evident from the increased proportion of wood failure. In this study, the dispersion of CNF and CNC in PVAc was achieved by premixing nanocellulose with water and subsequently, mixing the suspension with PVAc. This has caused a dilution of PVAc. Despite this, the results are quite encouraging. If CNF and CNC dispersion in PVAc can be achieved without dilution of the adhesive, then the reinforcing ability of CNF and CNC can be better realized.

ACKNOWLEDGMENTS

The author thanks for the financial support by operational research development and education in 4th industrial revolution no.CZ.02.1.01/0.0/0.0/16_019/0000803 of advance research supported by the forestry and wood science sector´s adaptation to global change, and by the International Grant Agency (IGA) of the Faculty of Forestry and Wood Science at Czech University of Life Science (B_06_2019).

REFERENCES

[1] Geng S, Haque MM, Oksman K. Crosslinked poly (vinyl acetate) (PVAc) reinforced with cellulose nanocrystals (CNC): Structure and mechanical properties. Composites Science and Technology. 2016 Apr 1;126:35-42.

[2] Gan PG, Sam ST, Abdullah MF, Omar MF. Thermal properties of nanocellulose-reinforced composites: A review. Journal of Applied Polymer Science. 2020 Mar 15;137(11):48544.

[3] Niinivaara E, Cranston ED. Bottom-up assembly of nanocellulose structures. Carbohydrate Polymers. 2020 Nov 1;247:116664.
[4] Zhao LF, Liu Y, Xu ZD, Zhang YZ, Zhao F, Zhang SB. State of research and trends in development of wood adhesives. Forestry Studies in China. 2011 Sep;13(4):321-6.
[5] Stoeckel F, Konnerth J, Gindl-Altmutter W. Mechanical properties of adhesives for bonding wood—A review. International Journal of Adhesion and Adhesives. 2013 Sep 1;45:32-41.
[6] Jaffe HL, Rosenblum FM, Daniels W. Polyvinyl acetate emulsions for adhesives. In Handbook of Adhesives 1990 (pp. 381-400). Springer, Boston, MA.
[7] Qiao L, Easteal AJ, Bolt CJ, Coveny PK, Franich RA. Improvement of the water-resistance of poly (vinyl acetate) emulsion wood adhesive. Pigment & resin technology. 2000 Jun 1.
[8] Qiao L, Easteal AJ. Aspects of the performance of PVAc adhesives in wood joints. Pigment & Resin Technology. 2001 Apr 1.
[9] Kaboorani A, Riedl B. Improving performance of polyvinyl acetate (PVA) as a binder for wood by combination with melamine-based adhesives. International Journal of Adhesion and Adhesives. 2011 Oct 1;31(7):605-11.
[10] Maksimov RD, Bitenieks J, Plume E, Zicans J, Merijs Meri R. The effect of introduction of carbon nanotubes on the physicomechanical properties of polyvinyl acetate. Mechanics of composite materials. 2010 Sep;46(3):237-50.
[11] Kaboorani A, Riedl B, Blanchet P, Fellin M, Hosseinaei O, Wang S. Nanocrystalline cellulose (NCC): A renewable nano-material for polyvinyl acetate (PVA) adhesive. European Polymer Journal. 2012 Nov 1;48(11):1829-37.
[12] Khan U, May P, Porwal H, Nawaz K, Coleman JN. Improved adhesive strength and toughness of polyvinyl acetate glue on addition of small quantities of graphene. ACS applied materials & interfaces. 2013 Feb 27;5(4):1423-8.
[13] Aydemir D, Gündüz G, Aşık N, Wang A. The Effects of Poly (vinyl acetate) Filled with Nanoclay and Cellulose Nanofibrils on Adhesion Strength of Poplar and Scots Pine Wood. Wood Industry/Drvna Industrija. 2016 Jan 1;67(1).
[14] Mabrouk AB, Dufresne A, Boufi S. Cellulose nanocrystal as ecofriendly stabilizer for emulsion polymerization and its application for waterborne adhesive. Carbohydrate polymers. 2020 Feb 1;229:115504.
[15] Singha AS, Thakur VK. Mechanical properties of natural fibre reinforced polymer composites. Bulletin of Materials Science. 2008 Oct;31(5):791-9.
[16] Wang Z, Gu Z, Hong Y, Cheng L, Li Z. Bonding strength and water resistance of starch-based wood adhesive improved by silica nanoparticles. Carbohydrate Polymers. 2011 Aug 1;86(1):72-6.
[17] Gupta PK, Raghunath SS, Prasanna DV, Venkat P, Shree V, Chithananthan C, Choudhary S, Surender K, Geetha K. An update on overview of cellulose, its structure and applications. Cellulose. 2019 May 13:846-1297.
[18] Henriksson M, Berglund LA, Isaksson P, Lindström T, Nishino T. Cellulose nanopaper structures of high toughness. Biomacromolecules. 2008 Jun 9;9(6):1579-85.
[19] Hon DN. Cellulosic adhesives. (1989)
[20] Zhang X, Young RA. Adhesion properties of cellulose films. MRS Online Proceedings Library (OPL). 1999;586.
[21] Bao-Xiu Z, Peng W, Tong Z, Chun-yun C, Jing S. Preparation and adsorption performance of a cellulosic-adsorbent resin for copper (II). Journal of applied polymer science. 2006 Mar 15;99(6):2951-6.

[22] Veigel S, Müller U, Keckes J, Obersriebnig M, Gindl-Altmutter W. Cellulose nanofibrils as filler for adhesives: effect on specific fracture energy of solid wood-adhesive bonds. Cellulose. 2011 Oct;18(5):1227-37.
[23] López-Suevos F, Eyholzer C, Bordeanu N, Richter K. DMA analysis and wood bonding of PVAc latex reinforced with cellulose nanofibrils. Cellulose. 2010 Apr;17(2):387-98.
[24] Ayrilmis N, Kwon JH, Lee SH, Han TH, Park CW. Microfibrillated-cellulose-modified urea-formaldehyde adhesives with different F/U molar ratios for wood-based composites. Journal of Adhesion Science and Technology. 2016 Sep 16;30(18):2032-43.
[25] Kojima Y, Isa A, Kobori H, Suzuki S, Ito H, Makise R, Okamoto M. Evaluation of binding effects in wood flour board containing ligno-cellulose nanofibers. Materials. 2014 Sep;7(9):6853-64.
[26] Cataldi A, Berglund L, Deflorian F, Pegoretti A. A comparison between micro-and nanocellulose-filled composite adhesives for oil paintings restoration. Nanocomposites. 2015 Oct 2;1(4):195-203.
[27] Mahrdt E, Pinkl S, Schmidberger C, van Herwijnen HW, Veigel S, Gindl-Altmutter W. Effect of addition of microfibrillated cellulose to urea-formaldehyde on selected adhesive characteristics and distribution in particleboard. Cellulose. 2016 Feb;23(1):571-80.
[28] Richter K, Bordeanu N, López-Suevos F, Zimmermann T. Performance of cellulose nanofibrils in wood adhesives. Proceedings of the Swiss Bonding, Rapperswil. 2009:239-46.
[29] Kawalerczyk J, Dziurka D, Mirski R, Siuda J, Szentner K. The effect of nanocellulose addition to phenol-formaldehyde adhesive in water-resistant plywood manufacturing. BioResources. 2020 May 22;15(3):5388-401.
[30] Rigg-Aguilar P, Moya R, Oporto-Velásquez GS, Vega-Baudrit J, Starbird R, Puente-Urbina A, Méndez D, Potosme LD, Esquivel M. Micro-and nanofibrillated cellulose (MNFC) from pineapple (Ananas comosus) stems and their application on polyvinyl acetate (PVAc) and urea-formaldehyde (UF) wood adhesives. Journal of Nanomaterials. 2020 Aug 1;2020.
[31] EN. Adhesives for load-bearing timber structures-test methods-part 1: determination of longitudinal tensile shear strength. EN 302-1.2013.
[32] ISO. Physical and mechanical properties of wood - Test methods for small clear wood specimens -- Part 1: Determination of moisture content for physical and mechanical tests. International Organization for Standardization. ISO 13061-1. 2014
[33] ISO. Physical and mechanical properties of wood - Test methods for small clear wood specimens -- Part 2: Determination of density for physical and mechanical tests. International Organization for Standardization. Geneva. Switzerland. ISO 13061-2. 2014.
[34] Mansoori Y, Akhtarparast A, Reza Zamanloo M, Imanzadeh G, Masooleh TM. Polymer–montmorillonite nanocomposites: chemical grafting of polyvinyl acetate onto Cloisite 20A. Polymer Composites. 2011 Aug;32(8):1225-34.
[35] Poletto M, Ornaghi HL, Zattera AJ. Native cellulose: structure, characterization and thermal properties. Materials. 2014 Sep;7(9):6105-19.
[36] Lu J, Askeland P, Drzal LT. Surface modification of microfibrillated cellulose for epoxy composite applications. Polymer. 2008 Mar 3;49(5):1285-96.
[37] Sanaeishoar H, Sabbaghan M, Argyropoulos DS. Ultrasound assisted polyacrylamide grafting on nano-fibrillated cellulose. Carbohydrate polymers. 2018 Feb 1;181:1071-7.

[38] Chaabouni O, Boufi S. Cellulose nanofibrils/polyvinyl acetate nanocomposite adhesives with improved mechanical properties. Carbohydrate Polymers. 2017 Jan 20; 156:64-70.
[39] Liese W, Bauch J. On anatomical causes of the refractory behavior of spruce and Douglas fir. Institute of Wood Science. Journal. 1967 Jan 1;4(1):3-14.
[40] Hajji P, Cavaille JY, Favier V, Gauthier C, Vigier G. Tensile behavior of nanocomposites from latex and cellulose whiskers. Polymer Composites. 1996 Aug;17(4):612-9.

4.2.2 Incorporating of cellulose nanofiber (CNF) and cellulose nanocrystals (CNC) to enhance the strength and stiffness property of polyurethane adhesive (1C-PUR)

Manuscript:

Kamboj G, Gaff M, Smardzewski J, Haviarová E, Hui D, Rousek, R, Das S, Rezaei F, Sethy A.K. (2022). Incorporating of cellulose nanofiber (CNF) and cellulose nanocrystals (CNC) to enhance the strength and stiffness property of polyurethane adhesive (1C-PUR).

Incorporating of cellulose nanofiber (CNF) and cellulose nanocrystals (CNC) to enhance the strength and stiffness property of polyurethane adhesive (1C-PUR)

Gourav Kamboj[1], Milan Gaff[1, 2], Jerzy Smardzewski[3], Eva Haviarová[4], David Hui[5], Radim Rousek[6], Sumanta Das[1], Fatemeh Rezaei[1], Anil Kumar Sethy[1,7]

[1]Department of Wood Processing and Biomaterials, Czech University of Life Sciences in Prague, Kamýcká 1176, Prague 6 - Suchdol, 16521 Czech Republic

[2]Department of Furniture, Design and Habitat (FFWT), Mendel University in Brno, Zemědělská 1665, 613 00 Brno-sever-Černá Pole, Czech Republic

[3]Poznan University of Life Sciences, Faculty of Forestry and Wood Technology, Department of Furniture Design, Wojska Polskiego 28, 60-637 Poznan, Poland

[4]Purdue University, Department of Forestry and Natural Resources, West Lafayette, IN 47907-2033, USA

[5]Deptartment of Mechanical Engineering, University of New Orleans, New Orleans, LA 70124, USA;

[6]Department of Wood Science, Faculty of Forestry and Wood Technology, Mendel University in Brno, Zemědělská 1665, 613 00 Brno-sever-Černá Pole, Czech Republic

[7]Institute of Wood Science and Technology, 18th Cross, Malleswaram, Bangalore-560003, India

ABSTRACT

In this study, nanocellulose reinforced adhesive was prepared by mixing the modified cellulose nanofiber (CNF) and cellulose nanocrystal (CNC) in PUR adhesive. The reinforced adhesive used to glue spruce (*Picea abies* L) and beech (*Fagus sylvatica* L*)* wood joints and elastic stiffness, shear strength were investigated to ascertain the bonding behavior of the glue line. The different concentrations of CNF and CNC (0.5%, 1%, and 2% w/w) affected the tensile properties at 12% moisture content and after moisture cycling conditions (8-19%) were studied. The elastic stiffness and shear strength increased and the optimum value at 1% of CNF and CNC reinforced PUR (polyurethane) adhesive was obtained. FTIR (Fourier-treansform infrared spectroscopy) and DSC (Differential scanning calorimeter) analyses showed the molecular interaction between nanocellulose and PUR adhesive; where the glass transition temperature increased for all the nanocomposite compared to the PUR adhesive. The glue line was assessed by SEM (Scanning electron microscope), and a significant improvement can be seen by the addition of nanocellulose at 12% moisture content and after moisture cycling condition.

Keywords: Cellulose Nanofiber, Cellulose Nanocrystal, PUR Adhesive, Chemical Modification

ABBREVIATION

PUR-N-B, Pure PUR beech wood joint (at 12% moisture);
PUR-C-B, Pure PUR beech wood joint (cycling 8-19-8%);
PUR-0.5-N-B, PUR reinforced 0.5% nanocellulose beech wood joint (at 12% moisture);

PUR-0.5-C-B, PUR reinforced 0.5% nanocellulose beech wood joint (cycling 8-19-8%);
PUR-1-N-B, PUR reinforced 1% nanocellulose beech wood joint (at 12% moisture);
PUR-1-C-B, PUR reinforced 1% nanocellulose beech wood joint (cycling 8-19-8%);
PUR-2-N-B, PUR reinforced 2% nanocellulose beech wood joint (at 12% moisture);
PUR-2-C-B, PUR reinforced 2% nanocellulose beech wood joint (cycling 8-19-8%);
PUR-0.5-N-S, PUR reinforced 0.5% nanocellulose spruce wood joint (at 12% moisture);
PUR-0.5-C-S, PUR reinforced 0.5% nanocellulose spruce wood joint (cycling 8-19-8%);
PUR-1-N-S, PUR reinforced 1% nanocellulose spruce wood joint (at 12% moisture);
PUR-1-C-S, PUR reinforced 1% nanocellulose spruce wood joint (cycling 8-19-8%);
PUR-2-N-S, PUR reinforced 2% nanocellulose spruce wood joint (at 12% moisture);
PUR-2-C-S, PUR reinforced 2% nanocellulose spruce wood joint (cycling 8-19-8%);

1. INTRODUCTION

The use of adhesive bonding is increasing in many industries, compared to the conventional joining technique. Polyurethane adhesive has become one of the most widely used for wood-based industry, packaging applications, and automotive industry, formed by the reaction of isocyanate groups and monomers of hydroxyl groups. It is well known for its excellent adhesion, flexibility, and exemplary performance in low-temperature conditions. Polyurethane is made from petrochemical products, which is costly and non-biodegradable. These chemical products cause severe environmental damage and contribute to the global supply shortage of petrochemical products. To reduce these types of problems, biomaterial-reinforced PUR adhesive has attracted attention from researchers.

Nowadays, the application of green, renewable, and sustainable materials is essential for industrial application and has increased researchers and industry's interest in seeking materials that are alternative to non-renewable sources. In this context, cellulose, starch, alginate, chitin, chitosan, and gelatin have been revealed to be promising candidates concerning their abundant availability from various sources [1]. During the last two decades, considerable academic and industrial research made efforts that have been devoted to developing cellulose nanocrystals and cellulose nanofibers [2]. There is a strong reason that: cellulose is the most abundant renewable material with its advantage of being available and obtained from plants, algae, tunicates, and some bacteria [3, 4, 5].

These nanocelluloses are in the form of cellulose nanofiber (CNF), cellulose nanocrystal (CNC), and bacterial nanocellulose (BC), which can be obtained by mechanical and chemical treatments. Cellulose nanocrystals (CNC) have a high crystalline region with a nano-rod thickness of 3-10nm and a length of a few hundred nanometers. They can be extracted from the pulp by using the acid hydrolysis process, which already has been industrialized. Cellulose nanofiber (CNF) is a semi-crystalline form of nanocellulose with a thickness of 5-30nm and a length of a few micrometers. The mechanical fibrillation of pulp fibers produces them by using the homogenization technique. These nanomaterials have excellent properties such as high strength and stiffness, low coefficient of thermal expansion, low density, dimensional stability, and ability to modify their surface chemistry [6, 7, 8, 9, 10]. Due to their excellent properties, both CNC and CNF have wide applications in the automotive industry, drug delivery, tissue engineering, packaging, water filtration, and wood-based adhesive industry. Researchers have improved the strength of PUR by adding nanofillers such as carbon nanotube, graphene, nano-silica, and nanocellulose [11, 12, 13].

The chemical modification allows nanocellulose reinforcing properties in the polymers and improves the mechanical properties of nanocomposites. In conventional adhesives, nanocellulose works as a bio-based reinforcing agent. The dispersion of nanocellulose in synthetic adhesive plays a vital role in enhancing the physical and mechanical properties. Nanocellulose is dispersed easily in a polar solvent, but polar solvents are not compatible with PUR adhesive. The surface modification of nanocellulose through its hydroxyl groups (-OH) makes it hydrophobic and has significantly increased its potential to disperse in non-polar solvents. With the reaction of oxidation and acetylation, a different range of chemical functionalities could be placed on the nanocellulose surface [14, 15]. These modifications have played an important role in modulating the surface properties of nanocellulose and improving the compatibility with non-polar matrices or changing its affinity from polar to non-polar molecules [16, 17].

Acetylation/Esterification is one of the most favorable modification methods where aromatics and carboxylic reagents are used in organic media. The mechanism of -OH group of cellulose with acetyl moieties causes plasticization of lignocellulosic strands [18]. Acid anhydride was used for acetylation which caused the mechanical disengagement in cellulose nanofiber (CNF) [19]. In this study, they put CNF suspension into ethanol solvent pursued by toluene and acetic anhydride. This process was done at 105 °C for 30 min there the highest degree of substitution (0.43) was accomplished. The above-mentioned treatment results in the production of hydrophobic cellulose nanofiber (CNF). N, N-dimethylformamide (DMF) is very useful and can be dissolved for both hydrophilic and hydrophobic polymers. Research should be focused on improving the interface, as the hydrophobic polymers have poor compatibility with nanocellulose [20]. Cao et al. 2009 [21] prepared a nanocomposite of waterborne polyurethane (WPU)-cellulose nanocrystal (CNC) by using polycaprolactone (PCL) as a compatibilizer, the partially presynthesized WPU was grafted on cellulose nanocrystalline surface, and the corresponding nanocomposite was obtained by the evaporation of DMF as a solvent. Experimental results showed that interface adhesion of CNC has been significantly enhanced, thereby improve the thermal stability and mechanical strength of the nanocomposites. Therefore, to improve the thermal and mechanical properties computability of nanocellulose and matrix should be improved, because both are forced to disperse by the solvent; if the compatibility of nanocellulose and polymer matrix is poor, then nanocellulose will be self-assembled rather than connected with polymer matrix. Second, it is also important to design a suitable dispersion and proper treatment, because the improper treatment might be led the high recovery cost and environmental pollution for industrialization.

The present research aims are to access the mechanical properties of nanocellulose (CNC and CNF) reinforced PUR adhesive. Chemical modification of CNF improves the compatibility between CNF and PUR adhesive. It provides a new strategy for the improvement of the properties of PUR adhesive and its wide application in the wood-based industry. The studies reported that inconsistent glue line thickness was a problem where the nanocellulose reinforcement obtained a thicker glue line to apply wood structural bonding. Such type of research has the advantages of green and renewable utilization of biomass materials, environmentally friendly wood-based adhesive. FTIR, DSC, and SEM analyses were examined to see the modification and dispersion of nanocellulose in PUR adhesive. In addition, a few studies are devoted to the preparation of nanocellulose reinforced thermosetting adhesives.

2. MATERIALS AND METHODS

2.1. Material

Cellulose nanofiber (CNF) and cellulose nanocrystal (CNC) in dry formed obtained from University of Maine, Orono, Maine, USA and CelluForce, Windsor, Quebec, Canada. Defect-free spruce (*Picea abies* L) and beech wood (*Fagus sylvatica*) have been taken from woodstore.cz and cut in the dimension of 150 × 20 × 5 mm (l × b × h). For equilibrium moisture content, samples were conditioned for 3 months at 65 ± 3% relative humidity (RH) and a temperature of 20 ± 2 °C. PUR (1C - AkzoNobel 2010) adhesive having viscosity 6000 to 19000 mPas at 25 °C with a density of 1160 kg/m³ and were used for this study. For chemical modification, acetic acid (CH_3COOH), acetone (C_3H_6O), and acetic anhydride ($C_4H_6O_3$) were purchased from Lach-Ner (Neratovice, Czech Republic), Potassium acetate (Reagent Plus ≥ 99%) used as a catalyst was purchased from Sigma-Aldrich.

2.2. Method

2.2.1 Prepareing and test of modified cellulose nanofiber

Modified cellulose nanofiber was prepared based on the acetylation method. According to Fig.1, CNF (0.25g) was mixed with 10ml acetic acid (CH_3COOH) at room temperature by using sonication (SONOPLUS HD 3100, Berlin, Germany) for 15 min. To remove acetic acid from the CNF suspension centrifuge process was followed at a speed of 15000 rpm for 15 min. After centrifugal, CNF suspension inside the centrifuge tube was separated into two layers, the acetic acid and a small layer of CNF.

Excess acetic acid was decanted, and the resultant CNF was washed with acetone. The obtained CNF was subjected to centrifuge (15000 rpm, 15min) by three times, decanting, and further dilution with distilled water. Then, extracted CNF from the previous step was mixed with 25ml of acetic anhydride with a 5% catalyst of potassium acetate (CH_3CO_2K). The suspension was heated at a temperature of 100 °C for 4 hrs continues stirring in the Soxhlet apparatus. The suspension was successfully centrifuged 3 times with acetone and last with distilled water to decant the unreacted acetic anhydride. The obtained CNF dried at room temperature.

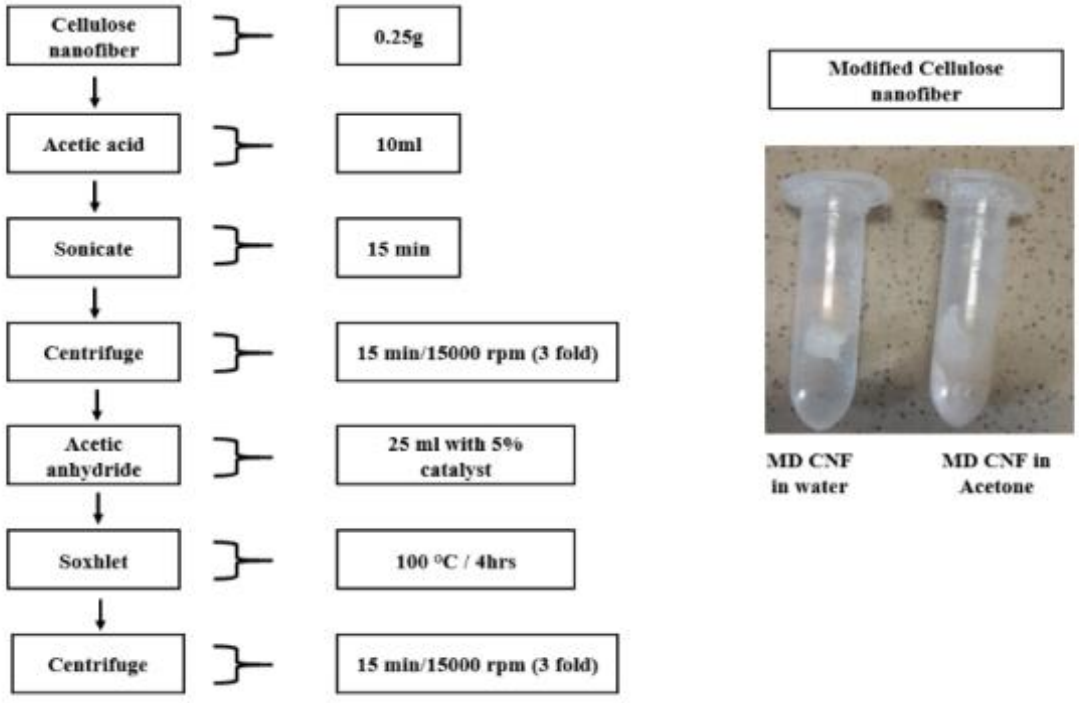

Fig. 1. Modification process of cellulose nanofiber

Fourier transform infrared spectroscopy studies were performed using FTIR spectrometer, Nicolet (Křelovická, Czech Republic). Before analysis modified CNF was adequately dried at room temperature for two days. The obtained modified CNF were pressed into the pallet and analyzed in the transmittance range of 4000 - 500 cm^{-1}.

Two-part of PUR adhesive mixed with one part of modified CNF and CNC content (0.5%, 1%, and 2%) with a high-speed homogenizer (T 18 digital ULTRA - TURRAX® IKA-Werke, Staufen, Germany) followed by sonication (SONOPLUS HD 3100, Berlin, Germany).

2.2.2 Preparation of overlap joint samples

Before gluing, the samples were conditioned for three months at 20 ± 2 °C and 65 ± 3% relative humidity to maintain the moisture content of 12%. Glue was applied on spruce and beech wood samples with a spread rate of 150 - 180g/m^2. After glue application, the samples were pressed at room temperature in a hydraulic press SCM (Villa, Verucchio, Rimini - Italy) with a pressure of 2 kg/cm^2 for 90 min. Before the shear test, the glued samples were placed in a climate chamber for two weeks and conditioned at 20 ± 2 °C and 65 ± 3% relative humidity. Ten replications of samples were prepared for each set of CNF and CNC reinforced PUR adhesive wood joints. The moisture content of the sample was determined according to [22] ISO 13061-1, and wood density was determined according to [23] ISO 13062-2. Samples were assessed per [24] EN 205-2003 with a video extensometer (INSTRON® 5882, NORWOOD, USA) at a constant speed of 5 ± 0.5 mm/min, and the data for the maximum force was acquired by a computer.

Ten replicates samples were prepared of PUR adhesive and each concentration (0.5%, 1%, and 2%) of CNF and CNC reinforced PUR adhesive for the moisture cycling condition. The effect of moisture cycling was studied by subjecting the glued samples at a constant temperature 30 ± 2 °C. The conditioned samples with 12% MC were first exposed to 8% MC (30 ± 2 °C and 43 ± 2 RH), followed by exposure to 30 ± 2 °C and 86 ± 2 RH to reach 19% EMC. Then the samples again brought down to 8% MC by exposing it to 30 ± 2 °C and 43 ± 2 RH and finally conditioned back to 12% MC by exposing them to 20 ± 2 °C and 65 ± 3% RH. Only one cycle was followed in this study. Samples were exposed at each combination of temperature and relative humidity until the weight got stabilized at that condition.

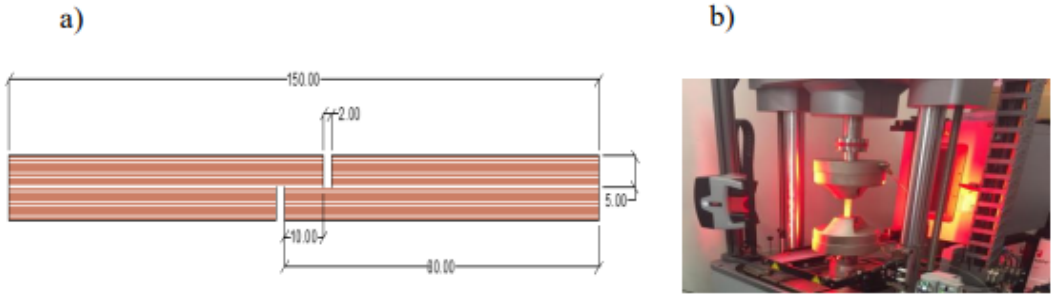

Fig. 2 a) Dimension of the test sample in mm; **b)** test sample attached to the testing machine

2.2.3 Differential scanning calorimeter (DSC)

Data were obtained by DSC 3 (METTLER, TOLEDO). Experiments were carried out by using approximately 4.5 mg of sample in a sealed aluminum pan. The samples were cooled to -30 °C at a rate of 10 °C/min and then heated to 180 °C to find out the glass transition (Tg), crystallization (Tc), and enthalpy (Δ Hc).

2.2.4 Scanning electron microscopy

The penetration adhesive was studied using a scanning electron microscope MIRA3 LMU (Tuscan, a. s., Brno, Czech Republic). The accelerating voltage of 0.8kV and a beam current of about 6pA were used for result visualizations.

2.2.5 Results calculation

Shear strength test was conducted according to [24] EN 205. Tensile shear strength was calculated as per the following equation No. 1.

$$\tau = \frac{F_{max}}{l \times b} \quad (1)$$

where τ represents tensile-shear strength along the fibers (MPa), Fmax is the maximum force at breaking point (N), l is the length of shear area (mm), and b is the width of shear area (mm).

The elastic modulus of wood joints was determined using equation 2.

$$E = \frac{\sigma_2 - \sigma_1}{\varepsilon_2 - \varepsilon_1} \quad (2)$$

where σ_1 and σ_2 are the stresses at 10% and 40% of maximum load and ε_1 and ε_2 are the corresponding strains at those stresses.

2.2.6 Statistical Analysis

The shear strength properties of nanocellulose reinforced PUR adhesive was evaluated by STATISTICA 13 software (TIBCO Inc., USA). All samples were analyzed with one-way variance analysis (ANOVA). All the results were verified at a 95% confidence level. To find out the interaction between the individual characters, a correlation analysis has been performed.

3. RESULTS AND DISCUSSION

Fig. 3a shows the elastic modulus of beech joints bonded with PUR, CNC reinforced PUR, and CNF reinforced PUR adhesive at 12% moisture content and after moisture cycle condition. At 12% moisture content, the elastic modulus of beech wood joints bonded with pure PUR adhesive was 3850 MPa. The reinforcement of CNC (0.5%, 1%, and 2%) affects the elastic modulus and is remarkable relative to the CNC content. The elastic modulus increased simultaneously up to 12% at 0.5% CNC reinforced PUR adhesive and then decreased continuously with further addition of CNC. The high elastic stiffness value was observed in the case of 0.5% CNC reinforced PUR adhesive, and the results are in line with the results reported by Santamaria-Echart et al. 2016 [25]. The author used different content of CNC reinforced with water based polyurethane adhesive and found the highest modulus with 0.5% CNC reinforced, further, addition of CNC content did not change the elastic stiffness value. Similar results has been observed by CNF (0.5%, 1%, and 2%) reinforced PUR adhesive. The highest elastic modulus was obtained by 0.5% CNF reinforced PUR adhesive, which was 4% higher compared to pure PUR adhesive at 12% moisture content, further, addition of CNF cause the decrease in elastic stiffness of beech wood joint.

After moisture cycle exposure, CNC reinforced PUR adhesive did not show any improvement in elastic stiffness of beech wood joint. In the case of CNF reinforced adhesive, 0.5% has a 5% higher elastic modulus than pure PUR adhesive after the moisture cycle exposure. Further increase of CNF content did not show any improvement in elastics modulus.

CNC and CNF reinforced PUR adhesive with 0.5% content showed higher modulus as compared to pure PUR adhesive at 12% moisture content and after moisture cycle exposure, which are in line with the results [26] where the author found that elastic modulus of CNC reinforced water based polyurethane increased below 1wt%, further, increased CNC contents, did not show any improvement might be self-aggregation that reduce the interface area between CNC and the polymer matrix relative to the overall surface area of CNC, resulting the lower hydrogen bonding density and transferring stress deficiency.

Elastic modulus of spruce wood joints bonded with PUR, CNC reinforced PUR, and CNF reinforced PUR adhesive at 12% moisture content and after moisture cycle condition have been shown in Fig. 3b. At 12% moisture content, spruce wood joints bonded with pure PUR adhesive have 3050 MPa elastic stiffness. Reinforcement of 0.5% CNC did not show any improvement in the elastic modulus, further, addition 1%, and 2% content increased the modulus from 25% to 33% compared to pure PUR adhesive. In case of CNF (0.5%, 1%, and 2%) reinforcement, the trend of elastic modulus increased simltenously from 10% to 12% as compared to pure PUR adhesive.

After moisture cycle exposure, 1% CNC reinforced PUR adhesive has the highest modulus, which was 16% higher than pure PUR adhesive joints. In the case of CNF, 0.5% CNF reinforced PUR adhesive has 11% higher elastic modulus than pure PUR adhesive, further, increase in CNF content decrease the elastic stiffness in spruce wood joints. The highest elastic modulus of nanocellulose reinforced PUR spruce wood joints has been observed up to 1%. The decrease in the elastic modulus with an increase in the filler fraction may be attributed to the higher number of voids formed during the mixing of nanocellulose with PUR adhesive. Overall the addition of nanocellulose (CNC and CNF) accerlated the elastic modulus at 12% moisture content and after moisture cycle exposure with limit content at 1%.

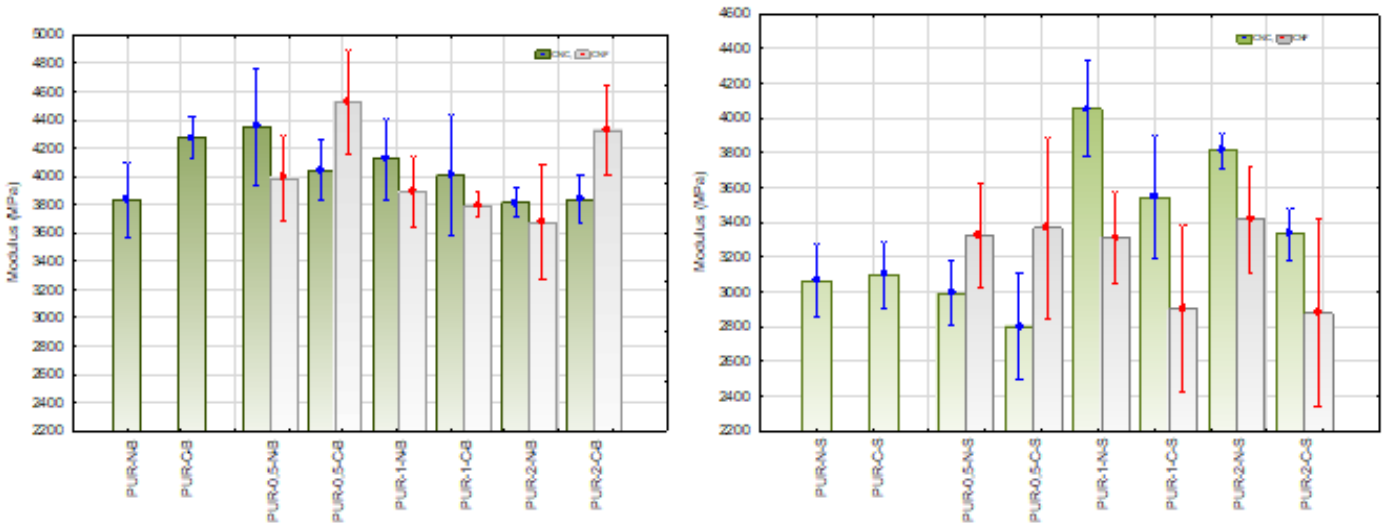

Fig. 3 Elastic modulus of joints bonded with PUR, CNC reinforced PUR, and CNF reinforced PUR adhesive at 12% MC and after moisture cycle condition; a) beech wood, b) spruce wood

Shear strength of beech wood joints bonded with PUR, CNC reinforced PUR, and CNF reinforced PUR adhesive is displayed in Fig. 4a. At 12% moisture content, it has been observed that, shear strength of PUR adhesive was 8 MPa. The addition of CNC improved the shear strength of adhesively bonded joints. The improvement in the shear strength of beech wood joints in the range of 3% to 5% as compared to PUR bonded joints depending on CNC content. Among the three concentration, 1% CNC gave the best results in terms of shear strength. The improvement in the shear strength, as compared to the joints bonded with PUR adhesive is marginal (2% to 4%) when different content of CNF was added as a reinforcing material. In fact both CNF/CNC have similar results and a limited improvement was noticed in shear strength. The results are in line with results reported by Cao et al. 2007 [27]. The author used CNF incorporating into the water based polyurethane matrix resulted a limited improvement of shear strength up to 2% of nanocomposites, further, addition of CNF shows a strong interactions between filler and between filler matrix, which restricted the motion of the matrix. After moisture cycle condition, beech wood joints bonded with PUR adhesive has 14 MPa shear strength. There was no significant difference in the shear strength of CNC/CNF (0.5%, 1%, and 2%) reinforced PUR adhesive.

Spruce wood joints bonded with PUR adhesive, CNC reinforced PUR, and CNF reinforced PUR adhesive are shown in Fig. 4b. At 12% moisture content, the joints bonded with PUR exhibited shear strength 7.5 MPa. Reinforcement of CNC improved the joint strength dramatically from 44% to 45%, as compared to PUR adhesive bonded joints. The highest improvement was noticed with 2% CNC reinforced PUR adhesive in spruce wood joints. In case of CNF reinforced, there was no significant improvement up to 1% content, further, addition of 2% CNF makes an improvement of 9% higher shear strength as compared to PUR adhesive joints.

After moisture cycle exposure, shear strength of spruce wood joints bonded with PUR adhesive was 6 MPa. The reinforcement of PUR with CNC improved the joint strength. The improvement in the shear strength of spruce wood joints was in the range of 25-42% as compared to PUR adhesive joints, 1% of CNC gave the best results in terms of shear strength after moisture cycle condition. The improvement in the shear strength joints bonded with CNF reinforced PUR adhesive are in the range of 8 to 22%, as compared to PUR adhesive. Among the three concentrations tried, 0.5% CNF reinforced gave the best results.

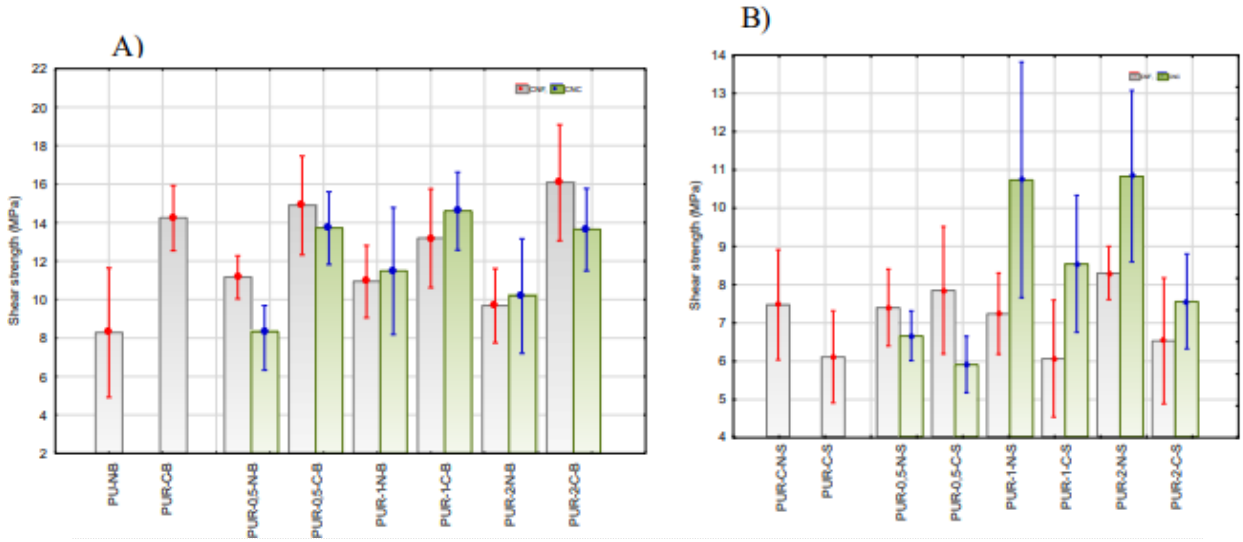

Fig. 4 Shear strength of joints bonded with PUR, CNC reinforced PUR, and CNF reinforced PUR adhesive at 12% MC and after moisture cycle condition; a) beech wood, b) spruce wood

Fourier transform infrared spectroscopy

The FTIR (Fourier-Transform Infrared Spectroscopy) spectra of PUR and CNF reinforced PUR adhesive is shown in Fig. 4. The hydroxyl group on the surface of CNF plays a significant role in PUR polymerization. These groups might participate in making the network with N-H and C=O functional groups, which influence the ultimate microstructure of PUR adhesive. The -OH group in CNF presents at 3300 cm^{-1}, slightly shifts to the right when reinforced with PUR adhesive. The intensity dropped sharply compared to the control samples, showing that -OH groups reacted with the isocyanate group (-NCO) in polyurethane adhesive. Due to molecular steric hindrance, not all the isocyanate groups reacted with the -OH group. PUR and CNF reinforced PUR adhesive shows a peak at 1720 cm^{-1} which shows urethane carbonyl groups, where the free N-H bond represents the N-H covalently bond connected with C=O groups in the urethane linkage. The FTIR peak at 2270 cm^{-1} is significant for PUR adhesive, which shows the free isocyanate groups in polyurethane structure. The free isocyanates reacted with -OH groups which cause reduced the peak by adding modified cellulose nanofiber. The peak observed at 2920 cm^{-1}, 1700 cm^{-1}, and 1370 cm^{-1} corresponds to C-H stretching, C=O stretching, and C-N stretching in polyurethane adhesive. The observation shows that the importance of modified cellulose nanofiber reinforced PUR adhesive and changes into the polymer matrix were observed significantly with the low amount of MD CNF.

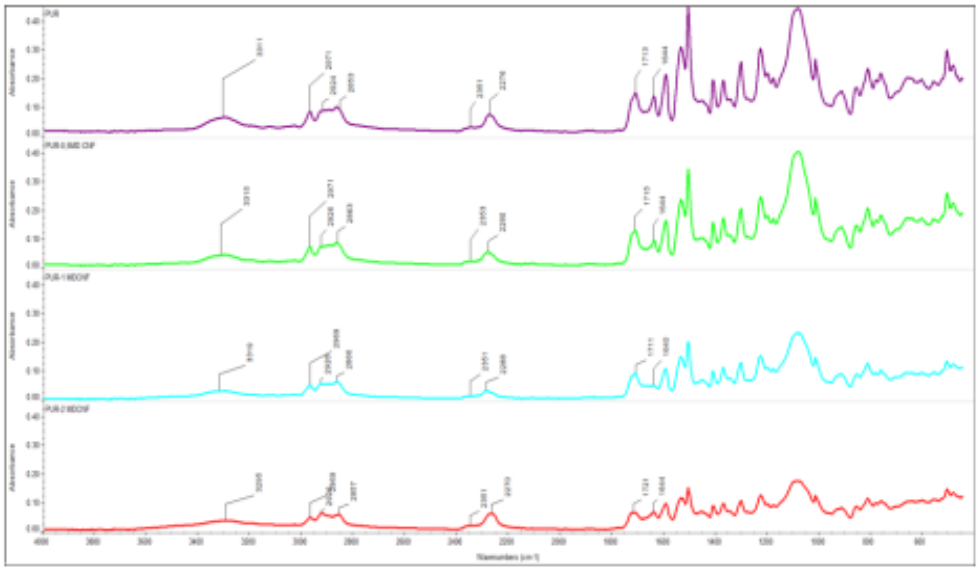

Fig. 4. FTIR spectra of PUR and CNF reinforced PUR adhesive

The FTIR spectra of the prepared PUR and CNC reinforced PUR adhesive are shown in Fig. 5. It was expected that the high -OH presence on the surface of CNC could play a significant role in the dispersion and physical appearance of CNC reinforced PUR adhesive. The typical polyurethane has extensive hydrogen bonding, where -NH group of

the urethane group plays a significant role. These hydrogen bonds can be accepted by the hard segment (the carbonyl group of the urethane group) or the soft segment (ester carbonyl or ether oxygen) [28]. The wide range of band 3300 cm^{-1} is related to -OH groups with strong intermolecular hydrogen bonds and 2900 cm^{-1} attributed CH stretching vibrations. The band around 3350 cm^{-1} shows in PUR and CNC reinforced PUR adhesive, which assigned the -NH stretching vibration of urethane groups and become more pronounced in reinforced adhesive, due to overlap with -OH stretching vibration [29, 30]. The peaks at 2900, 1700, and 1376 cm^{-1} correspond to the C-H stretching, C=O stretching and C-N bonding in polyurethane adhesive. The FTIR spectra of cellulose nanocrystalline-reinforced PUR adhesive have shown that peak reduced at 2926 cm^{-1} (C-H stretching) with the addition of cellulose nanocrystalline. The single peak at 1722 cm^{-1} shows the stretching vibration of the urethane and ester carbonyl groups, which further confirms the existing phase mixing between the hard and soft segment in the polyurethane matrix. Additionally, increased content of CNC in PUR adhesive shifts the carbonyl stretching vibration. This carbonyl shifting shows that incorporating CNC (0.5%, 1%, and 2%) disturbs the hydrogen bonding between -NH and C=O and improves the microphase separation between hard and soft segments due to strong hydrogen interaction between CNC and PUR adhesive.

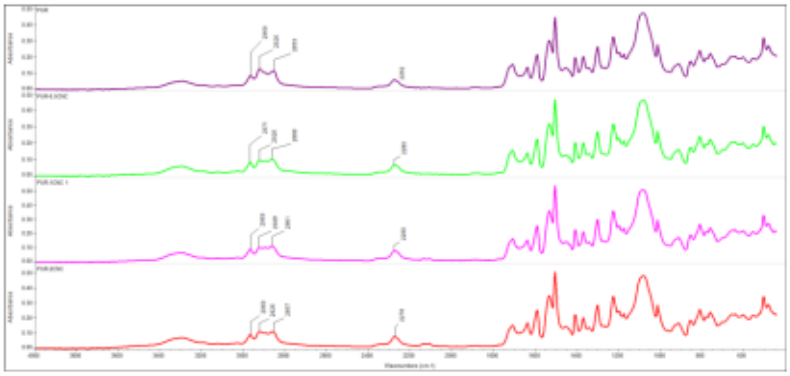

Fig.5. FTIR spectra of PUR and CNC reinforced PUR adhesive

To further understand the interaction between CNF and PUR adhesive, DSC studies of the PUR and CNF reinforced PUR adhesive were performed. Figure 6 shows the DSC thermograms of PUR and different CNF reinforced PUR adhesive content. In all curves, specific heat increment found near around -19 °C, which represents the glass transition state (T_g) and increased with the addition of 0.5%, 1%, and 2% CNF reinforced adhesive by -20.9 °C, -21.84 °C, and -21.52°C. The value of T_g increased by the addition of CNF in PUR adhesive. The presence of CNF influenced the values of T_g in two ways. Firstly, the addition of CNF makes a hydrogen bonding on the interfacial area, which can induce the restricted mobility of the PUR matrix. Another reason might be an interruption between the soft and hard segments which improves the microphase separation in PUR adhesive. The DSC curve shows that there were two endothermic peaks for both PUR and CNF reinforced PUR adhesive. The first endothermic peak was observed at 40 °C, which shifted up to 65 °C for 1% CNF and 60 °C for 2% CNF reinforced PUR adhesive. The first endothermic peak was related to rubbery transition forms of material. The reaction

between the -OH group of CNF and isocyanates groups (-NCO) of PUR makes a stronger cross-linkage matrix than PUR adhesive [31]. Since there is a stronger linkage, more energy is required to mobilize the structure, and glass transition temperature (T_g) increased after reinforcing CNF. The second endothermic peak for PUR 114 °C, while for 1% and 2% of CNF reinforced PUR adhesive was 145 °C. This endothermic peak was caused by the decomposition of the urethane group in the urea bond, which is made by the reaction of isocyanate with water [32, 33].

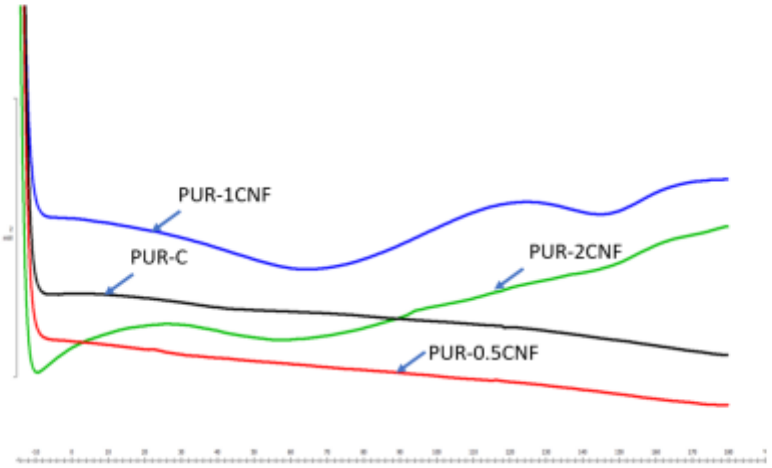

Fig. 6. DSC analysis of PUR and CNF reinforced PUR adhesive

Figure 7 shows DSC thermograms of PUR and CNC reinforced PUR adhesive. The thermograms measured for PUR matrix and CNC reinforced PUR adhesive were similar. However, a small difference in glass transition (T_g) has been noticed that could be related to the chemistry of CNC. Normally, PUR shows several changes related to soft and hard segments; both segments can present an order chain in the amorphous and crystalline region [34]. The soft segment which presents glass transition temperature is far below the room temperature, for PUR (-19 °C) and CNC (0.5%, 1%, and 2%) reinforced adhesive was (-21.98, -20.99, and -22.49 °C). Above room temperature transition is related to the disruption of hard segments, seen at the higher temperature. The thermal values of PUR matrix and CNC reinforced with different content are shown in Figure. 8. PUR matrix shows thermal relaxation at a higher temperature between 1–0 - 110 °C due to the short-range of hard segments. The incorporation of nanocellulose of a small amount of CNC (0.5%, 1%, and 2%) makes a measurable shift of the temperature of the melting of hard segments toward higher temperatures around 140 °C. These results indicated that the cellulose nanocrystal favors the crystallization and the betterment of crystals when they start to melt at a higher temperature. These observations ascribed the possible interaction of CNC with PUR matrix that nanocellulose acting as a nucleating agent for the polymer crystallization. A similar observation has been noticed by [35] who observed that the PU-silica interaction involved the polymer soft segment, resulting in less interaction between soft and hard segments, which increased the phase segregation, facilitates orientation and crystallization under tension. In another way, these types of behavior can attribute the soft segment alignment, which shows the direct interaction between PUR and silicates segment, which can correlate in the present case of CNC reinforced PUR. These observations have found the heat melting of soft segments, which indicates that the crystallization of the soft is favored with increasing CNC content and the chain mobility is not hindered to form increasingly better soft segments. These

behaviors might be due to CNC content increasing that maximizes the PUR-cellulose interactions.

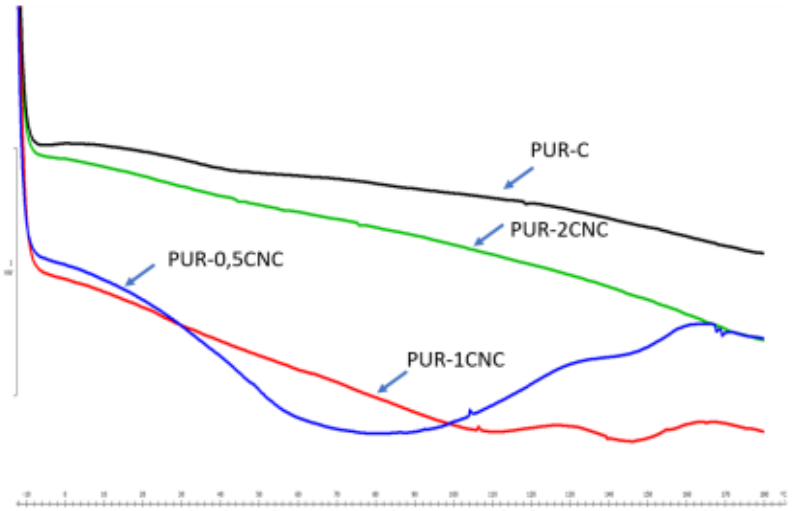

Fig.7. DSC analysis of PUR and CNC reinforced PUR adhesive

The fracture surface of neat PUR, 1% CNF reinforced PUR, and 1% CNC reinforced PUR adhesive is shown in Fig. 8 a, b, and c, respectively. The SEM images showed that there is a starved glue line in some regions with pure PUR adhesive in spruce wood joints. The addition of 1% of CNF changes the aspects of the crack and improves the glue line of spruce wood joints. The images showed an arrangement of nanofiber layer, which is due to the cellulose nanofiber reinforcement. This corresponds to the higher elastic modulus of CNF reinforced PUR adhesive as compared to the PUR adhesive. It seems that the reinforcing efficacy of CNF reinforced PUR adhesive is superior to that of PUR adhesive. From Fig. 8c, it can be noted that at 1% of CNC reinforced the glue line improved and the elastic stiffness of spruce wood joints is superior to that of the PUR adhesive. However, when compared the tensile strength there was no difference by the reinforcement of CNC. In our opinion, better compatibility between the CNC and PUR adhesive might be attributed to enhancing the interactions between the two phases, allowing stress to efficiently transfer from the matrix to the reinforcing phase and resulting in the better mechanical properties of reinforced as compared to the PUR adhesive.

Further changes in the moisture content (moisture cycling condition) of PUR and nanocellulose reinforced PUR adhesive also deserve consideration. Figure 8 d-f shows SEM images of spruce wood joints bonded with PUR adhesive and 1% CNF, 1% CNC reinforced PUR adhesive after moisture cycling condition. In PUR adhesive bonded joints, the most desirable fracture mode is a cohesive failure within the adhesive. All the joints of PUR after the moisture cycling condition exhibited cohesive failure. Further, the addition of 1% CNF in PUR adhesive improves the glue line, which shows CNF reinforcement may act as stress transfer whereby the results have lower crack initiate in the filler matrix. After moisture cycling condition, SEM analysis was carried out on the glue line surface of 1% CNC reinforced PUR adhesive Fig. 8 f. It was observed that CNC was well distributed in the matrix, and the debonding was not observed on the glue line. It indicates a strong chemical reaction between the PUR and CNC, which resulted in improvement in the bonding between the PUR matrix and CNC filler. This resulted in a

strong matrix/ filler interface and caused a low crack propagation after the moisture cycling condition and improved the wood bond joints. In spruce wood joints 1% CNC reinforcement PUR adhesive has better performance in glue line at 12% and after moisture cycling condition, which caused the higher elastic stiffness.

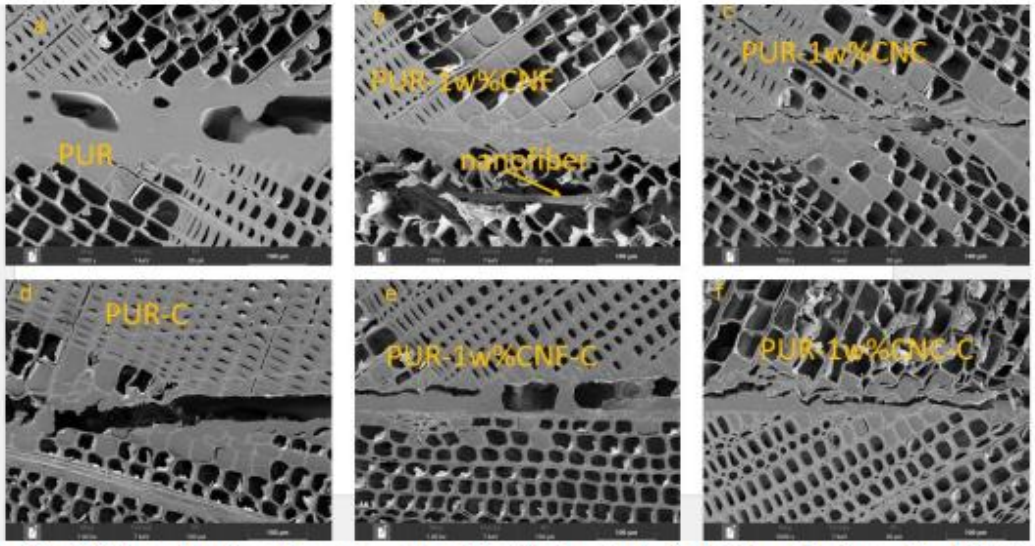

Fig. 8. SEM analysis of spruce wood joint bonded a) PUR adhesive, b) 1% CNF reinforced PUR adhesive, c) 1% CNC reinforced PUR adhesive at 12% MC; d) PUR adhesive, e) 1% CNF reinforced PUR adhesive, f) 1% CNC reinforced PUR adhesive after moisture cycling condition.

Figure 9 a-f shows the SEM images of beech wood joints bonded with PUR, 1% CNF reinforced PUR, and 1% CNC reinforced PUR adhesive at 12% MC and after moisture cycling condition. The results after the reinforcement of CNF and CNC in PUR adhesive do not show any significant improvement in the glue line of beech wood joints. This is mainly caused there is no significant difference in elastic stiffness after the reinforcement of CNF and CNC. As beech wood is more permeable than spruce wood [36] the penetration of reinforced PUR adhesive is very fast compared to the PUR adhesive. However, the lower elastic stiffness of reinforced PUR adhesive in beech wood joints could be attributed to the starved glue line due to the deeper penetration of reinforced adhesive compared to the PUR adhesive.

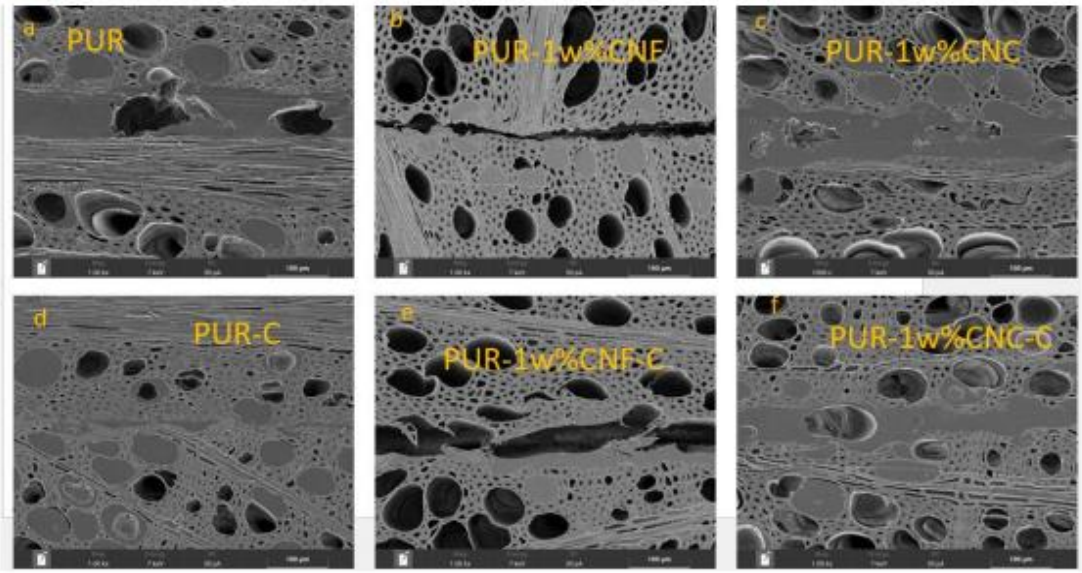

Fig. 9. SEM analysis of beech wood joint bonded a) PUR adhesive, b) 1% CNF reinforced PUR adhesive, c) 1% CNC reinforced PUR adhesive at 12% MC; d) PUR adhesive, e) 1% CNF reinforced PUR adhesive, f) 1% CNC reinforced PUR adhesive after moisture cycling condition.

CONCLUSIONS

Nanocellulose (CNF and CNC) reinforced adhesive was prepared by a mixture of modified CNF and CNC in PUR adhesive. The chemical modification of cellulose nanofiber (CNF) focused on the compatibilization with PUR adhesive matrices to improve the interfacial adhesion.

The addition of nanocellulose in PUR adhesive improved spruce wood joints' elastic stiffness and shear strength at 12% moisture and after moisture cycling condition (8-19%). In beech wood joints there is no significant difference after the addition of CNF and CNC in PUR adhesive.

Among the three (0.5%, 1%, and 2%) concentrations of nanocellulose (CNF and CNC) reinforcement, 1% addition was found to be the optimum for elastic stiffness and shear strength. Further increasing nanocellulose content, will lead to a significant drop in elastic stiffness and shear strength.

SEM analysis shows the morphology studies, and nanocellulose reinforced adhesive shows a relative improvement on the bond-line by the good dispersion of CNF and CNC addition to PUR adhesive.

The DSC study indicated that the glass transition temperature increased of PUR adhesive by the reinforcement of CNF and CNC.

ACKNOWLEDGMENTS

The author thanks for the financial support by operational research development and education in 4th industrial revolution no. CZ.02.1.01/0.0/0.0/16_019/0000803 of advance research supporting by the forestry and wood science sector´s adaptation to global change, and by the International Grant Agency (IGA) of the Faculty of Forestry and Wood Science at Czech University of Life Science (B_06_2019).

REFERENCE:

[1] Trache D. Nanocellulose as a promising sustainable material for biomedical applications. AIMS Mater. Sci. 2018 Jan 1;5(2):201-5.

[2] Hubbe MA, Rojas OJ, Lucia LA, Sain M. Cellulosic nanocomposites: a review. BioResources. 2008 Jul 31;3(3):929-80.

[3] Vazquez A, Foresti ML, Moran JI, Cyras VP. Extraction and production of cellulose nanofibers. In the handbook of polymer nanocomposites. Processing, performance and application 2015 (pp. 81-118). Springer, Berlin, Heidelberg.

[4] Trache D, Hussin MH, Chuin CT, Sabar S, Fazita MN, Taiwo OF, Hassan TM, Haafiz MM. Microcrystalline cellulose: Isolation, characterization and bio-composites application—A review. International Journal of Biological Macromolecules. 2016 Dec 1;93:789-804.

[5] Trache D, Khimeche K, Mezroua A, Benziane M. Physicochemical properties of microcrystalline nitrocellulose from Alfa grass fibres and its thermal stability. Journal of Thermal Analysis and Calorimetry. 2016 Jun;124(3):1485-96.

[6] Phanthong P, Reubroycharoen P, Hao X, Xu G, Abudula A, Guan G. Nanocellulose: Extraction and application. Carbon Resources Conversion. 2018 Apr 1;1(1):32-43.

[7] Rajinipriya M, Nagalakshmaiah M, Robert M, Elkoun S. Importance of agricultural and industrial waste in the field of nanocellulose and recent industrial developments of wood based nanocellulose: a review. ACS Sustainable Chemistry & Engineering. 2018 Feb 3;6(3):2807-28.

[8] Naz S, Ali JS, Zia M. Nanocellulose isolation characterization and applications: a journey from non-remedial to biomedical claims. Bio-Design and Manufacturing. 2019 Sep;2(3):187-212.

[9] Vineeth SK, Gadhave RV, Gadekar PT. Chemical modification of nanocellulose in wood adhesive. Open Journal of Polymer Chemistry. 2019 Nov 1;9(04):86.

[10] Köse K, Mavlan M, Youngblood JP. Applications and impact of nanocellulose based adsorbents. Cellulose. 2020 Apr;27(6):2967-90.

[11] Hou L, Zhou M, Wang S. Diamond Relat. 2018 Mater., 90, 166–171. 11

[12] Zhang S, Zhang D, Li Z, Yang Y, Sun M, Kong Z, Wang Y, Bai H, Dong W. Polydopamine functional reduced graphene oxide for enhanced mechanical and electrical properties of waterborne polyurethane nanocomposites. Journal of Coatings Technology and Research. 2018 Nov;15(6):1333-41.

[13] Wu G, Liu D, Chen J, Liu G, Kong Z. Preparation and properties of super hydrophobic films from siloxane-modified two-component waterborne polyurethane and hydrophobic nano SiO2. Progress in Organic Coatings. 2019 Feb 1;127:80-7.

[14] Fraschini C, Chauve G, Bouchard J. TEMPO-mediated surface oxidation of cellulose nanocrystals (CNCs). Cellulose. 2017 Jul;24(7):2775-90.

[15] Wu Z, Xu J, Gong J, Li J, Mo L. Preparation, characterization and acetylation of cellulose nanocrystal allomorphs. Cellulose. 2018 Sep;25(9):4905-18.

[16] Cervin NT, Aulin C, Larsson PT, Wågberg L. Ultra porous nanocellulose aerogels as separation medium for mixtures of oil/water liquids. Cellulose. 2012 Apr;19(2):401-10.

[17] Laitinen O, Hartmann R, Sirviö JA, Liimatainen H, Rudolph M, Ämmälä A, Illikainen M. Alkyl aminated nanocelluloses in selective flotation of aluminium oxide and quartz. Chemical Engineering Science. 2016 Apr 22;144:260-6.

[18] Bledzki AK, Mamun AA, Lucka-Gabor M, Gutowski VS. The effects of acetylation on properties of flax fibre and its polypropylene composites. Express polymer letters. 2008 Jun 1;2(6):413-22.
[19] Bulota M, Kreitsmann K, Hughes M, Paltakari J. Acetylated microfibrillated cellulose as a toughening agent in poly (lactic acid). Journal of Applied Polymer Science. 2012 Oct 25;126(S1):E449-58.
[20] Capron I, Rojas OJ, Bordes R. Behavior of nanocelluloses at interfaces. Current Opinion in Colloid & Interface Science. 2017 May 1;29:83-95.
[21] Cao X, Habibi Y, Lucia LA. One-pot polymerization, surface grafting, and processing of waterborne polyurethane-cellulose nanocrystal nanocomposites. Journal of Materials Chemistry. 2009;19(38):7137-45.
[22] ISO 13061-1 2014. Physical and mechanical properties of wood - Test methods for small clear wood specimens - Part 1: Determination of moisture content for physical and mechanical tests. International Organization for Standardization.
[23] ISO 13061-2 2014. Physical and mechanical properties of wood - Test methods for small clear wood specimens -- Part 2: Determination of density for physical and mechanical tests. International Organization for Standardization. Geneva. Switzerland.
[24] EN 205 2003. Adhesive for load-bearing timber structures - Test methods - Part 1: determination of longitudinal tensile shear strength
[25] Santamaria-Echart A, Ugarte L, García-Astrain C, Arbelaiz A, Corcuera MA, Eceiza A. Cellulose nanocrystals reinforced environmentally-friendly waterborne polyurethane nanocomposites. Carbohydrate Polymers. 2016 Oct 20;151:1203-9.
[26] Gao Z, Peng J, Zhong T, Sun J, Wang X, Yue C. Biocompatible elastomer of waterborne polyurethane based on castor oil and polyethylene glycol with cellulose nanocrystals. Carbohydrate Polymers. 2012 Feb 14;87(3):2068-75.
[27] Cao X, Dong H, Li CM. New nanocomposite materials reinforced with flax cellulose nanocrystals in waterborne polyurethane. Biomacromolecules. 2007 Mar 12;8(3):899-904.
[27] Seymour RW, Cooper SL. Thermal analysis of polyurethane block polymers. Macromolecules. 1973 Jan;6(1):48-53.
[28] Santamaria-Echart A, Ugarte L, Arbelaiz A, Gabilondo N, Corcuera MA, Eceiza A. Two different incorporation routes of cellulose nanocrystals in waterborne polyurethane nanocomposites. European Polymer Journal. 2016 Mar 1;76:99-109.
[29] Cao X, Dong H, Li CM. New nanocomposite materials reinforced with flax cellulose nanocrystals in waterborne polyurethane. Biomacromolecules. 2007 Mar 12;8(3):899-904.
[30] Marcovich NE, Auad ML, Bellesi NE, Nutt SR, Aranguren MI. Cellulose micro/nanocrystals reinforced polyurethane. Journal of materials research. 2006 Apr;21(4):870-81.
[31] Li Y, Ragauskas AJ. Ethanol organosolv lignin-based rigid polyurethane foam reinforced with cellulose nanowhiskers. RSC advances. 2012;2(8):3347-51.
[32] Liszkowska J, Czupryński B, Paciorek-Sadowska J. Thermal properties of polyurethane-polyisocyanurate (PUR-PIR) foams modified with tris (5-hydroxypenthyl) citrate. J. Adv. Chem. Eng. 2016;6(2).
[33] Hu W, Patil NV, Hsieh AJ. Glass transition of soft segments in phase-mixed poly (urethane urea) elastomers by time-domain 1H and 13C solid-state NMR. Polymer. 2016 Sep 25;100:149-57.

[34] Nunes RC, Pereira RA, Fonseca JL, Pereira MR. X-ray studies on compositions of polyurethane and silica. Polymer Testing. 2001 Jan 1;20(6):707-12.
[35] Kamboj G, Gaff M, Smardzewski J, Haviarová E, Borůvka V, Sethy AK. Numerical and experimental investigation on the elastic stiffness of glued dovetail joints. Construction and Building Materials. 2020 Dec 10;263:120613.

5 Discussion

5.1 Influence of Geometry on the Stiffness of Corner Finger Joints

This article focused on how wood species (spruce and beech), adhesive types (PVAc and PUR), and the number of teeth (2 and 5) effect on the elastic stiffness of finger joints under compression and tensile load. The highest elastic stiffness value was obtained from the beech wood samples with 5 teeth (30% higher) than 2 teeth bonded with polyvinyl acetate adhesive under tensile load. From the study it was concluded that elastic stiffness increased with the number of teeth in finger joints. Many researchers shows that the finger length is not a critical factor to determine the joint strength. Instead, that to acheive high strength in finger joints the critical factor is slope and sharpness. Study shows that tensile strength of finger joints lumber increased with decreasing slope (Mohammad 2004). The results have shown that the elastic stiffness was highly correlated with the wood species, wood density, and the joint geometry (Selbo 1963, Fisette and Rice 1988, Colling and Ehlbeck 1992). Walford (2000) determined the effect of finger length on tensile strength, which used for both structural and non-structural applications. The author found that shorter joints slightly stronger than longer ones but need a greater precision in manufacture. There was also a slight correlation with the loading type within the experiment.

5.2 Effect of Selected Factors on Spruce Dowel Joint Stiffness

we concluded that a higher glued surface area increases the elastic stiffness. It is therefore important to carefully consider the type of joinery used in furniture design. In the case of spruce dowel joints glued with PVAc and PUR adhesive, dowels one-half (1/2) and one-third (1/3) thickness of the joined elements were tested under compressive and tensile load. A higher elastic stiffness was obtained with PUR adhesive than PVAc adhesive under both types of loading with one-half and one-third dowel joint thickness. The test results showed that one-half thickness dowel joints had higher elastic stiffness than one-third thickness joints. The results are alined with O'Loinsigh et al., 2012. The author found that the better joint stiffness is generally achieved with a thicker joint, but this fact is also influenced by other factors, particularly the type of adhesive used. The maximum average elastic stiffness was obtained for half-thickness joints bonded with PUR adhesive under compressive load, which was 31% more than one-third thickness joints bonded with

PUR adhesive. Glue type used in bonding technology has played an essential role in the performance of wood dowel joints, Zaborsky et al., 2019 stated that the average elastic stiffness of dowel joint bonded with PUR adhesive approximately two time than joints bonded with PVAc adhesive. The strength and stiffness of dowel joints are determined by dowel diameter, dowel embedment depths, dowel space, glue type and fit tolerence.

5.3 Numerical and experimental investigation of the elastic stiffness of glued dovetail joints

In this publication, the elastic stiffness of spruce and beech wood dovetail joints bonded with PVAc and PUR adhesives was analysed by both experimental and numerical methods. In spruce wood, the joints bonded with PUR adhesive have 16% higher elastic stiffness than joints bonded with PVAc adhesive, which is already expected due to the higher stiffness of PUR adhesive. However, the results with beech wood were opposite; the elastic stiffness of joints bonded with PVAc was 28% higher than with PUR adhesive. This difference in elastic stiffness can be due to the differences in the penetration behaviour of both adhesives in these wood species (beech and spruce). The penetration ability of PUR adhesive is faster than PVAc. The penetration of the adhesive is further also influenced by the permeability of the wood (Hass et al., 2012). Beech wood is more permeable than spruce wood, and the penetration of PUR is faster compared to PVAc. The lower elastic stiffness of PUR-bonded beech wood could therefore be attributed to the starved bondline due to the deeper penetration of PUR resin into the wood. On the other hand, the bondline of PVAc in beech wood will be rather distinct due to its limited penetration.

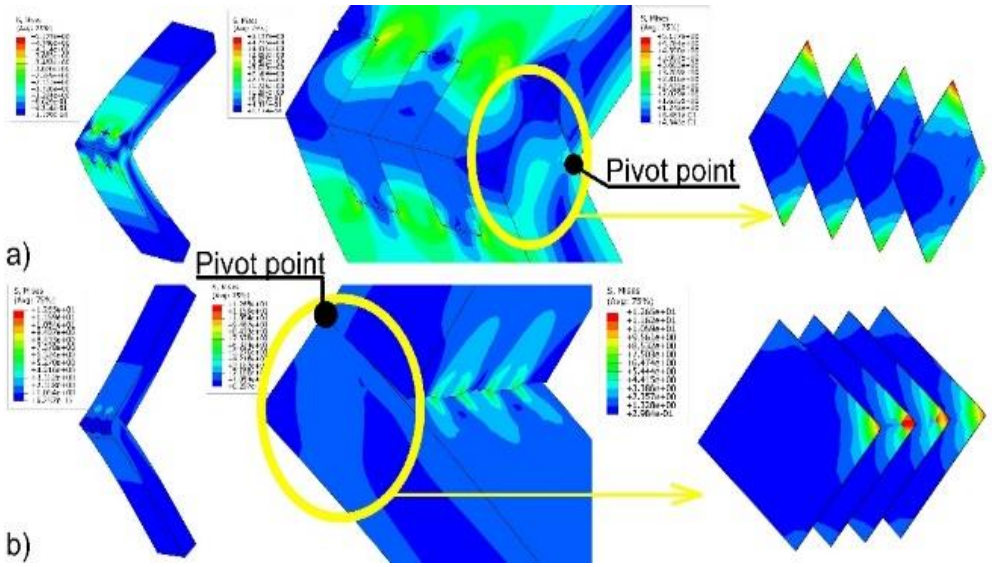

Figure 9 Distribution of reduced stress a) compression, b) tension

The numerical calculation has confirmed similar results as the experimental results for beech and spruce wood under compressive load. The numerical model provided important information about the distribution of reduced stress in joints, which can't be achieved by experimental studies. The mathematical model helps determine the location of stress in joints. Regardless of specific applications in the manufacturing of wood products, the requirement of wood adhesive is its bondability. The type of material, bondline geometry, and loading condition affect the adhesive strength. The addition of fillers that could enhance the joint strength therefore have huge potential.

5.4 Effect of nanocellulose (CNF and CNC) reinforcement on the strength and stiffness of PVAc bonded joints

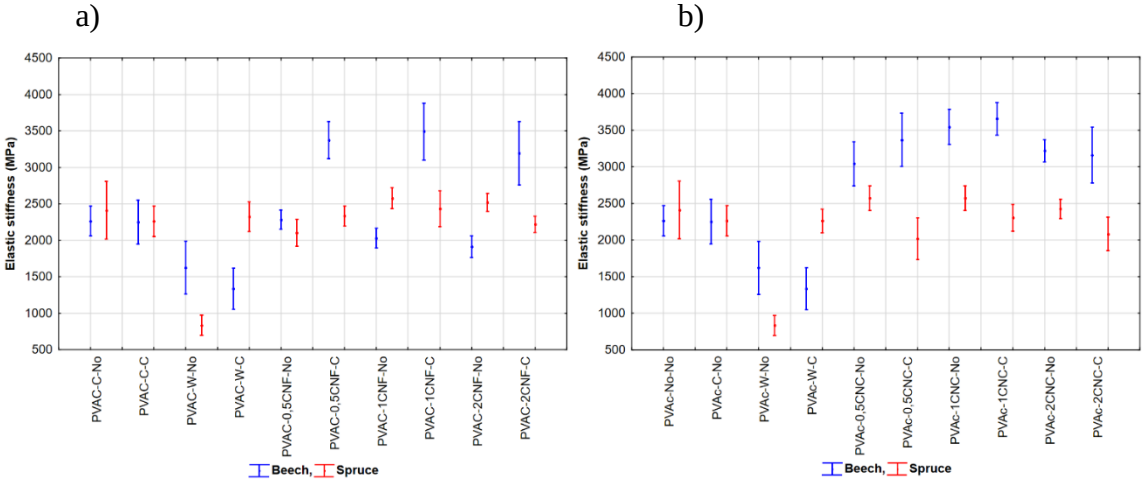

Figure 10 Elastic stiffness of wood joints bonded with PVAc and different contents of a) CNF and b) CNC reinforced adhesive

The effect of CNF content on the elastic stiffness of lap shear joints is shown in Fig. 10 a). For samples glued with nanocellulose reinforced adhesive, the elastic stiffness shows a clearly increasing trend with the CNF content. Direct dispersion of nanocellulose with pure PVAc adhesive was very complex; it was first dispersed in water and then added to the PVAc adhesive. The addition of water to the PVAc caused a significant decrease in the elastic stiffness of joints. However, the addition of CNF dramatically improved the elastic stiffness of adhesive joints.

The concentrations of (0.5w%, 1w%, and 2w%) of CNF and CNC reinforced PVAc adhesive were studied to find the best results in terms of elastic stiffness and shear strength at 12% moisture content and after moisture cycling condition (8-19%). The samples containing 1w% of CNF show the highest elastic stiffness and shear strength. The improvement was more significant in spruce wood as compared to beech wood. Spruce wood joints bonded with 1w% CNF reinforced PVAc show 4% and 219% higher elastic stiffness than pure and diluted PVAc adhesive. In the case of beech wood joints bonded with 1w% CNF reinforced PVAc, the difference was marginal compared to pure PVAc adhesive, while it was very significant compared to diluted PVAc (41%) higher. Fig. 10 b) shows that 1w% CNC reinforced PVAc adhesive resulted in the highest elastic stiffness. It was more significant in beech wood joints than in spruce joints. Beech wood joints bonded with 1w% CNC reinforced PVAc adhesive showed 35% and 54% higher elastic stiffness than pure PVAc and diluted PVAc adhesive. On the other hand, spruce wood joints bonded with 1w% CNC reinforced PVAc adhesive showed 8% and 70% higher elastic stiffness than pure PVAc and diluted PVAc adhesive. Chaabouni and Boufi (2017) investigated the influence of CNF addition on the properties of water borne polyvinyl acetate adhesive, they used very high CNF addition rates (up to 10 wt%) and observed a significant benefit in shear strength and water resistance performance. There are several studies on the application of nanocellulose reinforced adhesive in wood panels. Veigel et al. 2012 shows that the fracture energy and toughness of particle board and oriented strand board was increased by using urea formaldehyde and melamine urea formaldehyde reinforced CNF adhesive.

The effect of moisture cycling (8-19%) on the elastic stiffness of pure PVAc and CNF, CNC reinforced PVAc adhesive was also determined. After moisture cycling, the elastic stiffness of the CNF reinforced bonded joint significantly improved compared to the pure

and diluted PVAc adhesive. Beech wood joints bonded with 1w% CNF reinforced adhesive show 34% and 69% higher elastic stiffness compared to pure PVAc and diluted PVAc adhesive. On the other hand, the elastic stiffness of spruce wood at 1w% CNF reinforced adhesive did not have a significant effect compared to pure and diluted PVAc adhesive. However, the addition of CNC shows a similar trend in spruce wood. The elastic stiffness of beech wood joints bonded with 1w% CNC was 41% and 65% higher than that of pure and diluted PVAc adhesive. The result shows that the addition of nanocellulose dramatically improved the elastic stiffnss of wood-based polyvinyl acetate adhesive (PVAc) adhesive.

SEM (Scanning electron microscope) images of beech and spruce wood joints were also studied to understand the microscale bondline of PVAc and nanocellulose (CNF and CNC) reinforced PVAc adhesive at 12% moisture, shown in Fig. 11 a-f. A lap shear test showed that the elastic stiffness of nanocellulose reinforced adhesive increased after the addition of CNF and CNC. Fig.11 a-c compared the bondline of beech wood joints bonded with PVAc and 1w% nanocellulose reinforced PVAc adhesive, and Fig. 11 d-f compare the bondline of a spruce wood joint bonded with PVAc and 1w% nanocellulose reinforced PVAc adhesive. The general trend is that the thickness of the bondline increases with the addition of nanocellulose. The increase in the bondline is due to the presence of nanocellulose in PVAc adhesive, which becomes more obvious on the SEM images of the lap shear test, 1w% CNF and CNC reinforced PVAc adhesive shows that higher elastic stiffness can lead nano-reinforcement to a longer adhesive layer and surface of wood material being pulled off the surface.

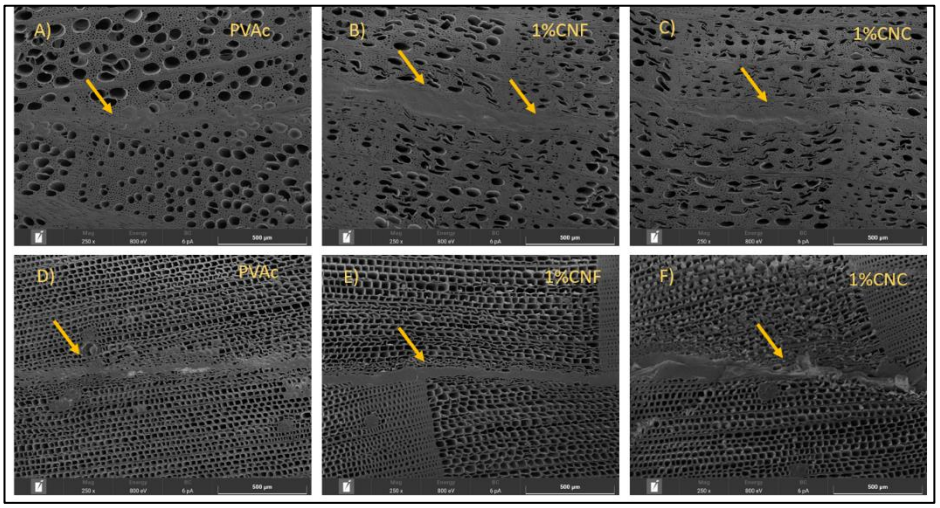

Figure 11 SEM images of beech wood joint: a) PVAc b) 1w% CNF reinforced PVAc c)1w% CNC reinforced PVAc; spruce wood joint: d) PVAc e) 1w% CNF reinforced PVAc f) 1w% CNC reinforced PVAc, at 12% of MC

Figure 12 shows SEM images of beech and spruce wood joints bonded with PVAc and nanocellulose (CNF and CNC) reinforced adhesives after exposure to moisture cycling conditions (8-19%). Neat PVAc glued joints developed a crack on the bondline after moisture cycle conditioning in beech and spruce wood. However, in the case of CNF and CNC reinforced adhesive joints, the effect of the relative humidity was minimal. This improvement can be explained by the interaction and distribution of nanofibres reinforcing PVAc adhesive. The presence of nanocellulose limit the absorption of water, cellulose is less hygroscopic; because of its rigid nature, nanocellulose also offsets the plasticising effect of water. Drying may cause shrinking of cellulose fibres, but it has some beneficial effects, such as a more intensely bonded structure, higher dimensional stability, and higher adhesion between fibres. It was observed that the moisture cycle affects the mechanical properties of pure PVAc bonded joints, while the addition of nanocellulose (CNF and CNC) stabilised the system against water absorption and improved the morphological and mechanical properties of reinforced adhesives. The results presented here support evidence of the efficient improvement of mechanical properties by the stress transfer between nanocellulose and PVAc polymers chain under moisture cycle condition.

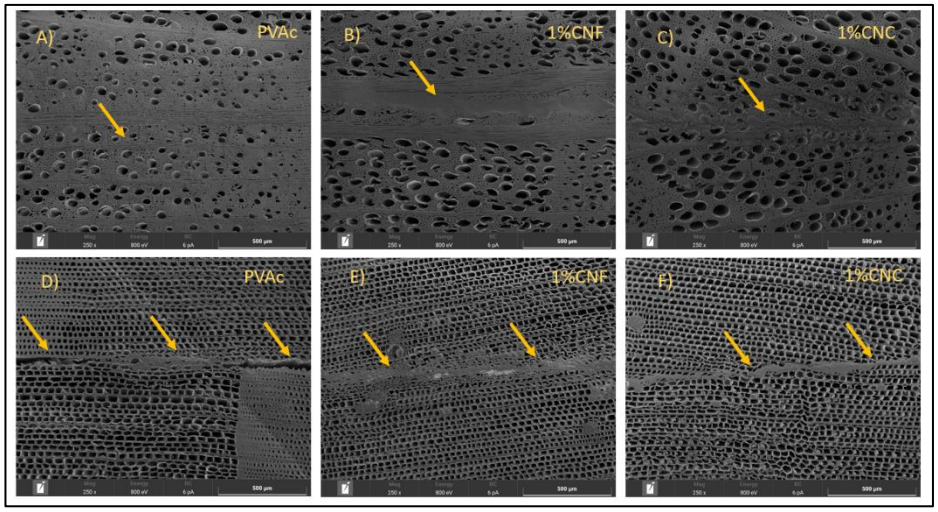

Figure 12 SEM images of beech wood joint: a) PVAc b) 1w% CNF reinforced PVAc c)1w% CNC reinforced PVAc; spruce wood joint: d) PVAc e) 1w% CNF reinforced PVAc f) 1w% CNC reinforced PVAc after moisture cycling

Fig. 13a Shows the FTIR spectra of pure PVAc and CNF reinforced PVAc adhesive. In FTIR spectra, the intensity at 1640 cm^{-1} increased, which is mainly due to the higher content of cellulose nanofibre. We can also see that the intensity increases at 3300 cm^{-1}, which is mainly attributed to -OH stretching vibration. There are no other new peaks due to the addition of CNF, which suggests that the interaction is not well between nanocellulose and PVAc adhesive.

A) B)

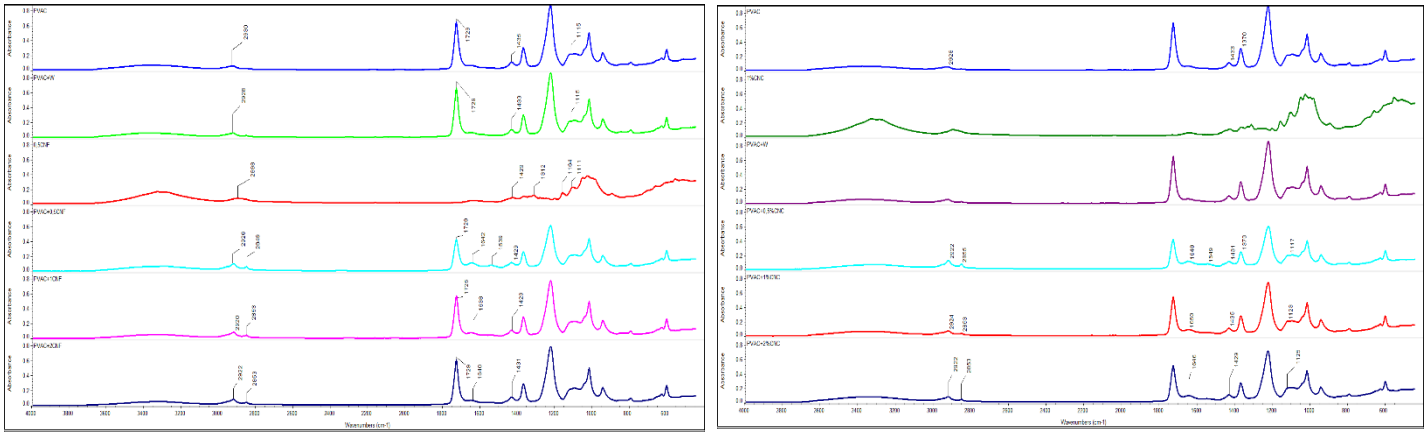

Figure 13 FTIR analysis of pure PVAc A) CNF and CNF reinforced PVAc adhesive, B) CNC and CNC reinforced PVAc adhesive

FTIR spectra of pure PVAc, CNC, and CNC reinforced PVAc adhesive are shown in Fig.13 b. The characteristics peak at 2924 cm^{-1} increased with CNC content increasing in PVAc adhesive, which shows stretching of C-H cellulose group. PVAc adhesive represent signal at 1730 cm^{-1} (carbonyl), 1433 cm^{-1} (methyl), 1370 cm^{-1} (methylene), 1245 – 1275 cm^{-1} (ester group). The absorption peak at 1642 cm^{-1}, 3392 cm^{-1}, and 3339 cm^{-1} shows the hydroxyl group of free water molecules absorbed onto the CNC surface.

Polyurethane materials are widely used in wood adhesives. Nanocellulose reinforced polyurethane are receiving steadily growing attention due to their unique and fascinating properties that potentially rival those of the most advanced materials in nature. Previously, nanometer-sized stiff and anisotropic filler with a high aspect ratio and an extremely large surface area, including graphite oxide nanoparticles, polyhedral oligomeric silsesquioxane, carbon nanotubes, and layered silicate clays, have been incorporated into polyurethane to enhance the mechanical properties and thermal

stability. Cellulose nanomaterial, including microfibrillated cellulose, microcrystalline cellulose (MCC) and CNC, have also been used as a reinforcing filler in polyurethane.

5.5 Comparative study on the properties of cellulose nanofiber (CNF) and cellulose nanocrystal (CNC) reinforced PUR adhesive bonded joints

The effect of CNF reinforced polyurethane adhesive in spruce and beech wood joints is shown in Fig. 14. The addition of CNF increased the elastic stiffness of spruce wood joints at 12% moisture content. Spruce wood joints have higher elastic stiffness at 2w%, which was 9% higher than PUR adhesive, while the elastic stiffness of beech wood, 0.5w% CNF, was 16% higher than that of PUR adhesive. The results are not significant in the case of spruce wood joints. The effect of CNF-reinforced polyurethane adhesive after moisture cycling conditioning (8-19%) was also studied. In spruce wood, joints bonded with 0.5w% CNF have 8% higher elastic stiffness than PUR adhesive, and beech wood joints bonded with 2w% CNF did not show any significant difference compared to pure PUR adhesive. The introduction of CNC as a reinforcing filler in PUR adhesive led to remarkable improvement in elastic stiffness; it is shown in Fig. 14 b. Spruce wood did not exhibit any changes with the addition of 0.5w% CNC, further, the addition of 1w% shows dramatic increment and 25% higher than PUR adhesive, while in beech wood joints, the elastic stiffness increased up to 0.5w% with CNC reinforced adhesive, which was 11% higher compared to PUR adhesive, Fig. 14 b. The addition of CNC does not show any improvement. The same results were achieved under moisture cycling conditions.

a) b)

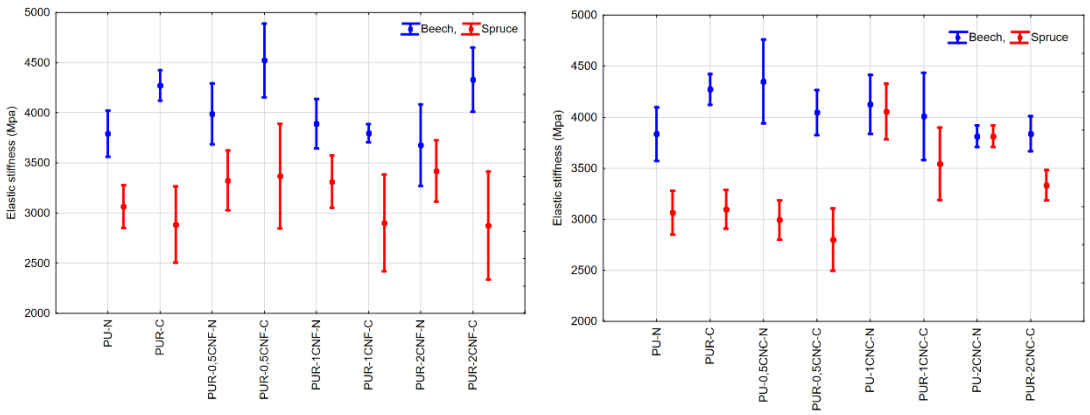

Figure 14 Elastic stiffness of spruce and beech wood joint bonded with a) CNF reinforced PUR adhesive, b) CNC reinforced PUR adhesive at 12% MC and after moisture cycling condition

nanocellulose reinforced adhesive, Fig. 15 and Fig. 16 compare the SEM images of spruce and beech wood joints bonded with PUR and nanocellulose (CNF and CNC) reinforced PUR adhesive. A general trend is that the elastic stiffness increases with 1w%

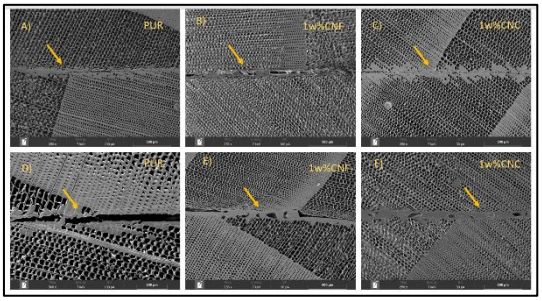

Figure 16 SEM images of a spruce wood joint: a) PUR b) 1w% CNF reinforced PUR c)1w% CNC reinforced PUR; spruce wood joint: d) PUR e) 1w% CNF reinforced PUR f) 1w% CNC reinforced PUR after moisture cycling conditioning

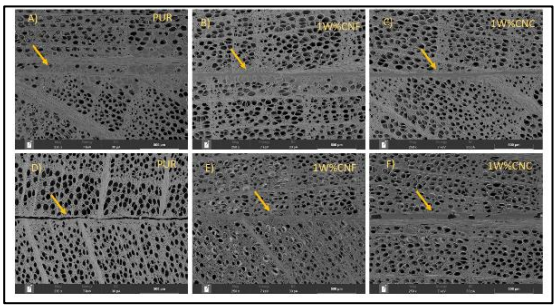

Figure 15 SEM images of a beech wood joint: a) PUR b) 1w% CNF reinforced PUR c)1w% CNC reinforced PUR; beech wood joint: d) PUR e) 1w% CNF reinforced PUR f) 1w% CNC reinforced PUR after moisture cycling conditioning

of CNF and CNC reinforced PUR adhesive. The increase in the elastic stiffness is due to the presence of nanofibre in the PUR adhesive, which can be visible on the SEM images taken under high magnification. For PUR adhesive, a crack on the bondline can be clearly seen. The addition of 1w% of nanocellulose also improved the bondline with nanofibre dispersion. This improvement was found in CNF and CNC, and it is shown in reinforced PUR adhesive spruce and beech wood joints in Fig.15 and Fig.16. The observation agrees with the elstic stiffness trend of the adhesive, which also increase the crosslinker content. During the lab shear test, the reinforced adhesive can bear a higher load without fracture, and this higher load can lead to the cross link of nanocellulose with PUR adhesive.

Fig. 17 a shows FTIR spectra of neat PUR and CNF reinforced PUR adhesive. The FTIR peak at 2270 cm^{-1} is significant for PUR adhesive, which represent a free isocyanate group in polyurethane structure. The addition of modified cellulose nanofibre to PUR adhesive causes a reduction in the -OH peak. The peak observed at 2920 cm^{-1}, 1700 cm^{-1}, and 1370 cm^{-1} corresponds to C-H stretching, C=O stretching, and C-N stretching in polyurethane (PUR) adhesive. The FTIR spectra of CNC reinforced

polyurethane adhesive are shown in Fig. 17 b FTIR spectra of CNC reinforced PUR adhesive have shown a peak reduced at 2926 cm^{-1} (C-H stretching) with the addition of CNC. Additionally, increased content of CNC in PUR adhesive shifts the carbonyl stretching vibration. This carbonyl shifting shows that incorporating CNC (0.5w%, 1w%, and 2w%) disturbs the hydrogen bonding between -NH and C=O, which further improves the microphase separation between the hard and soft segement due to a strong hydrogen interaction between CNC and PUR adhesive.

a) b)

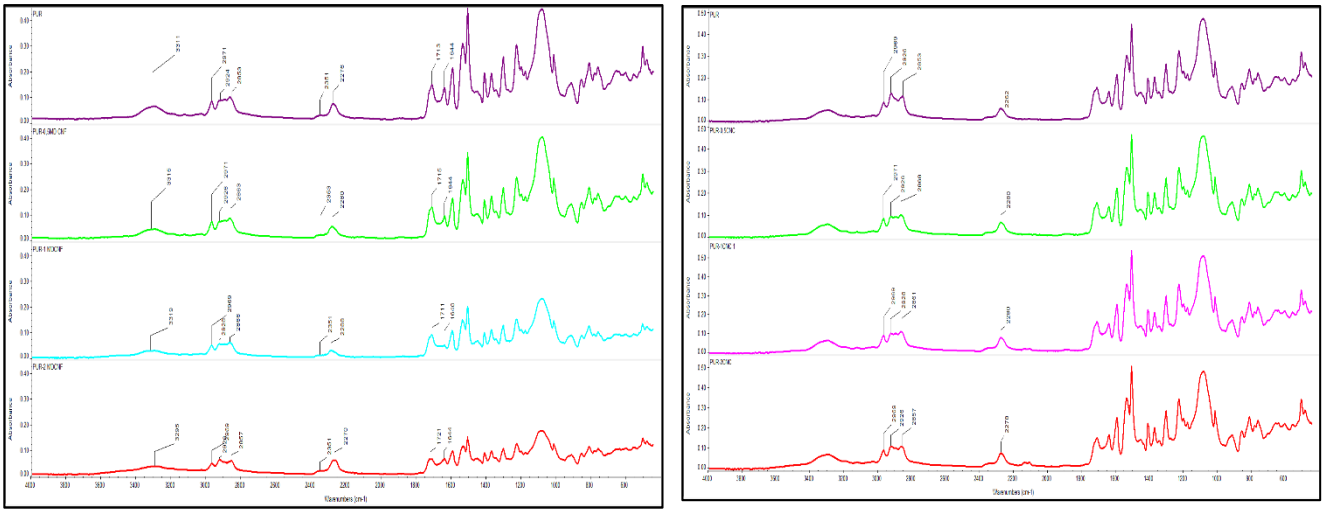

Figure 17 FTIR analysis of a) pure PUR, CNF, and CNF reinforced PUR adhesive, b) pure PUR, CNC, and CNC reinforced PUR adhesive

6 CONCLUSION AND FUTURE WORK

6.1 Conclusion

The general conclusion drawn from this study is shown in chapter 5. The below-mentioned points are brief summaries of the most important conclusions:

1. The elastic stiffness of beech and spruce wood finger joints (2 and 5 teeth) was investigated. The number of teeth in the finger joint plays a significant role; the higher the number of teeth, the higher the elastic stiffness. A 5-tooth finger joint has 30% higher elastic stiffness than 2-finger joint teeth. Wood density and adhesive type are positively correlated with the elastic stiffness of the tested adhesive bond. A high-quality bond was achieved with PUR adhesive.
2. Despite these results, the elastic stiffness of spruce wood dowel joints bonded with PUR and PVAc adhesive was investigated with half (1/2) and one-third (1/3) dowel thickness. The results show that joints with half-thickness bonded with PUR adhesive have twice the elastic stiffness as joints bonded with PVAc adhesive. The test results revealed that half-thickness joints have higher elastic stiffness than one-third thickness joints. The highest elastic stiffness of 921 Nm/rad was obtained with half-thickness joints bonded with PUR adhesive, and the lowest thickness, 209 Nm/rad, was found in joints bonded with PVAc adhesive under tensile load.
3. Further, to show the distribution of stresses in wood joints, numerical analysis on glued dovetail joints has been investigated based on experimental results. In these experiments, the elastic stiffness of beech and spruce dovetail joints bonded with PUR and PVAc adhesives under compression and tension load was calculated.
4. Beech wood joints bonded with PVAc have 28% higher elastic stiffness than joints bonded with PUR adhesive. In the case of spruce wood, joints bonded with PUR adhesive have 16% higher elastic stiffness than those bonded with PVAc adhesive. This may be due to the penetration ability of the adhesive, which is influenced by the permeability of wood. Because beech wood is more permeable than spruce wood, the penetration of PUR is faster than in spruce wood due to the starved bondline and deeper penetration of the adhesive, which results in lower elastic stiffness of beech wood with PUR adhesive.
5. Numerical calculations confirmed similar results as the experimental results for beech and spruce wood under compression load, while the results were the opposite under tensile load. Moreover, the numerical model provided important information

related to the stress distribution in joints, which can't be achieved by experimental studies. This model also helps provide the location of stress and precisely identify that the stress in compression was recorded to be higher than under tensile load.

6. Nanocellulose (CNC and CNF) reinforced adhesives (PVAc and PUR) at 12% moisture content and after moisture cycling conditioning (8-19-8%) were also observed in this study. The effect of CNC and CNF and their concentration (0.5w%, 1w%, and 2w%) were studied with a beech and spruce wood lap shear test. With PVAc adhesive, a higher elastic stiffness was achieved at 1w% concentration of CNC and CNF reinforced PVAc adhesive in beech and spruce wood lap shear test at 12% moisture content and after moisture cycling condition (8-19-8%). The same results were achieved with CNC and CNF reinforced PUR adhesive. The nanocellulose reinforcement improved the water resistance of both adhesives and strongly enhanced the mechanical properties in moisture cycle conditions.
7. SEM studies with fracture bondlines were performed to understand the pure PVAc, PUR and nanocellulose reinforced PVAc, PUR wood bond mechanism. With added nanocellulose, the bondline was improved and a minimum crack were found compared to the pure PVAc, PUR adhesive at 12% mc and after moisture cycling conditioning.
8. Pure PVAc, PUR, nanocellulose reinforced adhesive with 0.5w%, 1w%, and 2w% concentrations were also investigated through FTIR, but no clear difference was detected.

6.2 Future work

In this thesis, we mostly focused on the experimental investigation of the mechanical behaviour of joints bonded with adhesive (PVAc and PUR). It is believed that some additional investigation would be of great value, such as long-term loading and joint fatigue, and nanocellulose reinforced adhesives to improve the mechanical properties of glued wood joints. Further studies with other factors, such as proper dispersion of nanocellulose and improving interfacial compatibility in nanocomposites to maximise material properties, would be beneficial. It is also necessary to get a better understanding of adhesion interactions and the mechanical interlocking of nanofibres with adhesive polymers. Several studies have promoted the properties of nanocomposites, but only a few related to nanocelluose reinforced wood adhesives. Another area is improvement of the water-resistance of nanocellulose based

adhesives, which is possible through the chemical modification of nanocellulose, cross-linking to get a denser network, or mixing with synthetic adhesives and improving its interface for better compatibility. Future work should therefore focus on the application of nanocellulose wood-based adhesives that have better properties and economic justification than the existing material. The research needs for nanocellulose adhesion ensure a bright future for renewable polymer resources.

7 List of used literature

1. Aranguren, M.I., Marcovich, N.E., Salgueiro, W., Somoza, A. (2013) Effect of the nano-cellulose content on the properties of reinforced polyurethanes. A study using mechanical tests and positron anihilation spectroscopy. Polym Test;32(1):115-122.
2. Azeredo HMC, Mattoso LHC, Avena-Bustillos RJ, et al. (2010). Nanocellulose Reinforced Chitosan Composite Films as Affected by Nanofiller Loading and Plasticizer Content. J Food Sci.75(1):N1-N7.
3. Auad, M.L., Mosiewicki, M.A., Richardson, T., Aranguren, M.I., Marcovich, N.E. (2010). Nanocomposites made from cellulose nanocrystals and tailored segmented polyurethanes. J Appl Polym Sci.;115(2):1215-1225. J.
4. Asomani (2009). The performance of dovetail halving joint in Leg-and rail construction using Chrysophyllum albidum. Case study: the working chair M. Phil Thesis Kwame Nkrumah University of Science and Technology, Kumasi, p. 71
5. Boadu, K. B., Antwi-Boasiako, C. (2017). Assessment of the bending strength of mortise-tenon and dovetail joints in leg-and-rail construction using Klainedoxa gabonensis Pierre Ex Engl. and Entandrophragma cylindricum (Sprague) Sprague. Wood Material Science & Engineering, 12(4): 242-250.
6. Burdurlu, E., Kilic, Y., Elibol, G.C., Kilic, M. (2006). The shear strength of Calabrian pine (Pinus brutia Ten.) bonded with polyurethane and polyvinyl acetate adhesives. J. Appl. Polym. Sci., 99, 3050–3061.
7. Brandmair, A., Clauß, S., Haß, P., Niemz, P. (2012) Gluing of hardwoods with 1C-PUR-adhesives for engineered wood elements. [Verklebung von Laubhölzern mit 1 K-PUR-Klebstoffen für den Holzbau]. Bauphysik 34(5):210–216
8. Chuan, D.Y.E., Fragiacomo, M., Aldi, P., Mazzilli, M. and Kuhlmann, U., 2008. Performance of notched coach screw connection for timber-concrete composite floor system. NZ Timber Design Journal, 17(1), pp.4-10.
9. Chawla, K. K. (1998). Reinforcements, in: Composite Materials—Science and Engineering (3rd Ed.), Springer, New York, pp. 7-72.
10. Chaabouni, O., Boufi, S. (2017). Cellulose nanofibrils/polyvinyl acetate nanocomposite adhesives with improved mechanical properties, Carbohyd. Polym. 156, 64-70. DOI: 10.1016/j.carbpol.2016.09.016
11. Ceccotti, A., J.-W. van de Kuilen, The WCTE 2010 conference proceedings, June 20–24, 2010, Riva del Garda, Italy.
12. Cai, Z., Niska, K.O. (2012) Nanocelluloses: Potential Materials for Advanced Forest Products Proceedings of Nanotechnology in Wood Composites Symposium.
13. Colling, F. and Ehlbeck, J., 1992. Tragfähigkeit von Keilzinkenverbindungen im Holzleimbau. Bauen mit Holz, 94(7), pp.586-593.

14. Dou, Z.J., Cheng, M., Qin, Y.F., Chen, L., Qin, Z.Y. (2014). Simultaneous improvement of mechanical properties and thermal stability of polyurethane by polyethylene glycol grafted cellulose nanocrystals Adv. Mater. Res., 1052, pp. 249-253, 10.4028/www.scientific.net/amr.1052.249
15. Ebnesajjad, S. (2008). Adhesives Technology Handbook, 2nd ed.; William Andrew: Norwich, NY, USA, 2008; pp. 1–6, 114–115
16. Eckelman, C.A., Akcay, H., Leavitt, R., Haviarova, E. (2002). Demonstration building constructed with round mortise and tenon joints and salvage material from small-diameter tree stems. Forest Products Journal. 52: 82-86.
17. Eckelman, C.A., Kwiatkowski, K. (1978). Experimental testing of the theory of deformations of cabinet designs llolztechnologie, 19 (4), pp. 202-206
18. Eckelman, C.A., Rabiej, R.A. (1985). A comprehensive method of analysis of case furniture Forest Prod. J., 35 (4), pp. 62-68
19. EN 205 (2003): Adhesive for load-bearing timber structures – Test methods – Part 1: determination of longitudinal tensile shear strength.
20. Floros, M., Hojabri, L., Abraham, E., et al. (2012) Enhancement of thermal stability, strength and extensibility of lipid-based polyurethanes with cellulose-based nanofibers. Polym Degrad Stab.97(10):1970-1978.
21. Frihart, C. R. (2013). Wood adhesion and adhesives, in: Handbook of Wood Chemistry and Wood Composites (2nd Ed.), R. M. Rowell (ed.), CRC Press, Boca Raton, FL, USA, pp. 255-313., DOI: 10.1016/j.jclepro.2015.07.070
22. Fisette, P.R. and Rice, W.W., 1988. An analysis of structural finger-joints made from two northeastern species. Forest products journal (USA).
23. Gavrilović-Grmuša, I., Dunky, M., Djiporović-Momčilović, M., Popović, M., Popović J. (2016). Influence of pressure on the radial and tangential penetration of adhesive resin into poplar wood and on the shear strength of adhesive joints. BioRES. 11: 2238–2255. DOI: 10.15376/biores.11.1.2238-2255
24. Girouard, N.M., Xu, S., Schueneman, G.T., Shofner, M.L., Meredith , J.C. (2016). Site-selective modification of cellulose nanocrystals with isophorone diisocyanate and formation of polyurethane-CNC composites ACS Appl. Mater. Inter., 8, pp. 1458-1467, 10.1021/acsami.5b10723
25. Ganowicz, R., Dziuba, T. Ozarska-Bergandy, B. (1978). Theorie der verformungen von schrankkonstruktionen Holztechnologie, 19 (2), pp. 100-107
26. Hass, P., Wittel, F.K., Mendoza, M., Herrmann, H.J., Niemz, P. (2012). Adhesive penetration in beech wood: experiments, Wood Sci. Technology 46 (1-3) 243-256.
27. Haviarova, E., Kasal, A., Efe, H., Eckelman, C. A., Erdil, Y. Z. (2013). Effect of adhesive type and tenon size on bending moment capacity and rigidity of T-shaped furniture joints constructed of Turkish Beech and Scots Pine. Wood and Fiber Science, 45 (3): 1–7.
28. Hoadley, R.B. (2000). Understanding Wood: A Craftsman's Guide to Wood Technology Taunton Press, p. 280

29. Ivdre, A., Mucci, V., Stefani, P.M., Aranguren, M.I., Cabulis, U. (2016) Nanocellulose reinforced polyurethane obtained from hydroxylated soybean oil. IOP Conference Series: Mater Sci Eng.;111(1):012011.
30. ISO 13061–1 Physical and Mechanical Properties of Wood – Test Method for Small Clear Wood Specimens – Part 1: Determination of Moisture Content for Physical and Mechanical Tests International Organization for Standardization, Geneva, Switzerland (2014)
31. ISO 13061–2 Physical and Mechanical Properties of Wood – Test Method for Small Clear Wood Specimens – Part 2: Determination of Density for Physical and Mechanical Tests International Organization for Standardization, Geneva, Switzerland (2014)
32. Jokerst, R.W. (1981) Finger-jointed wood products. Res Pap FPL-RP-382. USDA For Serv Forest Prod Lab,Madison,WI
33. Jiang, W., Haapala, A., Tomppo, L., Pakarinen, T., Sirviö, J.A. Liimatainen, H. (2018). Effect of Cellulose Nanofibrils on the Bond Strength of Polyvinyl Acetate and Starch Adhesives for Wood. BioResources, 13, 2283-2292. https://doi.org/10.15376/biores.13.2.2283-2292
34. Kamke, F.A., Lee, J.N. (2007). Adhesive penetration in wood – A review. Wood and Fiber Science. 39: 205–220
35. Kaboorani, A., Riedl, B. (2011) Improving Performance of Polyvinyl Acetate (PVA) as a Binder for Wood by Combination with Melamine Based Adhesives. International Journal of Adhesion and Adhesives, 31, 605-611. https://doi.org/10.1016/j.ijadhadh.2011.06.007
36. Kaboorani, A., Riedl, B., Blanchet, P., Fellin, M., Hosseinaei, O. and Wang, S., 2012. Nanocrystalline cellulose (NCC): A renewable nano-material for polyvinyl acetate (PVA) adhesive. European Polymer Journal, 48(11), pp.1829-1837.
37. Kotaś, T., Sztywność. (1957). mebli skrzyniowych. Przemysł Drzewny, 1957, vol. 10, pp. 15–18.
38. Kotaś, T. (1957). Sztywność mebli skrzyniowych (cz. II) Przemysł Drzewny, 11, pp. 10-14
39. Kiaei, M., Samariha, A. (2011). Fiber dimensions, physical and mechanical properties of five important hardwood plants. Indian Journal of Science and Technology 4(11): 1460- 1463
40. Kägi, A., Niemz, P., Mandallaz, D. (2006). Influence of moisture content and selected technological parameters on the adhesion of one-part polyurethane adhesives under extreme climatical conditions. [Einfluss der Holzfeuchte und ausgewählter technologischer Parameter auf die Verklebung mit 1K-PUR Klebstoffen unter extremen klimatischen Bedingungen]. Holz Roh Werkst 64(4):261–268
41. Kläusler, O., Clauss, S., Lübke, L., Trachsel, J., Niemz, P. (2013) Influence of moisture on stress–strain behaviour of adhesives used for structural bonding of wood. International Journal of Adhesion and Adhesives 44:57-65. DOI: 10.1016/j.ijadhadh.2013.01.015

42. López-Suevos, F., Eyholzer, C., Bordeanu, N., and Richter, K. (2010). DMA analysis and wood bonding of PVAc latex reinforced with cellulose nanofibrils, Cellulose 17(2), 387-398. DOI: 10.1007/s10570-010-9396-8
43. Lei,W.Q., Zhou, X., Fang, C.Q., Song, Y.H., Li ,Y.G. (2019). Eco-friendly waterborne polyurethane reinforced with cellulose nanocrystal from office waste paper by two different methods Carbohydr. Polym., 209, pp. 299-309, 10.1016/j.carbpol.2019.01.013
44. Lu, G. (1996). Improvement of polyvinyl acetate emulsions Huagong Shikan, 10 (6), p. 17
45. Müller, U., Veigel, S., Follrich, J., Gabriel, J., Gindl, W. (2009). Performance of 1C polyurethane in comparison to other wood adhesives. Paper presented at the ICWA 09 International Conference on Wood Adhesives, Lake Tahoe, Nevada, 28–30.
46. Mohammad, M., 2004. Finger-joint process and products quality. Value to Wood Project Report (FCC3), FP Innovations–Forintek Division, St-Foy, Quebec, Canada.
47. Nutsch, W., Eckerhard, M., Ehrmann, W., Hammerl, W., Hammler, D., Nestle, H., Nutsch, T., Schulz, P. (2006). Příručka pro Truhláře [Carpenter's Guide], Europ-Sabotales, Praha, Czech Republic.
48. Ng, H.M., Sin, L.T., Tee, T.T., Bee, S.T., Hui, D., Low, C.Y., Rahmat, A.R. (2015). Extraction of cellulose nanocrystals from plant source for application as a reinforcing agent in polymers, Composite Part -B: Engineering, volume 75, page 176-200, https://doi.org/10.1016/j.compositesb.2015.01.008
49. Özçifçi, A., Yapici, F. (2008). Effects of machining method and grain orientation on the bonding strength of some wood species. J. Mater. Process. Technol., 202, 353–358.
50. O'Loinsigh, C., Oudjene, M., Shotton, E., Pizzi, A. and Fanning, P., 2012. Mechanical behaviour and 3D stress analysis of multi-layered wooden beams made with welded-through wood dowels. Composite Structures, 94(2), pp.313-321.l
51. Pei, A., Malho, J-M., Ruokolainen, J., Zhou, Q., Berglund, L.A. (2011) Strong Nanocomposite Reinforcement Effects in Polyurethane Elastomer with Low Volume Fraction of Cellulose Nanocrystals. Macromolecules.44(11):4422-4427.
52. Proulx, E. (1996). Yankee Magazine's Make It Last: Over 1,000 Ingenious Ways to Extend the Life of Everything You Own. Rodale Press, Incorporated, 5.
53. Pizzi, A., Mittal, K.L. (2003) The handbook of adhesive technology. Dekker, New York
54. Pizzi, A. (2005). Wood adhesives-basic. In Handbook of Adhesion, 2nd ed.; Packham, D.E., Ed.; John Wiley & Sons, Ltd.: Bath, UK, pp. 603–606.
55. Segovia, C., and Pizzi, P.A. (2012). Performance of dowel-welded wood furniture linear joints, Journal of Adhesion Science and Technology 23(9), 1293-1301. DOI: 101163/ 156856109X434017.

56. Su, W.C., Wang, Y. (2007) Withdrawal properties of single dovetail joints Taiwan J. Forestry Sci., 22 (3), pp. 321-328
57. Smardzewski, J., 2015 b: Furniture design, Springer, Heidelberg, Germany 377 pp.
58. Smardzewski, J., 2008. Effect of wood species and glue type on contact stresses in a mortise and tenon joint. Proceedings of the Institution of Mechanical Engineers, Part C: Journal of Mechanical Engineering Science, 222(12), pp.2293-2299.
59. Smardzewski, J., 1998. Numerical analysis of furniture constructions. Wood Science and Technology, 32(4), pp.273-286.
60. Smardzewski, J. and Prekrat, S., 2002. Stress distribution in disconnected furniture joints. Electronic Journal of Polish Agricultural Universities, Wood Technology, 5(2).
61. Singha, A. S., Thakur, V. K. (2008). Effect of fibre loading on urea-formaldehyde matrix based green composites, Iran. Polym. J. 17(11), 861-873.
62. Selbo, M.L., 1963. Effect of joint geometry on tensile strength of finger joints. Forest Products Journal, 13(9), pp.390-400.
63. Tonoli, G.H.D., Teixeira,E.M., Corrêa, A.C. MarconciniJ.M., Caixeta, L.A. Pe reira-da-Silva, M.A. et al. Cellulose micro/nanofibres from Eucalyptus kraft pulp: preparation and properties Carbohyd Polym, 89 (2012), pp. 80-88
64. Tas, H. H., Altinok, M., Cimen, M. (2014). The strength properties changing according to type corner joints and adhesive wood-based furniture under the effect of dynamic forces, Wood Research 59(2), 359-372.
65. Ülker, O., 2016. Wood adhesives and bonding theory. Adhesives–Applications and Properties.
66. Vineeth, S., Gadhave, R., Gadekar, P. (2019) Nanocellulose Applications in Wood Adhesives-Review. Open Journal of Polymer Chemistry, 9, 63-75. doi: 10.4236/ojpchem.2019.94006.
67. Veigel, S., Rathke, J., Weigl, M. and Gindl-Altmutter, W., 2012. Particle board and oriented strand board prepared with nanocellulose-reinforced adhesive. Journal of Nanomaterials, 2012.
68. Wu, Q., Henriksson, M., Liu, X., Berglund, L.A. (2007). A High Strength Nanocomposite Based on Microcrystalline Cellulose and Polyurethane. Biomacromolecules;8(12):3687-3692.
69. Walford, B.G., 2000. Effect of finger length on finger-joint strength in radiata pine. In World Conference on Timber Engineering, Jul.-Aug (pp. 31-3).
70. Zhou, H. (1991). Research on the improvement of water resistance of polyvinyl acetate emulsion Nianjie, 12 (4), pp. 11-12
71. Zhang, J.L. Eckelman, C.A. (1993). The bending moment resistance of single-dowel corner joints in case construction Forest Prod J., 43 (6), pp. 19-24
72. Záborský, V., Kamboj, G., Sikora, A. and Borůvka, V., 2019. Effects of selected factors on Spruce dowel joint stiffness. BioResources, 14(1), pp.1127-1140.